

# Linear and Nonlinear Analysis of DC biased Coupled Microbeams

Gyanadutta Swain

A Thesis Submitted to  
Indian Institute of Technology Hyderabad  
In Partial Fulfillment of the Requirements for  
The Degree of Master of Technology



भारतीय प्रौद्योगिकी संस्थान हैदराबाद  
Indian Institute of Technology Hyderabad

Department of Mechanical Engineering

June 2013

## Declaration

I declare that this written submission represents my ideas in my own words, and where ideas or words of others have been included, I have adequately cited and referenced the original sources. I also declare that I have adhered to all principles of academic honesty and integrity and have not misrepresented or fabricated or falsified any idea/data/fact/source in my submission. I understand that any violation of the above will be a cause for disciplinary action by the Institute and can also evoke penal action from the sources that have thus not been properly cited, or from whom proper permission has not been taken when needed.

Gyanadutta Swain

(Signature)

GYANADUTTA SWAIN

(Gyanadutta Swain)

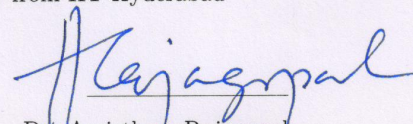
ME11M05

(Roll No.)

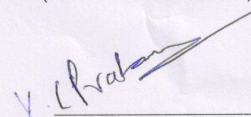


## Approval Sheet

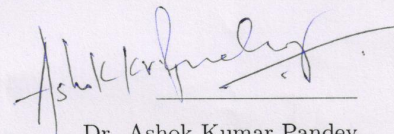
This Thesis entitled Linear and Nonlinear Analysis of DC biased Coupled Microbeams by Gyanadutta Swain is approved for the degree of Master of Technology from IIT Hyderabad



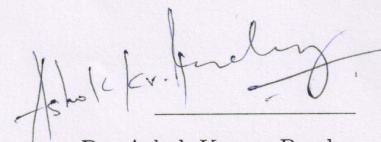
Dr. Amirtham Rajagopal  
Dept. of Civil Engg., IITH  
(External Examiner)



Dr. Chandrika Prakash Vyasarayani  
Dept. of Mechanical Engg., IITH  
(Internal Examiner)



Dr. Ashok Kumar Pandey  
Dept. of Mechanical Engg., IITH  
(Adviser)



Dr. Ashok Kumar Pandey  
Dept. of Mechanical Engg., IITH  
(Chairman)

## Acknowledgements

I am thankful to all the people who have guided and supported me throughout my thesis work. First of all, I express my immense gratitude to my advisor Dr. Ashok Kumar Pandey, for giving me a chance to work in such an interesting field and believing in me during the research work. I also thank him for his excellent guidance and all time valuable support and encouragement.

I would like to extend my gratitude to my committee members who have made interesting and useful remarks during my thesis work. I also wish to thank Professor V. Eswaran, H.O.D, Department of Mechanical Engineering, IIT Hyderabad and Professor U.B Desai, Director, IIT Hyderabad for their support in various ways. I acknowledge all the faculty members of Mechanical Engg. Dept., IIT Hyderabad, specially Dr. M. Ramji, Dr. B. Venkatesham, Dr. R. Prasanth Kumar, being a student of who during the course work, I got the opportunity to learn many new techniques as well as concepts which were directly or indirectly useful in my thesis work. I would also like to thank all Staff members, Project Associate Staffs, Research scholars and M Tech colleagues in CAE as well as Nano Lab, Department of Mechanical Engineering, IIT Hyderabad for their help and suggestions, whenever needed. I must not ignore the special contributions of the institute library for providing all the necessary books, articles and access to many useful domains to enrich my asset list in this research work.

Many, many thanks go to my family for their blessings and support. I wish to express my special gratitude to my lovable mother Malati Lata for her care and love and to my elder sisters Smita, Nameeta, Arpita and brother Bibhu for giving me the base support through out this period. I am also thankful to my IIT Hyderabad friends for the warmth of their friendship and providing a supportive environment, which has made my stay at IIT Hyderabad wonderful. I sincerely acknowledge some of my close friends Pinaki, Nikhil, Anup, Rakesh, Jaeson, Prashil, Mayank, Anil, Jabir and others for their role as tension healers and as rich sources of entertainment. And above all to Asha kiran, my wonderful mate for her love and encouragement and for all her supports on and off the work.

At the end, I would like to pay special homage to my late father. He could be the most happiest person in this occasion. I deeply regret for this uncommon happening. But I feel proud to say, "Papa, wherever I am today, it is just because of your small right decision about my life, when I was unable to foresee and predict my future. You are deeply missed."

# Dedication

Dedicated To

My Beloved Parents

(Mr. Binod Kumar Swain and Mrs. Malati Lata Swain)

# Abstract

Now-a-days, micro electro-mechanical system based sensors and actuators are widely used in almost every field due to their uncommon advantages over the conventional devices in terms of stability, accuracy, sensitivity and operating flexibility etc. There are different mechanisms to increase the sensitivity as well as the frequency range of dynamic resonators. Frequency tuning due to an electrostatic effect, nonlinear mid-plane stretching, a thermo mechanical effect, etc., are some of the major techniques used to widen the operating frequency range of these devices. However, the majority of these techniques are applied to a single operation mode in an individual MEMS structure. But the tuning of different modes in an array of beams is of great interest which could possibly provide an idea to develop more sensitive as well as stable micro-resonators.

In this study, we describe the combined thermal and electrostatic effects in tuning the frequencies of different modes in a beam. The thermal effects such as cooling or heating are introduced by the varying tensions in the beams, which affect the frequencies. On the other hand, the electrostatic effects, due to the application of large dc bias, result in the softening of one of the modes and hardening of other mode. With sufficiently large dc voltage, the modal coupling of the two modes of the beam is achieved. Understanding the coupling of different modal frequencies and their tuning mechanisms is essential for design of multi-frequency MEMS sensors and actuators. First we take a clamped-clamped Au-Pd beam separated from two side electrodes and a bottom electrode. We experimentally find the first two bending modes of the beam and vary their dependence with respect to an electrostatic DC bias. Subsequently, we develop a theoretical model to predict the variation of these two coupled modes. It is found that the coupling strength of the modes can be controlled by effectively changing the differential gaps between the beam and the side electrodes. Finally, we extend this analysis to an array of three similar fixed-fixed beams and then generalize it for an array with  $N$  beams. It is found that with proper application of thermal and electrostatic tuning in an array, it is possible to get multi-modal coupling as well as large frequency range. we analytically determine the coupling of an array of 40 beams and validate the theoretical outcome experimentally.

After analyzing the frequencies based on linear formulations, the dynamic analysis for the single coupled micro-beam is performed for linear as well as nonlinear regions. Here, to obtain the dynamic behavior of the device, we apply method of multiple scales to the original modal equations. finally using the method of reconstitution, we get first order uniform expansion for the solution of the system, governing the dynamic response.

# Contents

Declaration . . . . .	i
Approval Sheet . . . . .	i
Acknowledgements . . . . .	iv
Abstract . . . . .	vi
<b>Nomenclature</b>	<b>viii</b>
<b>1 Introduction</b>	<b>1</b>
1.1 Motivation . . . . .	1
1.2 Literature Survey . . . . .	2
1.3 Outline of the thesis . . . . .	6
<b>2 Mathematical modeling and solution of a single fixed-fixed beam</b>	<b>8</b>
2.1 Full static and dynamic governing equation . . . . .	8
2.2 Frequency analysis based on linear equations . . . . .	12
2.3 Nonlinear response of dynamic equation . . . . .	14
2.3.1 Numerical solution (based on rk5 or ode45) . . . . .	15
2.3.2 Solution based on Method of Multiple Scales . . . . .	17
2.3.3 Stability Analysis . . . . .	26
2.4 Results and discussion . . . . .	27
2.4.1 Linear frequency analysis . . . . .	27
2.4.2 Numerical solution (based on rk5 or ode45) . . . . .	28
2.4.3 Solution based on Method of Multiple Scales . . . . .	29
<b>3 Mathematical modeling and solution of an array of three fixed-fixed beams</b>	<b>31</b>
3.1 Full static and dynamic governing equations . . . . .	31
3.2 Frequency analysis for $N = 3$ beam. . . . .	37
3.3 Results and discussions . . . . .	40

<b>4</b>	<b>Mathematical modeling and solution of an array of <math>N</math> fixed-fixed beams</b>	<b>43</b>
4.1	Full static and dynamic governing equations . . . . .	43
4.2	Linear frequency analysis for $N$ beams. . . . .	46
4.3	Results and discussions . . . . .	48
<b>5</b>	<b>Conclusions and Future work</b>	<b>50</b>



# Chapter 1

## Introduction

Micro-Electro-Mechanical Systems, or MEMS, is a technology that in its most general form can be defined as miniaturized mechanical and electro-mechanical elements that are made using the techniques of microfabrication. With the evolution of such new sophisticated techniques and stepping in the third generation of Nanotechnology, the MEMS / NEMS (Nano-Electro-Mechanical-Systems) devices are more often pursued to be used in the risk governance frame. To facilitate this, in parallel to the manufacturing flexibility, The functional advancements of these devices have become the present focus of interest. In this work, frequency tuning of MEMS devices due to dc biasing is presented, which gives the advantage of modal coupling both in linear and nonlinear region.

### 1.1 Motivation

At this present scenario, the applications of MEMS devices are not only limited as high sensitive sensors of mass[1, 2, 3] , force, pressure, temperature[4] or actuators and micro mirrors but also they have become a major breakthrough in the field of biotechnology, medicine, communications, avionics, robotics and research etc. MEMS inertial sensors, specifically accelerometers and gyroscopes, are quickly gaining market acceptance for high accuracy. The easy combination of MEMS technology in other fields such as optical-MEMS and bio-MEMS, have led to the production of some futuristic devices, MEMS encoders, automation airplane, millibot etc. As a boon of sophisticated microfabrication processes, these extreme small devices which consume less power can be fabricated in bulk, considerably reducing the cost of production.

At the same time due to their reduced size or increased aspect ratio, the early onset of non-linearity limits the useful linear dynamic range and effectively alters the dynamic behavior of the device[5] . Since non-linearity is the frequent rule of nature, we often encounter several systems that operate beyond linear range where the output response is suppressed by noise and the natural frequency is shifted considerably from the original value showing regions of instabilities. So controlling these devices in the nonlinear region is equally important from the application point of view as well as performance enhancement of the system.

Thinking from the control side, the ultra high natural frequency of the MEMS device can be tuned using different techniques[4],[6]-[12] which adds favors in the dynamic operation of these devices through several coupling mechanisms. Among them, the phenomena of electrostatic coupling through dc biasing has become an interesting domain of MEMS research in the recent years as it facilitates visualization of the frequency band of multiple beams in an array . The competitive behavior of simultaneous softening and hardening may result in mixing of dispersed modes which are important from the sensitivity point of view. So the collective thermal and electrostatic effects may be of greater importance to get the dual advantages of increasing the operating range as well as sensitivity of the devices through multiple modal interactions. The generated noise can also be suppressed by operating it near the coupling region, hence increasing the efficiency of the device. Such multiple modal interactions can be described through an array of micro-beams.

## 1.2 Literature Survey

Microelectromechanical system based devices as mechanical resonators are widely used in many areas replacing other conventional devices. These are used in almost every electronic device using digital and communication circuits, where frequency reference for synchronization[13] is essential. Although quartz crystal oscillators are capable to provide a stable frequency reference over a range of operating conditions, MEMS devices are successfully replacing them in many fields due to their miniaturization capabilities, compatibility, low power consumption, reasonable accuracy and economic batch fabrication. These superior capabilities are ensured because of high sensitivity and ultra-high frequency of operation which is possible with the extreme small size of the device. Still high performance MEMS devices are desired with wide operating range and long term stability to completely replace the crystal resonators.

From literature, it is revealed that the sensitivity as well as frequency bandwidth of a resonant sensor or an actuator can be improved using different frequency tuning mechanisms. Among these, the most commonly used techniques are tuning by electrostatic DC biasing, thermal stressing, structural hardening, etc., which are generally applied to a particular mode of a single or an array of resonators. Application of these tuning techniques to two or more modes have recently been explored to get the coupled region where the performance can be significantly enhanced. Therefore, it is crucial to understand the coupling mechanism of two or more modes.

Recently, Suzuki et al.[6] have proposed method of electrostatic frequency tuning in a fish bone shaped MEMS resonator for the first five vibration modes. The resonator consists of one main beam and several sub beams attached to the main beam. By suitably choosing the location and numbers of exciting electrodes, they are able to get a wide frequency range. Their frequency tuning covers a range of 178 Hz to 1746 kHz for the first five modes along with enhanced Q factor due to selection of tapered anchor.

Similarly Wan-Sul Lee et al.[7] have modeled a 3D micromechanical actuator using FEM and

BEM to explain the frequency shifting due to electrostatic tuning and compared the numerical result with experimental data.

In another experiment Quirin et al.[8] have used the concept of dielectric force in frequency tuning. A doubly clamped high stressed silicon nitride beam when actuated by means of four bottom gold electrodes separated through certain gap experiences dielectric force which is a function of the gap between beam and electrodes and applied voltages. Using such tuning mechanism they were able to get a frequency bandwidth of more than 100 kHz.

Eyal Buks and Michael L. Roukes[9] have applied the method of electrostatic tuning to an array of 67 fixed-fixed microbeam resonators made of Au and explained the significance of collective response due to induced inter-device mechanical coupling using optical diffraction method. The electrostatic interaction between the individual mechanical resonators gives rise to the formation of a band of normal modes of vibration otherwise called as phonons. Finally they have proposed the concept of such type of tuning in an array to be used in the field of spectral analysis.

Using temperature dependence of the tension in the beam, Ashok et al.[4] are able to use the concept of frequency change with temperature for proposing an AuPd temperature sensor. Since the resonant frequency of a system under the action of large tension is significantly dependent on the stress developed, and the stress induced is a function of the temperature, hence varying the temperature results in tuning the frequency. In another experiment, Todd Remtema and Liwei Lin[10] have adopted the frequency tuning using localized thermal stressing effect on comb shaped micro resonator to get a frequency tuning of 6.5 percent at around the central frequency of 31 kHz experimentally.

By suitably tuning different modes of vibration so that they come close to each other, it is possible to get another interesting phenomena where modes interact with each other. The existence of such mode mixing region in InAs nanowire resonator has been shown experimentally by Solanki et al.[11]. They have explained the nonmonotonic dispersion of resonant frequency and the presence of mixed mode region with respect to applied gate voltage. They have also shown this modal interaction in nonlinear region by increasing the amplitude of driving force.

Kozinsky et al.[12, 14] have used the electrostatic frequency tuning mechanism to tune the nonlinearity of NEMS resonators both upward and downward. They have applied this tuning procedure to a doubly clamped SiC resonator to increase its dynamic range. By tuning two orthogonal modes closer to each other they are able to observe the anti-crossing region in two different devices namely SiC and gold beam, using two different detection techniques.

Further as the dimensions of the devices shrink to smaller scale, they exhibit nonlinearities which considerably alter the dynamics of the device. It becomes highly sensitive to excitation showing regions of instability under certain operating conditions.

Most of the systems in nature are nonlinear as a rule, hence they can be modeled effectively using nonlinear governing equations or considering nonlinear boundary conditions[15]. There are many sources of nonlinearities that can exist in a system[15, 16] such as material nonlinearity, geometric nonlinearity, inertial nonlinearity, forcing nonlinearity and dissipative nonlinearity. The material or constitutive nonlinearity arises due to the nonlinear stress-strain relation for the material of the system whereas the geometric nonlinearity is due to the nonlinear strain-displacement relationship. Inertial nonlinearity arises because of unbalanced concentrated or distributed masses. The remaining two are due to nonlinearity in the applied or dissipating forcing terms.

However, the nonlinearity is easily reachable in case of MEMS devices, where its influence is important even at small amplitude of response. Hence a proper analysis of the dynamics including nonlinearities should be carried out so as to understand the system and its controlling parameters thoroughly before implementing any idea.

In recent years many researchers based on their studies on nonlinearities have proposed numerous techniques to get highly stable MEMS / NEMS devices with more sensitivity and applicability. Lee et al.[18] proposed a concept of frequency tuning of resonating device in nonlinear range by stiffness adjustment by which two vibrational modes can be coupled with each other through internal resonance that can be used for frequency stabilization.

Antonio et al.[19] have investigated the nonlinear response and internal resonance conditions in clamped-clamped microbeam array for fixed DC bias and variable AC excitation over critical amplitude of vibration. They have shown the state of 3:1 internal resonance where the first in-plane flexural mode couples with the principal torsional mode and transfer of energy between the two occurs. Finally they have proposed a method of amplitude and frequency stabilization using internal resonance mechanism and verified it experimentally using a closed loop configuration.

The nonlinear vibration of a suspended cable with 1:1 internal resonance has been investigated by Akira Abe[20] using two different numerical approaches. He has considered both quadratic and cubic nonlinearities in his formulation and adopted the method of multiple scales and shooting method for the analysis. The effect of second and third in-plane and out-of-plane modal interactions has been shown in his work. Using the same approach of MMS (method of multiple scales), Yan et al.[21] have studied the nonlinear vibration in double-walled carbon nanotubes, where there exists 1:3 internal resonance condition between coupled coaxial and non-coaxial vibration modes.

In another study by S. Murat et al.[22] nonlinear transverse vibration of an Euler-Bernoulli beam with multiple supports is investigated. They have considered the beam with initial tension subjected to 3:1 internal resonance. The stretching of the neutral axis due to fixed boundary conditions is considered in the nonlinear governing equation. The internal resonance condition is achieved corresponding to particular positions of supports and initial tension values. Frequency and force response curves are plotted for 3:1 internal resonance corresponding to 3, 4 and 5 supports cases.

Usama H. Hegazy[23] studied the dynamic behavior and chaotic motion of a string-beam coupled system subjected to parametric excitation. The beam and string are coupled through 3:1 internal resonance with cubic nonlinearity. He has applied the method of multiple scales for the analysis of system and influence of different parameters on the system dynamics. Finally the presence of multi-valued region, jumps, instabilities etc. are illustrated. Similar 3:1 internal resonance in the nonlinear oscillation of a shallow arch has been reported by El-Bassiouny [24].

Ashwin Vyas et al.[25] have considered a T-shaped microresonator to study the nonlinear 1:2 internal resonance in flexural structural modes. The analytical model includes pre-stress with geometric, inertial and forcing nonlinearities. Using a reduced order two mode expansion and asymptotic analysis, the dynamics of the T-beam is studied and the coupled responses are obtained. As a concluding remark, after comparing the analytical results qualitatively with experimental data, they have mentioned the high sensitiveness of the device to mass perturbations and thus, holds great potential as a radio frequency filter-mixer or mass sensor.

Another important analysis on 2:1 internal resonance has been performed by M. F. Daqaq et al.[26] in microscanners. They have electrostatically tuned the frequencies of the device to get two to one internal resonance condition between torsional and bending vibration modes. Applying MMS to the governing equations including nonlinearities in forcing, they are able to get the coupled nonlinear responses corresponding to primary excitation of the first and second modes respectively. Subsequently they have introduced the concept of energy transfer mechanism through internal resonance.

Many works so far has been done on the nonlinear analysis of clamped-clamped Nanoelectromechanical resonators due to their simplicity in fabrication and extensive practical use because of their higher resonant frequencies than other structures with similar dimensions.

Candler et al.[27] have reported nonlinear characterization and mechanism of clamped-clamped resonator under electrostatic excitation. Another similar doubly clamped AuPd resonator has been studied by Zaitsev et al.[28]. They have shown that nonlinear dissipation plays an important role along with nonlinear elastic effects on the dynamics of the device. Hyung et al.[29] have demonstrated the possibility of stable operation of MEMS oscillators beyond critical vibration amplitude using closed-loop control system. Kozinsky et al.[14] have also investigated the nonlinear behavior of fixed-fixed beams and confirmed the presence of mixed mode region between two orthogonal modes from their experimental results.

Few works have also been reported on array of coupled resonators considering the nonlinearity in the system. In these cases, it is possible to get multiple coupling between different modes giving rise to modified dynamic behavior of the system and more complicated energy transfer process. Internal resonance and bifurcations in an array of nonlinearly coupled microbeams has been studied by S. Gutschmidt and O. Gottlieb [30, 31]. Using a nonlinear continuum model they have



investigated the dynamics of the system below its first pull-in instability. Applying asymptotic multiple scale approach, the response of two elements and three elements system near 3:1 internal resonance subjected to parametric excitation are analyzed.

In a similar way, the parametric resonance in electrostatically coupled array of carbon nanotubes has been studied by A. Isacsson and J. M. Kinaret [32]. They have analyzed a model of one-dimensional array of carbon nanotube resonators in two different configurations. They have shown that both transverse and longitudinal parametric resonances can be excited along with primary resonances. The electrostatic interactions between adjacent tubes affect the dynamics and mode stability.

In another study, Chotorlishvili et al.[33] have analytically modeled two NEMS resonators with arbitrary coupling strength between them. They have analyzed the nonlinear dynamics of the system using perturbation technique considering cubic nonlinearity in restoring forces. Finally they have proposed how to control the energy transfer between coupled modes by tuning the driving field frequency.

### 1.3 Outline of the thesis

This thesis altogether consists of four chapters. In the first chapter, we have described the motivation behind the selection of this work related to linear and nonlinear analysis of coupled microbeams along with a brief introduction to different terms like MEMS, NEMS, modal coupling, frequency tuning etc. Various causes of nonlinearities that influence a system are explained with the importance of study of nonlinearity. Towards the end, a review of different works performed by various researchers in this area and their contributions are presented in short.

The second chapter wraps entire studies including modeling, analysis, results and discussions for a single microbeam. This chapter is further divided into various subsections; Initially, we have derived the static and dynamic governing equations for a single fixed-fixed beam based on available literature. Subsequently the frequency analysis is done based on linear governing equations. Then the nonlinear formulation is carried out so as to facilitate numerical studies using method of multiple scales and stability analysis is done based on different criteria. In the last subsection, the results for the case of single beam are discussed.

In the third chapter, we have modeled for an array of three microbeams, which are actuated by two side electrodes and one bottom electrode. Considering different types of forcing acting on individual components, we have completed the static analysis as well as dynamic analysis of the system. Here the case of multiple modal coupling is illustrated while discussing the results.

The fourth chapter is basically an extension of third chapter, where we have extended all the formulations and analysis steps for the case of three beams to an array of  $N$  beams. After

generalization of all the procedures for  $N$  beams, we have specifically solved for a 40 beams array ( $N = 40$ ). To the later stage, both linear and nonlinear results for the beam array are discussed.

In the fifth or last chapter, we have summarized our results corresponding to linear and nonlinear responses for single beam as well as array of beams. Finally, the conclusion is drawn based on the usefulness of this work along with its future perspectives.

## Chapter 2

# Mathematical modeling and solution of a single fixed-fixed beam

This chapter presents the theoretical foundation and modeling of a single microbeam subjected to electric excitation. We derive the governing equations using elastic beam theory considering large deformations in the structure. Different electrostatic forces acting on the beam are considered while modeling the beam. Based on the mathematical model, we analyze the frequencies in two orthogonal directions. Subsequently, we apply method of multiple scales to solve the nonlinear governing equations and perform dynamic analysis.

### 2.1 Full static and dynamic governing equation

In this section, we theoretically model a doubly clamped microbeam with rectangular cross section surrounded by two semi-infinite side electrodes and one bottom electrode. we take a fixed-fixed beam of length  $L$ , width  $B$  and thickness  $H$ , which is separated from the two side electrodes  $E_1$  and  $E_2$  by the air-gaps of  $g_0$  and  $g_1$ , respectively (Fig. 2.1). It is also separated from the bottom electrode  $E_g$  by a gap of  $d$ . Taking the deflection of the beam along in-plane and out-of-plane as  $y(x, t)$  and  $z(x, t)$ , respectively, as shown in Fig. 2.2(a) the governing equations after neglecting damping and considering residual tension and mid-plane stretching can be written as

$$EI_z y_{xxxx} + \rho A y_{tt} - [N_0 + T_N] y_{xx} = Q_y \quad (2.1)$$

$$EI_y z_{xxxx} + \rho A z_{tt} - [N_0 + T_N] z_{xx} = Q_z \quad (2.2)$$

where,  $T_N = \frac{E_x A}{2L} \int_0^L (y_x^2 + z_x^2) dx$  is the tension induced by mid-plan stretching [34],  $N_0$  is the initial tension induced by fabrication processes [35], heating, etc., We take  $\alpha_{corr.} = \frac{E}{E_x}$  as the correction factor, to take care of the transverse isotropic property of the beam.  $EI$  is the bending rigidity

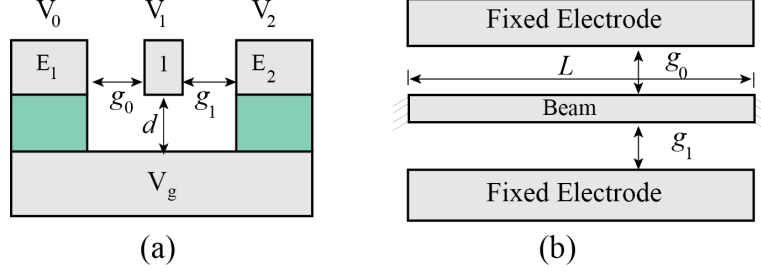


Figure 2.1: (a) Side view of a single beam separated from the the side electrodes,  $E_1$  and  $E_2$ , and the ground electrode  $E_g$ ; (b) Top view of single beam shown with the two side electrodes on either side of the beam.

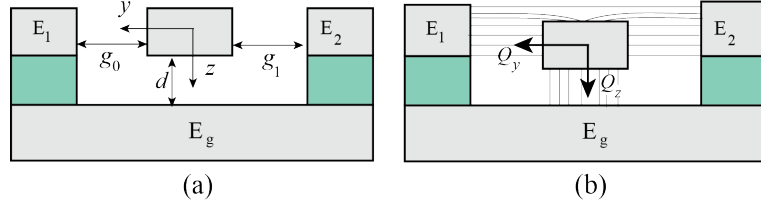


Figure 2.2: (a) Displacement of the beam in two different directions are represented by  $y$  and  $z$ ; (b) The corresponding forces are represented by  $Q_z$  and  $Q_y$ . (Note that the fringing effect is neglected in  $Q_z$  and  $Q_y$ ).

and  $\rho$  is the material density. The boundary conditions for the fixed-fixed beam are taken as:

$$\begin{aligned} y(0, t) = y(L, t) = 0, \quad z(0, t) = z(L, t) = 0, \\ y_x(0, t) = y_x(L, t) = 0, \quad z_x(0, t) = z_x(L, t) = 0. \end{aligned} \quad (2.3)$$

$Q_y$  and  $Q_z$  are the effective electrostatic forcing per unit length along  $y$  and  $z$  directions as shown in Fig. 2.2(b). The expression of the forcing can be obtained under two important assumptions. First, the parallel plate capacitors with neglected fringing effects are assumed. Secondly, we consider the contribution of inhomogeneous electric field due to the deflection of the beam in  $z$ -direction [8]. Such forcing can have significant effect in  $z$ -direction. Thus, the final expression of the forcing can be assumed as,

$$Q_y = \frac{1}{2}\epsilon_0(1 - k_1|z|)H \left[ \frac{(V_{10} + v(t))^2}{(g - y)^2} - \frac{(V_{21} + v(t))^2}{(g_1 + y)^2} \right] \quad (2.4)$$

$$Q_z = \frac{1}{2}\epsilon_0B \left[ \frac{(V_{1g} + v(t))^2}{(d - z)^2} \right] - k_2z \left[ (V_{21} + v(t))^2 + (V_{10} + v(t))^2 \right] \quad (2.5)$$

Where  $\epsilon_0 = 8.85 \times 10^{-12}$  F/m is the free space permittivity.  $V_{ij}$  and  $v(t)$  are the DC and AC components of applied voltage. In the above expressions,  $k_1$  represents the contribution of the net effective change in area due to  $z$ -deflection. However, it is assumed to be negligible in the present study.  $k_2$  represents the strength of forcing due to inhomogeneous electric field generated because of  $z$ -deflection, which is found to be very effective in the present test case.  $V_{ij} = V_i - V_j$  is the

difference in the DC voltage applied between the beam and electrodes.

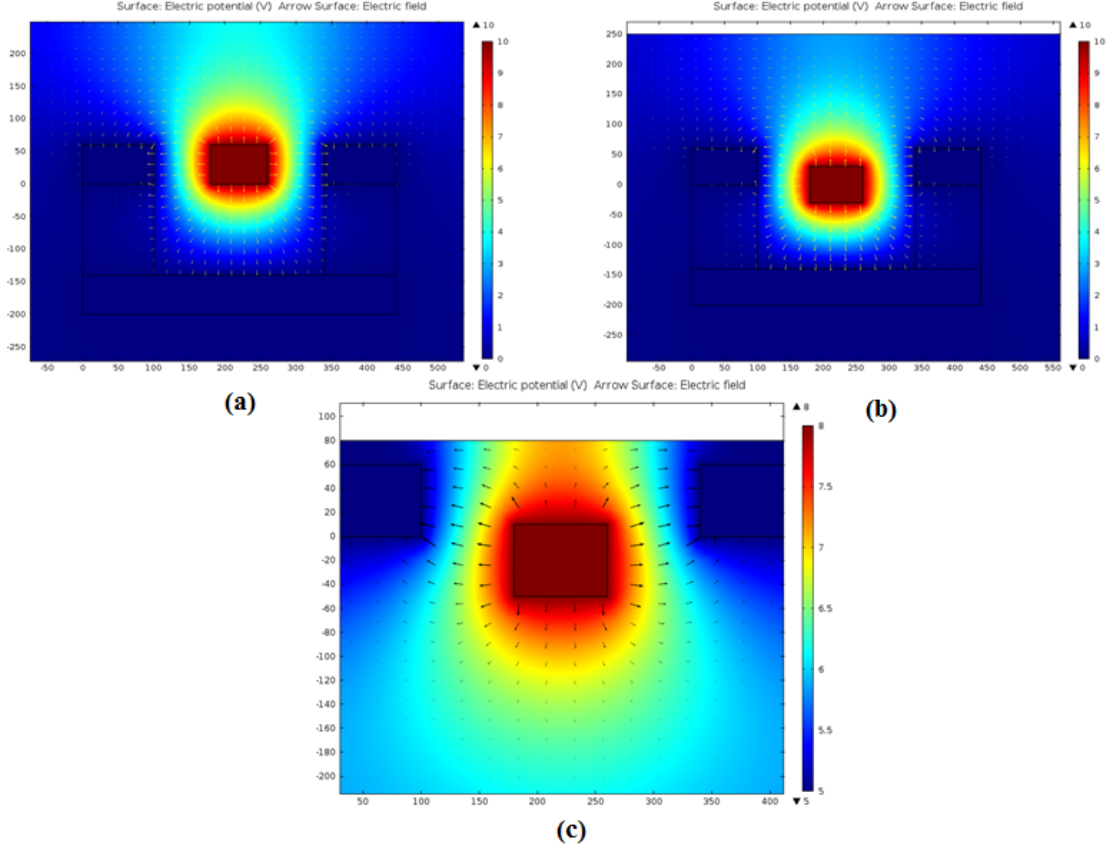


Figure 2.3: COMSOL results showing variation of electric field due to different positions of beam. (a) homogeneous electric field when beam is undeflected, (b) Inhomogeneous electric field when the beam is deflected downward, (c) Inhomogeneous electric field strength shown by arrow length.

For convenience, we introduce new non-dimensional variables as denoted by hat in the governing equations,

$$\hat{x} = \frac{x}{L}, \quad \hat{y}_n = \frac{y_n}{g}, \quad \hat{z}_n = \frac{z_n}{d}, \quad \hat{t} = \frac{t}{T} \quad (2.6)$$

where,  $T$  is the time scale used to non-dimensionalize time  $t$  and is equal to  $\sqrt{\frac{\rho_B H L^4}{E I_z}}$ . Subsequently dropping hats for convenience, we get nondimensionalized form of equations,

$$y_{xxxx} + y_{tt} - [N + \alpha_1 \Gamma(y, y) + \alpha_2 \Gamma(z, z)] y_{xx} = \alpha_3 \times \left[ \frac{(V_{10} + v(t))^2}{(1 - y)^2} - \frac{(V_{21} + v(t))^2}{r_1^2 (1 + \frac{y}{r_1})^2} \right] \quad (2.7)$$

$$z_{xxxx} + \alpha_4 z_{tt} - \alpha_4 [N + \alpha_1 \Gamma(y, y) + \alpha_2 \Gamma(z, z)] z_{xx} = \alpha_5 \frac{(V_{1g} + v(t))^2}{(1 - z)^2} - \alpha_6 [(V_{10} + v(t))^2 + (V_{21} + v(t))^2] z \quad (2.8)$$



subjected to the following modified boundary conditions,

$$\begin{aligned} y(0, t) = y(1, t) = 0, \quad z(0, t) = z(1, t) = 0, \\ y_x(0, t) = y_x(1, t) = 0, \quad z_x(0, t) = z_x(1, t) = 0. \end{aligned} \quad (2.9)$$

We Take the ratio of the beam and side electrode gaps as  $r_1 = (g_1/g_0)$ , and other terms appearing in Eqn (2.7),(2.8) are written as below,

$$\begin{aligned} \alpha_1 = \frac{6E_x g_0^2}{EB^2}, \quad \alpha_2 = \frac{6E_x d^2}{EB^2}, \quad \alpha_3 = \frac{6\epsilon_0 L^4}{EB^3 g_0^3}, \\ \alpha_4 = \frac{I_z}{I_y}, \quad \alpha_5 = \frac{6\epsilon_0 L^4}{EH^3 d^3}, \quad \alpha_6 = \frac{k_2 L^4}{EI_y}, \quad N = \frac{N_0 L^2}{EI_z}, \end{aligned} \quad (2.10)$$

and the function  $\Gamma$  is defined as,

$$\Gamma(m(x, t), n(x, t)) = \int_0^1 \frac{\partial m}{\partial x} \frac{\partial n}{\partial x} dx. \quad (2.11)$$

We assume the displacements in both the orthogonal directions consisting of two parts; static part which depends on position  $x$  from the fixed support and the dynamic component which depends on position as well as time.

$$y(x, t) = u_s(x) + u(x, t), \quad z(x, t) = w_s(x) + w(x, t). \quad (2.12)$$

where  $u_s(x)$  and  $w_s(x)$  are static deflections. The static deflections are obtained by substituting Eqn.(2.12) into Eqn.(2.7) and (2.8) and subsequently setting the time derivatives and dynamic terms equal to zero and solving the resulting equations. Now, the static equations are written as,

$$u_{sxxxx} - [N + \alpha_1 \Gamma(u_s, u_s) + \alpha_2 \Gamma(w_s, w_s)] u_{sxx} = \alpha_3 \times \left[ \frac{(V_{10})^2}{(1 - u_s)^2} - \frac{(V_{21})^2}{r_1^2 (1 + \frac{u_s}{r_1})^2} \right] \quad (2.13)$$

$$w_{sxxxx} - \alpha_4 [N + \alpha_1 \Gamma(u_s, u_s) + \alpha_2 \Gamma(w_s, w_s)] w_{sxx} = \alpha_5 \times \frac{(V_{1g})^2}{(1 - w_s)^2} - \alpha_6 \left[ (V_{10}^2 + V_{21}^2) w_s \right] \quad (2.14)$$

subjected to the following static boundary conditions,

$$u_s(0) = u_s(1) = w_s(0) = w_s(1) = 0 \quad (2.15)$$

For the governing dynamic equations, we again substitute Eqn.(2.12) into Eqn.(2.7) and (2.8). Using the static equations Eqn.(2.13) and (2.14) and then expanding the forcing terms about the

equilibrium using Taylor series method, the dynamic equations are obtained as follows,

$$\begin{aligned}
& u_{xxxx} + u_{tt} - [\alpha_1\Gamma(u, u) + 2\alpha_1\Gamma(u_s, u) + \alpha_2\Gamma(w, w) + 2\alpha_2\Gamma(w_s, w)]u_{sxx} \\
& - [N + \alpha_1\Gamma(u_s, u_s) + \alpha_1\Gamma(u, u) + 2\alpha_1\Gamma(u_s, u) + \alpha_2\Gamma(w, w) + \alpha_2\Gamma(w_s, w_s) \\
& + 2\alpha_2\Gamma(w_s, w)]u_{xx} = 2\alpha_3 \left[ (V_{10} + v(t))^2 \times \frac{u}{(1 - u_s)^3} + (V_{21} + v(t))^2 \times \frac{u}{r_1^3(1 + \frac{u_s}{r_1})^3} \right] \\
& + \alpha_3 \left[ (2V_{10}v(t) + v(t)^2) \times \frac{1}{(1 - u_s)^2} - (2V_{21}v(t) + v(t)^2) \times \frac{1}{r_1^2(1 + \frac{u_s}{r_1})^2} \right] \quad (2.16)
\end{aligned}$$

$$\begin{aligned}
& w_{xxxx} + \alpha_4 w_{tt} - \alpha_4 [\alpha_1\Gamma(u, u) + 2\alpha_1\Gamma(u_s, u) + \alpha_2\Gamma(w, w) + 2\alpha_2\Gamma(w_s, w)]w_{sxx} \\
& - \alpha_4 [N + \alpha_1\Gamma(u_s, u_s) + \alpha_1\Gamma(u, u) + 2\alpha_1\Gamma(u_s, u) + \alpha_2\Gamma(w, w) + \alpha_2\Gamma(w_s, w_s) \\
& + 2\alpha_2\Gamma(w_s, w)]w_{xx} = 2\alpha_5 \frac{V_{1g}^2}{(1 - w_s)^3} w + \alpha_5 \frac{2V_{1g}v(t) + v(t)^2}{(1 - w_s)^2} \left( 1 + \frac{2w}{(1 - w_s)} \right) \\
& - \alpha_6 \left[ (V_{10} + v(t))^2 + (V_{21} + v(t))^2 \right] w - 2\alpha_6 \left[ V_{10}v(t) + V_{21}v(t) + v(t)^2 \right] w_s \quad (2.17)
\end{aligned}$$

To perform frequency analysis, we find the linear equations from Eqn.(2.16) and (2.17) by neglecting nonlinear and forcing terms. Finally, the linear dynamic equations in terms of  $u_s, u, w_s$  and  $w$  are obtained as,

$$\begin{aligned}
& u_{xxxx} + u_{tt} - [2\alpha_1\Gamma(u_s, u) + 2\alpha_2\Gamma(w_s, w)]u_{sxx} - [N + \alpha_1\Gamma(u_s, u_s) + \alpha_2\Gamma(w_s, w_s)]u_{xx} \\
& = 2\alpha_3 \left[ V_{10}^2 \times \frac{u}{(1 - u_s)^3} + V_{21}^2 \times \frac{u}{r_1^3(1 + \frac{u_s}{r_1})^3} \right] \quad (2.18)
\end{aligned}$$

$$\begin{aligned}
& w_{xxxx} + \alpha_4 w_{tt} - \alpha_4 [2\alpha_1\Gamma(u_s, u) + 2\alpha_2\Gamma(w_s, w)]w_{sxx} - \alpha_4 [N + \alpha_1\Gamma(u_s, u_s) \\
& + \alpha_2\Gamma(w_s, w_s)]w_{xx} = 2\alpha_5 \frac{V_{1g}^2}{(1 - w_s)^3} w - \alpha_6 \left[ (V_{10}^2 + V_{21}^2)w \right] \quad (2.19)
\end{aligned}$$

subjected to the following boundary conditions,

$$\begin{aligned}
& u(0, t) = u(1, t) = w(0, t) = w(1, t) = 0 \\
& u_x(0, t) = u_x(1, t) = w_x(0, t) = w_x(1, t) = 0 \quad (2.20)
\end{aligned}$$

In the next section, we have considered these two linear dynamic equations for performing frequency analysis. The variations of frequencies in both the directions are obtained from the reduced order model of the single beam system using Rayleigh-Ritz-Galerkin (RRG) procedure.

## 2.2 Frequency analysis based on linear equations

In order to find the modal equations and the corresponding natural frequencies of the system subjected to DC biasing, we reduce the linear equations Eqn.(2.17) and (2.18) using Rayleigh-Ritz-Galerkin procedure which is based on modal superposition concept and using the orthogonality

conditions, we obtain the final reduced form.

Considering only one mode in the analysis, the static and dynamic deflections of the beam along both the planes are assumed as,

$$\begin{aligned} u_s(x) &= A_1(y, z)\phi(x) \quad , \quad w_s(x) = A_2(y, z)\phi(x), \\ u(x, t) &= P_1(t)\phi(x) \quad , \quad w(x, t) = P_2(t)\phi(x). \end{aligned} \quad (2.21)$$

Here,  $\phi(x)$  is the first normalized linear undamped mode shape for the fixed-fixed beam and  $P_1(t), P_2(t)$  are the non-dimensional modal coordinates.  $A_1, A_2$  are the static deflections of the beam in two orthogonal directions due to DC biasing. We assume the mode shape  $\phi(x)$  which satisfies the orthogonality condition given as  $\int_0^1 (\phi_1(x))^2 dx = 1$  and the mode shape also satisfies the geometric boundary conditions.

$$\phi(x) = \sqrt{\frac{2}{3}} \left( 1 - \cos(2\pi x) \right) \quad (2.22)$$

Using Eqn.(2.21), (2.22) in Eqn.(2.13) and (2.14), the static equations in terms of  $A_1, A_2$  are written as:

$$\begin{aligned} \frac{16}{9}\pi^4\alpha_1 A_1^3 + \left( \frac{16}{3}\pi^4 + \frac{16}{9}\pi^4\alpha_2 A_2^2 + \frac{4}{3}\pi^2 N \right) A_1 - \alpha_3 \left[ V_{10}^2 \sqrt{\frac{2/3}{(1 - 2\sqrt{\frac{2}{3}}A_1)^3}} \right. \\ \left. - \frac{V_{21}^2}{r_1^2} \sqrt{\frac{2/3}{(1 + 2\sqrt{\frac{2}{3}}\frac{A_1}{r_1})^3}} \right] = 0 \end{aligned} \quad (2.23)$$

$$\begin{aligned} \frac{16}{9}\pi^4\alpha_2 A_2^3 + \left( \frac{16}{3}\frac{\pi^4}{\alpha_4} + \frac{16}{9}\pi^4\alpha_1 A_1^2 + \frac{4}{3}\pi^2 N \right) A_2 - \frac{\alpha_5}{\alpha_4} V_{1g}^2 \sqrt{\frac{2/3}{(1 - 2\sqrt{\frac{2}{3}}A_2)^3}} \\ + \frac{\alpha_6}{\alpha_4} (V_{21}^2 + V_{10}^2) A_2 = 0 \end{aligned} \quad (2.24)$$

These above two equations show the coupling of static deflections  $A_1$  and  $A_2$  through the elongation of the beam in two directions by quantities  $\alpha_1$  and  $\alpha_2$ . They are also functions of induced tension  $N$  and vary with respect to applied DC. Solving these equations simultaneously, we get static deflections of the beam corresponding to a fixed applied voltage. As the applied DC voltage increases, the magnitude of static deflection in both the directions increases. At a particular value of DC voltage, the electrostatic attraction exceeds elastic restoring force which results in collapse of the structure. This particular value of DC is known as pull-in voltage. Here the slope of amplitude- $V_{DC}$  curve becomes infinity. The pull-in voltages can be found by differentiating Eqn.(2.23) and (2.24) with respect to  $A_1, A_2$ .

The modal equations are similarly obtained by substituting Eqn.(2.21), (2.22) in Eqn.(2.18) and (2.19). In matrix form, the modal equations are given by,

$$\begin{bmatrix} \ddot{P}_1 \\ \ddot{P}_2 \end{bmatrix} + \begin{bmatrix} \lambda_1^2 & c_{12} \\ c_{21} & \lambda_2^2 \end{bmatrix} \begin{bmatrix} P_1 \\ P_2 \end{bmatrix} = 0,$$

where,  $c_{12}$  and  $c_{21}$  are the coupling terms in two modal directions and  $\lambda_1, \lambda_2$  are the uncoupled natural frequencies of the beam in both the directions given by,

$$\lambda_1^2 = \left[ \frac{16}{3}\pi^4 + \frac{16}{9}\pi^4\alpha_2A_2^2 + \frac{16}{3}\pi^4\alpha_1A_1^2 + \frac{4}{3}\pi^2N - 2\alpha_3 \left( V_{10}^2(1 - 2\sqrt{\frac{2}{3}}A_1)^{-\frac{5}{2}} + \frac{V_{21}^2}{r_1^3}(1 + 2\sqrt{\frac{2}{3}}\frac{A_1}{r_1})^{-\frac{5}{2}} \right) \right]$$

$$\lambda_2^2 = \left[ \frac{16}{3}\frac{\pi^4}{\alpha_4} + \frac{16}{9}\pi^4\alpha_1A_1^2 + \frac{16}{3}\pi^4\alpha_2A_2^2 + \frac{4}{3}\pi^2N - 2\frac{\alpha_5}{\alpha_4}V_{1g}^2(1 - 2\sqrt{\frac{2}{3}}A_2)^{-\frac{5}{2}} + \frac{\alpha_6}{\alpha_4}(V_{10}^2 + V_{21}^2) \right]$$

$$c_{12} = \frac{32}{9}\alpha_2A_1A_2\pi^4, \quad c_{21} = \frac{32}{9}\alpha_1A_1A_2\pi^4 \quad (2.25)$$

Hence, the modal equations are written as,

$$P_{1tt}(t) + \lambda_1^2P_1(t) + c_{12}P_2(t) = 0 \quad (2.26)$$

$$P_{2tt}(t) + \lambda_2^2P_2(t) + c_{21}P_1(t) = 0 \quad (2.27)$$

To obtain the perturbed natural frequencies, we assume the solution of Eqn.(2.26), (2.27) considering the system oscillating in one of its normal modes frequency  $\omega$  and starts from the rest.

$$P_1(t) = \beta e^{i\omega t}, \quad P_2(t) = \gamma e^{i\omega t} \quad (2.28)$$

Substituting these assumed solutions in the modal equations, we get

$$(\lambda_1^2 - \omega^2)\beta + c_{12}\gamma = 0 \quad (2.29)$$

$$(\lambda_2^2 - \omega^2)\gamma + c_{21}\beta = 0 \quad (2.30)$$

For non-trivial solution, the determinant of these system of equations should be zero. After solving the resulting equations, we get two values of  $\omega$  corresponding to two directions.

$$\omega_{1,2} = \sqrt{\frac{1}{2} \left[ (\lambda_1^2 + \lambda_2^2) \pm \sqrt{(\lambda_1^2 - \lambda_2^2)^2 + 4c_{12}c_{21}} \right]} \quad (2.31)$$

The corresponding eigen-vectors (mode shapes) for  $\omega_1$  and  $\omega_2$  are given as,

$$\begin{pmatrix} \beta \\ \gamma \end{pmatrix}_{1,2} = -\frac{2c_{12}}{(\lambda_1^2 - \lambda_2^2) \mp \sqrt{(\lambda_1^2 - \lambda_2^2)^2 + 4c_{12}c_{21}}} \quad (2.32)$$

## 2.3 Nonlinear response of dynamic equation

After analyzing the modal frequencies based on linear dynamic equations, we consider the nonlinear and forcing terms to obtain the nonlinear response of the dynamic system consisting of single beam. In this section, we consider linear damping in both the directions and obtain the non-dimensional equations as discussed earlier. Subsequently, we reduce the non-dimensional equations using single mode RRG procedure to get static as well as reduced nonlinear modal equations. First, we solve the nonlinear modal equations directly using numerical techniques such as Runge-kutta method and after that we apply perturbation technique to get the dynamic response of the beam.

### 2.3.1 Numerical solution (based on rk5 or ode45)

After including linear damping terms  $c_1$  and  $c_3$  in both the directions, the non-dimensional governing equations for the beam using Eqn.(2.6) are written as,

$$y_{xxxx} + y_{tt} + C_1 y_t - [N + \alpha_1 \Gamma(y, y) + \alpha_2 \Gamma(z, z)] y_{xx} = \alpha_3 \left[ \frac{(V_{10} + v(t))^2}{(1-y)^2} - \frac{(V_{21} + v(t))^2}{r_1^2 (1 + \frac{y}{r_1})^2} \right] \quad (2.33)$$

$$z_{xxxx} + \alpha_4 z_{tt} + C_3 z_t - \alpha_4 [N + \alpha_1 \Gamma(y, y) + \alpha_2 \Gamma(z, z)] z_{xx} = \alpha_5 \frac{(V_{1g} + v(t))^2}{(1-z)^2} - \alpha_6 [(V_{10} + v(t))^2 + (V_{21} + v(t))^2] z \quad (2.34)$$

subjected to the following modified boundary conditions,

$$\begin{aligned} y(0, t) = y(1, t) = 0, \quad z(0, t) = z(1, t) = 0, \\ y_x(0, t) = y_x(1, t) = 0, \quad z_x(0, t) = z_x(1, t) = 0. \end{aligned} \quad (2.35)$$

Here,  $C_1 = \frac{c_1 L^4}{EI_z T}$  and  $C_3 = \frac{c_3 L^4}{\alpha_4 EI_y T}$  are the non-dimensional parameters including damping coefficients. All other terms are defined as earlier and given in Eqn.(2.10) and (2.11). Applying Rayleigh-Ritz-Galerkin procedure with single mode shape, the reduced order static equations are obtained as shown in Eqn.(2.23) and (2.24). Proceeding as discussed in the previous section and using Eqn.(2.21) and (2.22) we obtain the nonlinear modal equations in both the directions from Eqn.(2.33) and (2.34), which are given as

$$\begin{aligned} P_{1tt}(t) + \lambda_1^2 P_1(t) + \frac{16}{9} \alpha_1 \pi^4 P_1(t)^3 + \frac{16}{3} \alpha_1 A_1 \pi^4 P_1(t)^2 + \left[ \frac{16}{9} \alpha_2 \pi^4 P_2(t)^2 + \frac{32}{9} \alpha_2 A_2 \pi^4 P_2(t) \right. \\ \left. - 2\alpha_3 \frac{(2V_{10}v(t) + v(t)^2)}{(1 - 2\sqrt{\frac{2}{3}} A_1)^{\frac{5}{2}}} - 2\alpha_3 \frac{(2V_{21}v(t) + v(t)^2)}{r_1^3 (1 + 2\sqrt{\frac{2}{3}} \frac{A_1}{r_1})^{\frac{5}{2}}} \right] P_1(t) + C_1 P_{1t}(t) + \frac{16}{9} \alpha_2 A_1 \pi^4 P_2(t)^2 \\ + \frac{32}{9} \alpha_2 A_1 A_2 \pi^4 P_2(t) = \sqrt{\frac{2}{3}} \alpha_3 \frac{(2V_{10}v(t) + v(t)^2)}{(1 - 2\sqrt{\frac{2}{3}} A_1)^{\frac{3}{2}}} + \sqrt{\frac{2}{3}} \alpha_3 \frac{(2V_{21}v(t) + v(t)^2)}{r_1^2 (1 + 2\sqrt{\frac{2}{3}} \frac{A_1}{r_1})^{\frac{3}{2}}} \end{aligned} \quad (2.36)$$



$$\begin{aligned}
& P_{2tt}(t) + \lambda_2^2 P_2(t) + \frac{16}{9} \alpha_2 \pi^4 P_2(t)^3 + \frac{16}{3} \alpha_2 A_2 \pi^4 P_2(t)^2 + \left[ \frac{16}{9} \alpha_1 \pi^4 P_1(t)^2 + \frac{32}{9} \alpha_1 A_1 \pi^4 P_1(t) \right. \\
& - 2 \frac{\alpha_5 (2V_{1g}v(t) + v(t)^2)}{\alpha_4 (1 - 2\sqrt{\frac{2}{3}}A_2)^{\frac{5}{2}}} + \left. \frac{\alpha_6 (2V_{10}v(t) + 2V_{21}v(t) + 2v(t)^2)}{\alpha_4} \right] P_2(t) + C_3 P_{2t}(t) + \frac{16}{9} \alpha_1 A_2 \pi^4 P_1(t)^2 \\
& + \frac{32}{9} \alpha_1 A_1 A_2 \pi^4 P_1(t) = \sqrt{\frac{2}{3}} \frac{\alpha_5 (2V_{1g}v(t) + v(t)^2)}{\alpha_4 (1 - 2\sqrt{\frac{2}{3}}A_2)^{\frac{3}{2}}} - \frac{\alpha_6}{\alpha_4} [2(V_{10} + V_{21} + v(t))v(t)] A_2
\end{aligned} \tag{2.37}$$

Where  $\lambda_1$  and  $\lambda_2$  are the unperturbed natural frequencies of the system and are given as:

$$\begin{aligned}
\lambda_1 &= \sqrt{\frac{16}{3} \pi^4 + \frac{4}{3} N \pi^2 + \frac{16}{3} \alpha_1 A_1^2 \pi^4 + \frac{16}{9} \alpha_2 A_2^2 \pi^4 - 2\alpha_3 \left( \frac{V_{10}^2}{(1 - 2\sqrt{\frac{2}{3}}A_1)^{\frac{5}{2}}} + \frac{V_{21}^2}{r_1^3 (1 + 2\sqrt{\frac{2}{3}}\frac{A_1}{r_1})^{\frac{5}{2}}} \right)} \\
\lambda_2 &= \sqrt{\frac{16}{3} \frac{\pi^4}{\alpha_4} + \frac{4}{3} N \pi^2 + \frac{16}{3} \alpha_2 A_2^2 \pi^4 + \frac{16}{9} \alpha_1 A_1^2 \pi^4 - 2 \frac{\alpha_5}{\alpha_4} \frac{V_{1g}^2}{(1 - 2\sqrt{\frac{2}{3}}A_2)^{\frac{5}{2}}} + \frac{\alpha_6}{\alpha_4} (V_{10}^2 + V_{21}^2)}
\end{aligned} \tag{2.38}$$

These two equations are coupled through several terms and govern the dynamic behavior of the beam subjected to different AC excitation along with DC biasing. Now, for convenience we define new terms and rewrite Eqn.(2.37) and (2.38) as below,

$$\begin{aligned}
P_{1tt}(t) + \lambda_1^2 P_1(t) + t_1 P_1(t)^3 + t_2 P_1(t)^2 + \left[ t_3 P_2(t)^2 + t_4 P_2(t) - t_5 (2V_{10}v(t) + v(t)^2) \right. \\
\left. - t_6 (2V_{21}v(t) + v(t)^2) \right] P_1(t) + C_1 P_{1t}(t) + t_7 P_2(t)^2 + t_8 P_2(t) \\
= t_9 (2V_{10}v(t) + v(t)^2) - t_{10} (2V_{21}v(t) + v(t)^2)
\end{aligned} \tag{2.39}$$

$$\begin{aligned}
P_{2tt}(t) + \lambda_2^2 P_2(t) + s_1 P_2(t)^3 + s_2 P_2(t)^2 + \left[ s_3 P_2(t)^2 + s_4 P_2(t) - s_5 (2V_{1g}v(t) + v(t)^2) \right. \\
\left. + s_6 (2V_{10}v(t) + 2V_{21}v(t) + 2v(t)^2) \right] P_2(t) + C_3 P_{2t}(t) + s_7 P_1(t)^2 + s_8 P_1(t) \\
= s_9 (2V_{1g}v(t) + v(t)^2) - s_{10} (2(V_{10} + V_{21} + v(t))v(t))
\end{aligned} \tag{2.40}$$

Where, different coefficients  $t_i$ 's and  $s_i$ 's are defined in the appendix. Equations (2.39) and (2.40) are second order nonlinear and coupled equations in  $P_1(t)$  and  $P_2(t)$ . To find the modal displacements, we solve them numerically using Runge-kutta method. For this, we convert these above two second order nonlinear equations into four first order equations as follows,

$$P_{1t}(t) = P_3(t) \tag{2.41}$$

$$\begin{aligned}
P_{3t}(t) = & -\lambda_1^2 P_1(t) - t_1 P_1(t)^3 - t_2 P_1(t)^2 - \left[ t_3 P_2(t)^2 + t_4 P_2(t) - t_5 (2V_{10}v(t) + v(t)^2) \right. \\
& \left. - t_6 (2V_{21}v(t) + v(t)^2) \right] P_1(t) - C_1 P_3(t) - t_7 P_2(t)^2 - t_8 P_2(t) \\
& + t_9 (2V_{10}v(t) + v(t)^2) - t_{10} (2V_{21}v(t) + v(t)^2) \quad (2.42)
\end{aligned}$$

$$P_{2t}(t) = P_4(t) \quad (2.43)$$

$$\begin{aligned}
P_{4t}(t) = & -\lambda_2^2 P_2(t) - s_1 P_2(t)^3 - s_2 P_2(t)^2 - \left[ s_3 P_2(t)^2 + s_4 P_2(t) - s_5 (2V_{1g}v(t) + v(t)^2) \right. \\
& \left. + s_6 (2V_{10}v(t) + 2V_{21}v(t) + 2v(t)^2) \right] P_2(t) - C_3 P_4(t) - s_7 P_1(t)^2 - s_8 P_1(t) \\
& + s_9 (2V_{1g}v(t) + v(t)^2) - s_{10} (2(V_{10} + V_{21} + v(t))v(t)) \quad (2.44)
\end{aligned}$$

We solve above four first order equations in MATLAB to obtain the dynamic response of the beam by finding the modal co-ordinates  $P_1(t)$  and  $P_2(t)$ .

### 2.3.2 Solution based on Method of Multiple Scales

Solving the nonlinear modal equations directly in MATLAB by converting the system of equations into first order forms has the limitation of separating the stable and unstable regions. It gives only the stable part of the solution. In this section, we use perturbation technique for the nonlinear modal equations and solve them to obtain the dynamic response of the beam and subsequently do the stability analysis.

we apply the method of multiple scales (MMS) to equations (2.39) and (2.40) to obtain a first-order uniform expansion for the solution of the system. For this the modal displacements are assumed to be functions of two time scales; the fast time scale  $T_0 = t$  which characterizes motions occurring at different frequencies and the slow time scale  $T_1 = \epsilon t$  and  $T_2 = \epsilon^2 t$  which characterize the time variations of the amplitudes and phases of the modes of oscillation. Here  $\epsilon$  is a dimensionless small positive number used as booking keeping parameter. We assume the displacements as the summation of terms with coefficients of different powers of  $\epsilon$ .

$$\begin{aligned}
P_1(t) = x_1 = & \epsilon x_{11}(T_0, T_1, T_2) + \epsilon^2 x_{12}(T_0, T_1, T_2) + \epsilon^3 x_{13}(T_0, T_1, T_2) + O(\epsilon^4) \\
P_2(t) = x_2 = & \epsilon x_{21}(T_0, T_1, T_2) + \epsilon^2 x_{22}(T_0, T_1, T_2) + \epsilon^3 x_{23}(T_0, T_1, T_2) + O(\epsilon^4) \quad (2.45)
\end{aligned}$$

The derivative terms with respect to  $t$  are now defined in terms of new time scales as

$$\frac{d}{dt} = \frac{\partial}{\partial T_0} \frac{dT_0}{dt} + \frac{\partial}{\partial T_1} \frac{dT_1}{dt} + \frac{\partial}{\partial T_2} \frac{dT_2}{dt} = (D_0 + \epsilon D_1 + \epsilon^2 D_2)$$

$$\frac{d^2}{dt^2} = \left( \frac{d}{dt} \right)^2 = (D_0 + \epsilon D_1 + \epsilon^2 D_2)^2 = (D_0^2 + 2\epsilon D_0 D_1 + \epsilon^2 D_1^2 + 2\epsilon^2 D_0 D_2) + H.O.T \quad (2.46)$$

Terms like damping and forcing are re-scaled by multiplying with different powers of  $\epsilon$  so that they will be balanced as the same order terms in the equation.

$$C_1 = \epsilon C_1 \quad , \quad C_3 = \epsilon C_3 \quad , \quad v(t) = \epsilon^2 V_{ac} \cos(\omega_{ac} t) \quad (2.47)$$

By multiplying different terms with different powers of  $\epsilon$  we scale them as strong, weak or more weak terms. Hence they are treated separately while solving the system of equations.

Substituting equations (2.45)-(2.47) in equations (2.39) and (2.40), subsequently separating different powers of  $\epsilon$  upto third order, we get the following three sets of equations.

$$\begin{aligned} O(\epsilon^1) \rightarrow D_0^2 x_{11} + \lambda_1^2 x_{11} + t_8 x_{21} &= 0 \\ D_0^2 x_{21} + \lambda_2^2 x_{21} + s_8 x_{11} &= 0 \end{aligned} \quad (2.48)$$

$$\begin{aligned} O(\epsilon^2) \rightarrow D_0^2 x_{12} + \lambda_1^2 x_{12} + t_8 x_{22} &= -2D_0 D_1 x_{11} - C_1 D_0 x_{11} - t_2 x_{11}^2 - t_4 x_{11} x_{21} \\ &\quad - t_7 x_{21}^2 + t_9 \eta_{11} \cos(\omega_{ac} t) - t_{10} \eta_{12} \cos(\omega_{ac} t) \\ D_0^2 x_{22} + \lambda_2^2 x_{22} + s_8 x_{12} &= -2D_0 D_1 x_{21} - C_3 D_0 x_{21} - s_2 x_{21}^2 - s_4 x_{11} x_{21} \\ &\quad - s_7 x_{11}^2 + s_9 \eta_{21} \cos(\omega_{ac} t) - s_{10} (\eta_{11} + \eta_{12}) \cos(\omega_{ac} t) \end{aligned} \quad (2.49)$$

$$\begin{aligned} O(\epsilon^3) \rightarrow D_0^2 x_{13} + \lambda_1^2 x_{13} + t_8 x_{23} &= -C_1 (D_0 x_{12} + D_1 x_{11}) - (2D_0 D_1 x_{12} + D_1^2 x_{11} + 2D_0 D_2 x_{11}) \\ &\quad - t_1 x_{11}^3 - 2t_2 x_{11} x_{12} - t_3 x_{11} x_{21}^2 - t_4 (x_{11} x_{22} + x_{12} x_{21}) \\ &\quad + t_5 \eta_{11} \cos(\omega_{ac} t) x_{11} - t_6 \eta_{12} \cos(\omega_{ac} t) x_{11} - 2t_7 x_{21} x_{22} \\ D_0^2 x_{23} + \lambda_2^2 x_{23} + s_8 x_{13} &= -C_3 (D_0 x_{22} + D_1 x_{21}) - (2D_0 D_1 x_{22} + D_1^2 x_{21} + 2D_0 D_2 x_{21}) \\ &\quad - s_1 x_{21}^3 - 2s_2 x_{21} x_{22} - s_3 x_{21} x_{11}^2 - s_4 (x_{11} x_{22} + x_{12} x_{21}) \\ &\quad + s_5 \eta_{21} \cos(\omega_{ac} t) x_{21} - s_6 (\eta_{11} + \eta_{12}) \cos(\omega_{ac} t) x_{21} - 2s_7 x_{11} x_{12} \end{aligned} \quad (2.50)$$

These three sets of coupled homogeneous / non-homogeneous equations are solved separately and the final solutions for modal displacements are obtained using Eqn.(2.45). Now the two homogeneous second order coupled equations given by (2.48) are solved to find the values of  $x_{11}$  and  $x_{21}$ . We assume the solution of these two equations as

$$\begin{aligned} x_{11} &= A_1(T_1, T_2) e^{i\omega_1 T_0} + A_2(T_1, T_2) e^{i\omega_2 T_0} + \bar{A}_1(T_1, T_2) e^{-i\omega_1 T_0} + \bar{A}_2(T_1, T_2) e^{-i\omega_2 T_0} \\ x_{21} &= k_1 A_1(T_1, T_2) e^{i\omega_1 T_0} + k_2 A_2(T_1, T_2) e^{i\omega_2 T_0} + k_1 \bar{A}_1(T_1, T_2) e^{-i\omega_1 T_0} + k_2 \bar{A}_2(T_1, T_2) e^{-i\omega_2 T_0} \end{aligned} \quad (2.51)$$

where,  $\omega_1$  and  $\omega_2$  are the coupled natural frequencies of the system in two orthogonal directions obtained from linear analysis and are given in Eqn.(2.31).  $A_1(T_1, T_2)$  and  $A_2(T_1, T_2)$  represents the displacement as well as phase of oscillation and are expressed in polar form later. With this assumed solution for the first set of equations, we solve for Eqn.(2.49). Substituting back Eqn.(2.51) into (2.48) we get,

$$\begin{aligned} [(\lambda_1^2 - \omega_1^2) + t_8 k_1] A_1 e^{i\omega_1 T_0} + [(\lambda_1^2 - \omega_2^2) + t_8 k_2] A_2 e^{i\omega_2 T_0} &= 0 \\ [(\lambda_2^2 - \omega_1^2) k_1 + s_8] A_1 e^{i\omega_1 T_0} + [(\lambda_2^2 - \omega_2^2) k_2 + s_8] A_2 e^{i\omega_2 T_0} &= 0 \end{aligned} \quad (2.52)$$

In Eqn.(2.52) equating coefficients of different terms on both sides, we get

$$(\lambda_1^2 - \omega_1^2) + t_8 k_1 = 0; \quad (\lambda_1^2 - \omega_2^2) + t_8 k_2 = 0; \quad (2.53)$$

$$(\lambda_2^2 - \omega_1^2) k_1 + s_8 = 0; \quad (\lambda_2^2 - \omega_2^2) k_2 + s_8 = 0; \quad (2.54)$$

Solving Eqn.(2.53) and (2.54) for  $k_1, k_2$  we get,

$$k_n = \left( \frac{\omega_n^2 - \lambda_1^2}{t_8} \right) = \left( \frac{s_8}{\omega_n^2 - \lambda_2^2} \right) \quad (2.55)$$

for  $n=1,2$ . To obtain the solution for (2.49), we substitute (2.51) into it and eliminate the secular terms arising on the right hand side of the equations by considering the solvability conditions. Here to describe the nearness of  $\omega_2$  to  $\omega_1$  and  $\omega_{ac}$  to  $\omega_1$  quantitatively, we have taken two detuning parameters  $\sigma_1$  and  $\sigma_2$  defined by,

$$\omega_{ac} = \omega_1 + \epsilon\sigma_1; \quad \omega_2 = \omega_1 + \epsilon\sigma_2 \quad (2.56)$$

After substituting for  $x_{11}$  and  $x_{21}$  in eq(2.49), it can be written as,

$$\begin{aligned} D_0^2 x_{12} + \lambda_1^2 x_{12} + t_8 x_{22} &= -2i(\omega_1 D_1 A_1 e^{i\omega_1 T_0} + \omega_2 D_1 A_2 e^{i\omega_2 T_0}) - iC_1(A_1 \omega_1 e^{i\omega_1 T_0} + A_2 \omega_2 e^{i\omega_2 T_0}) \\ &\quad - t_2(A_1^2 e^{2i\omega_1 T_0} + A_1 \bar{A}_1 + A_2^2 e^{2i\omega_2 T_0} + A_2 \bar{A}_2 + 2A_1 \bar{A}_2 e^{i(\omega_1 - \omega_2) T_0} + 2A_1 A_2 e^{i(\omega_1 + \omega_2) T_0}) \\ &\quad - t_4(A_1^2 k_1 e^{2i\omega_1 T_0} + A_1 \bar{A}_1 k_1 + A_2^2 k_2 e^{2i\omega_2 T_0} + A_2 \bar{A}_2 k_2 + A_1 \bar{A}_2 (k_1 + k_2) e^{i(\omega_1 - \omega_2) T_0} \\ &\quad + A_1 A_2 (k_1 + k_2) e^{i(\omega_1 + \omega_2) T_0}) - t_7(k_1^2 A_1^2 e^{2i\omega_1 T_0} + k_1^2 A_1 \bar{A}_1 + k_2^2 A_2^2 e^{2i\omega_2 T_0} + k_2^2 A_2 \bar{A}_2 \\ &\quad + 2k_1 k_2 A_1 \bar{A}_2 e^{i(\omega_1 - \omega_2) T_0} + 2k_1 k_2 A_1 A_2 e^{i(\omega_1 + \omega_2) T_0}) + \frac{t_9}{2} \eta_{11} e^{i\omega_{ac} T_0} - \frac{t_{10}}{2} \eta_{12} e^{i\omega_{ac} T_0} + cc \end{aligned} \quad (2.57)$$

$$\begin{aligned} D_0^2 x_{22} + \lambda_2^2 x_{22} + s_8 x_{12} &= -2i(\omega_1 k_1 D_1 A_1 e^{i\omega_1 T_0} + k_2 \omega_2 D_1 A_2 e^{i\omega_2 T_0}) - iC_3(k_1 A_1 \omega_1 e^{i\omega_1 T_0} \\ &\quad + k_2 A_2 \omega_2 e^{i\omega_2 T_0}) - s_2(k_1^2 A_1^2 e^{2i\omega_1 T_0} + k_1^2 A_1 \bar{A}_1 + k_2^2 A_2^2 e^{2i\omega_2 T_0} + k_2^2 A_2 \bar{A}_2 + 2k_1 k_2 A_1 \bar{A}_2 e^{i(\omega_1 - \omega_2) T_0} \\ &\quad + 2k_1 k_2 A_1 A_2 e^{i(\omega_1 + \omega_2) T_0}) - s_4(A_1^2 k_1 e^{2i\omega_1 T_0} + A_1 \bar{A}_1 k_1 + A_2^2 k_2 e^{2i\omega_2 T_0} + A_2 \bar{A}_2 k_2 \\ &\quad + A_1 \bar{A}_2 (k_1 + k_2) e^{i(\omega_1 - \omega_2) T_0} + A_1 A_2 (k_1 + k_2) e^{i(\omega_1 + \omega_2) T_0}) - s_7(A_1^2 e^{2i\omega_1 T_0} + A_1 \bar{A}_1 + A_2^2 e^{2i\omega_2 T_0} \\ &\quad + A_2 \bar{A}_2 + 2A_1 \bar{A}_2 e^{i(\omega_1 - \omega_2) T_0} + 2A_1 A_2 e^{i(\omega_1 + \omega_2) T_0}) + \frac{s_9}{2} \eta_{21} e^{i\omega_{ac} T_0} - \frac{s_{10}}{2} (\eta_{11} + \eta_{12}) e^{i\omega_{ac} T_0} + cc \end{aligned} \quad (2.58)$$

We assume the homogeneous solution for  $O(\epsilon^2)$  as:

$$\begin{aligned}x_{12} &= P_{11}e^{i\omega_1 T_0} + P_{12}e^{i\omega_2 T_0} + cc, \\x_{22} &= P_{21}e^{i\omega_1 T_0} + P_{22}e^{i\omega_2 T_0} + cc\end{aligned}\quad (2.59)$$

Using eq(2.59); eq(2.57) and eq(2.58) can be written as,

$$(\lambda_1^2 - \omega_1^2)P_{11}e^{i\omega_1 T_0} + (\lambda_1^2 - \omega_2^2)P_{12}e^{i\omega_2 T_0} + t_8(P_{21}e^{i\omega_1 T_0} + P_{22}e^{i\omega_2 T_0}) = R_{11}e^{i\omega_1 T_0} + R_{12}e^{i\omega_2 T_0}\quad (2.60)$$

$$(\lambda_2^2 - \omega_1^2)P_{21}e^{i\omega_1 T_0} + (\lambda_2^2 - \omega_2^2)P_{22}e^{i\omega_2 T_0} + s_8(P_{11}e^{i\omega_1 T_0} + P_{12}e^{i\omega_2 T_0}) = R_{21}e^{i\omega_1 T_0} + R_{22}e^{i\omega_2 T_0}\quad (2.61)$$

In general form for  $n = 1, 2$  eq (2.60),(2.61) can be written in matrix form as below

$$\begin{bmatrix} (\lambda_1^2 - \omega_n^2) & t_8 \\ s_8 & (\lambda_2^2 - \omega_n^2) \end{bmatrix} \begin{bmatrix} P_{1n} \\ P_{2n} \end{bmatrix} = \begin{bmatrix} R_{1n} \\ R_{2n} \end{bmatrix}$$

where,  $R_{1n}$ ,  $R_{2n}$  are the coefficients of  $e^{i\omega_1 T_0}$  and  $e^{i\omega_2 T_0}$  respectively appearing in the equations (2.57) and (2.58) and are given below,

$$\begin{aligned}R_{11} &= -2i\omega_1 D_1 A_1 - 2i\omega_2 D_1 A_2 e^{i\sigma_2 T_1} - iC_1 A_1 \omega_1 - iC_1 A_2 \omega_2 e^{i\sigma_2 T_1} \\ &\quad + \left( \frac{t_9 \eta_{11} - t_{10} \eta_{12}}{2} \right) e^{i\sigma_1 T_1}\end{aligned}$$

$$\begin{aligned}R_{12} &= -2i\omega_1 D_1 A_1 e^{-i\sigma_2 T_1} - 2i\omega_2 D_1 A_2 - iC_1 A_1 \omega_1 e^{-i\sigma_2 T_1} - iC_1 A_2 \omega_2 \\ &\quad + \left( \frac{t_9 \eta_{11} - t_{10} \eta_{12}}{2} \right) e^{i(\sigma_1 - \sigma_2) T_1}\end{aligned}$$

$$\begin{aligned}R_{21} &= -2i\omega_1 k_1 D_1 A_1 - 2ik_2 \omega_2 D_1 A_2 e^{i\sigma_2 T_1} - iC_3 k_1 A_1 \omega_1 - iC_3 k_2 A_2 \omega_2 e^{i\sigma_2 T_1} \\ &\quad + \left( \frac{s_9 \eta_{21} - s_{10}(\eta_{11} + \eta_{12})}{2} \right) e^{i\sigma_1 T_1}\end{aligned}$$

$$\begin{aligned}R_{22} &= -2i\omega_1 k_1 D_1 A_1 e^{-i\sigma_2 T_1} - 2i\omega_2 k_2 D_1 A_2 - iC_3 k_1 A_1 \omega_1 e^{-i\sigma_2 T_1} - iC_3 k_2 A_2 \omega_2 \\ &\quad + \left( \frac{s_9 \eta_{21} - s_{10}(\eta_{11} + \eta_{12})}{2} \right) e^{i(\sigma_1 - \sigma_2) T_1}\end{aligned}\quad (2.62)$$

Solving for eq (2.60) and (2.61) simultaneously, using the homogeneous equation (2.52), we get the solvability conditions in terms of  $R_{1n}$  and  $R_{2n}$ .

$$R_{1n} = \frac{t_8}{(\lambda_2^2 - \omega_n^2)} R_{2n} = -\left( \frac{t_8}{s_8} \right) k_n R_{2n} = -\bar{k}_n R_{2n}\quad (2.63)$$



Corresponding to  $n=1$ , the solvability condition  $R_{11} + \bar{k}_1 R_{21} = 0$ , for  $\bar{k}_1 = (\frac{t_s}{s_s})k_1$  gives

$$\begin{aligned} & -2i\omega_1(1 + k_1\bar{k}_1)D_1A_1 - 2i\omega_2(1 + k_2\bar{k}_1)D_1A_2 e^{i\sigma_2 T_1} = i\omega_1 A_1(C_1 + C_3 k_1 \bar{k}_1) \\ & + i\omega_2 A_2(C_1 + C_3 k_2 \bar{k}_1) e^{i\sigma_2 T_1} - \left( \frac{t_9 \eta_{11} - t_{10} \eta_{12} + \bar{k}_1 s_9 \eta_{21} - \bar{k}_1 s_{10}(\eta_{11} + \eta_{12})}{2} \right) e^{i\sigma_1 T_1} \end{aligned} \quad (2.64)$$

For  $n=2$ , the solvability condition  $R_{12} + \bar{k}_2 R_{22} = 0$ , for  $\bar{k}_2 = (\frac{t_s}{s_s})k_2$  is written as,

$$\begin{aligned} & -2i\omega_1(1 + k_1\bar{k}_2)D_1A_1 e^{-i\sigma_2 T_1} - 2i\omega_2(1 + k_2\bar{k}_2)D_1A_2 = i\omega_2 A_2(C_1 + C_3 k_2 \bar{k}_1) \\ & + i\omega_1 A_1(C_1 + C_3 k_1 \bar{k}_2) e^{-i\sigma_2 T_1} - \left( \frac{t_9 \eta_{11} - t_{10} \eta_{12} + \bar{k}_2 s_9 \eta_{21} - \bar{k}_2 s_{10}(\eta_{11} + \eta_{12})}{2} \right) e^{i(\sigma_1 - \sigma_2) T_1} \end{aligned} \quad (2.65)$$

Solving Eqn.(2.64) and (2.65) simultaneously we find the expressions for  $D_1A_1$  and  $D_1A_2$ .

$$\begin{aligned} D_1A_1 &= \frac{(B_3G_2 - B_2G_4)A_1 + (B_4G_2 - B_2G_3)A_2 e^{i\sigma_2 T_1} - i(B_2G_5 - B_5G_2) e^{i\sigma_1 T_1}}{(B_2G_1 - B_1G_2)} \\ D_1A_2 &= \frac{(B_4G_1 - B_1G_3)A_2 + (B_3G_1 - B_1G_4)A_1 e^{-i\sigma_2 T_1} - i(B_1G_5 - B_5G_1) e^{i(\sigma_1 - \sigma_2) T_1}}{(B_1G_2 - B_2G_1)} \end{aligned} \quad (2.66)$$

Now we substitute for  $D_1A_1$  and  $D_1A_2$  back from Eqn.(2.66) into the second order modified equations Eqn.(2.57) and (2.58) and the complete solution for second order equations (2.49) is written as,

$$\begin{aligned} x_{12} &= A_3(T_1, T_2) e^{i\omega_1 T_0} + A_4(T_1, T_2) e^{i\omega_2 T_0} + c_{11} A_1^2 e^{2i\omega_1 T_0} + c_{12} A_1 \bar{A}_1 + c_{13} A_2^2 e^{2i\omega_2 T_0} \\ & + c_{14} A_2 \bar{A}_2 + c_{15} A_1 \bar{A}_2 e^{i(\omega_1 - \omega_2) T_0} + c_{16} A_1 A_2 e^{i(\omega_1 + \omega_2) T_0} + cc \\ x_{22} &= k_1 A_3(T_1, T_2) e^{i\omega_1 T_0} + k_2 A_4(T_1, T_2) e^{i\omega_2 T_0} + c_{21} A_1^2 e^{2i\omega_1 T_0} + c_{22} A_1 \bar{A}_1 + c_{23} A_2^2 e^{2i\omega_2 T_0} \\ & + c_{24} A_2 \bar{A}_2 + c_{25} A_1 \bar{A}_2 e^{i(\omega_1 - \omega_2) T_0} + c_{26} A_1 A_2 e^{i(\omega_1 + \omega_2) T_0} + cc \end{aligned} \quad (2.67)$$

The coefficients  $c_{ij}$  are determined by comparing similar terms on both sides of Eqn. (2.57),(2.58) after substituting Eqn.(2.67) into them (given in the appendix). Substituting Eqn.(2.51) and (2.67) into Eqn.(2.50), subsequently separating secular terms and following Eqn.(2.63), we get the following two solvability conditions.

$$\begin{aligned} & -2i\omega_1 B_{11}(D_1A_3 + D_2A_1) - B_{11}D_1^2A_1 - B_{13}D_1A_1 - [2i\omega_2 B_{12}(D_1A_4 + D_2A_2) + B_{12}D_1^2A_2 \\ & + B_{14}D_1A_2] e^{i\sigma_2 T_1} = i\omega_1 B_{13}A_3 + i\omega_2 B_{14}A_4 e^{i\sigma_2 T_1} + \bar{g}_1 \bar{A}_2 A_1^2 e^{-i\sigma_2 T_1} + \bar{g}_2 \bar{A}_2 A_2^2 e^{i\sigma_2 T_1} \\ & + \bar{g}_3 A_1 A_2 \bar{A}_1 e^{i\sigma_2 T_1} + \bar{g}_4 A_2^2 \bar{A}_1 e^{2i\sigma_2 T_1} + \bar{g}_5 A_1^2 \bar{A}_1 + \bar{g}_6 A_1 \bar{A}_2 A_2 \end{aligned} \quad (2.68)$$

$$\begin{aligned} & -2i\omega_2 G_{12}(D_1A_4 + D_2A_2) - G_{12}D_1^2A_2 - G_{13}D_1A_2 - [2i\omega_1 G_{11}(D_1A_3 + D_2A_1) + G_{11}D_1^2A_1 \\ & + G_{14}D_1A_1] e^{-i\sigma_2 T_1} = i\omega_2 G_{13}A_4 + i\omega_1 G_{14}A_3 e^{-i\sigma_2 T_1} + \bar{f}_1 \bar{A}_1 A_2^2 e^{i\sigma_2 T_1} + \bar{f}_2 \bar{A}_1 A_1^2 e^{-i\sigma_2 T_1} \\ & + \bar{f}_3 A_1 A_2 \bar{A}_2 e^{-i\sigma_2 T_1} + \bar{f}_4 A_1^2 \bar{A}_2 e^{-2i\sigma_2 T_1} + \bar{f}_5 A_2^2 \bar{A}_2 + \bar{f}_6 A_1 \bar{A}_1 A_2 \end{aligned} \quad (2.69)$$

We define  $\bar{g}_n = g_{1n} + \bar{k}_1 g_{2n}$  and  $\bar{f}_n = f_{1n} + \bar{k}_2 f_{2n}$ , where  $f_{1n}$  and  $g_{1n}$  are given in the appendix. Following Nayfeh[36] we choose  $A_3, A_4$  so as to eliminate  $D_1^2 A_1$  and  $D_1^2 A_2$  from Eqn.(2.68) and (2.69). That leads to,

$$D_1[2i\omega_1 A_3 + D_1 A_1] = 0 \quad \Rightarrow [2i\omega_1 A_3 + D_1 A_1] = h_{11}(T_2),$$

$$D_1[2i\omega_2 A_4 + D_1 A_2] = 0 \quad \Rightarrow [2i\omega_2 A_4 + D_1 A_2] = h_{12}(T_2); \quad (2.70)$$

But from Eqn.(2.66), it is quiet clear that  $D_1 A_1$  and  $D_1 A_2$  are implicit functions of slow time scale  $T_2$ . Hence we make  $h_{11}(T_2) = h_{12}(T_2) = 0$ . Now from Eqn.(2.66) and (2.70), expressions for  $A_3, A_4$  can be written as,

$$A_3 = i \left[ \frac{(B_3 G_2 - B_2 G_4) A_1 + (B_4 G_2 - B_2 G_3) A_2 e^{i\sigma_2 T_1} - i(B_2 G_5 - B_5 G_2) e^{i\sigma_1 T_1}}{2\omega_1 (B_2 G_1 - B_1 G_2)} \right]$$

$$A_4 = i \left[ \frac{(B_4 G_1 - B_1 G_3) A_2 + (B_3 G_1 - B_1 G_4) A_1 e^{-i\sigma_2 T_1} - i(B_1 G_5 - B_5 G_1) e^{i(\sigma_1 - \sigma_2) T_1}}{2\omega_2 (B_1 G_2 - B_2 G_1)} \right] \quad (2.71)$$

Using Eqn.(2.70) in Eqn.(2.68) and (2.69), we can find the values for  $D_2 A_1$  and  $D_2 A_2$  by simultaneously solving these following equations,

$$-2i\omega_1 B_{11} D_2 A_1 - 2i\omega_2 B_{12} D_2 A_2 e^{i\sigma_2 T_1} = B_{13} D_1 A_1 + B_{14} D_1 A_2 e^{i\sigma_2 T_1} + i\omega_1 B_{13} A_3$$

$$+ i\omega_2 B_{14} A_4 e^{i\sigma_2 T_1} + \bar{g}_1 \bar{A}_2 A_1^2 e^{-i\sigma_2 T_1} + \bar{g}_2 \bar{A}_2 A_2^2 e^{i\sigma_2 T_1} + \bar{g}_3 A_1 A_2 \bar{A}_1 e^{i\sigma_2 T_1}$$

$$+ \bar{g}_4 A_2^2 \bar{A}_1 e^{2i\sigma_2 T_1} + \bar{g}_5 A_1^2 \bar{A}_1 + \bar{g}_6 A_1 \bar{A}_2 A_2; \quad (2.72)$$

$$-2i\omega_1 G_{11} D_2 A_1 e^{-i\sigma_2 T_1} - 2i\omega_2 G_{12} D_2 A_2 = G_{13} D_1 A_2 + G_{14} D_1 A_1 e^{-i\sigma_2 T_1} + i\omega_2 G_{13} A_4$$

$$+ i\omega_1 G_{14} A_3 e^{-i\sigma_2 T_1} + \bar{f}_1 \bar{A}_1 A_2^2 e^{i\sigma_2 T_1} + \bar{f}_2 \bar{A}_1 A_1^2 e^{-i\sigma_2 T_1} + \bar{f}_3 A_1 A_2 \bar{A}_2 e^{-i\sigma_2 T_1}$$

$$+ \bar{f}_4 A_1^2 \bar{A}_2 e^{-2i\sigma_2 T_1} + \bar{f}_5 A_2^2 \bar{A}_2 + \bar{f}_6 A_1 \bar{A}_1 A_2; \quad (2.73)$$

After solving, we get the expressions for  $D_2 A_1$  and  $D_2 A_2$  as,

$$D_2 A_1 = \frac{i}{2\omega_1 (B_{11} G_{12} - B_{12} G_{11})} \left[ (B_{14} G_{12} - B_{12} G_{13}) D_1 A_2 e^{i\sigma_2 T_1} + (B_{13} G_{12} - B_{12} G_{14}) D_1 A_1 \right.$$

$$\left. + i\omega_1 (B_{13} G_{12} - B_{12} G_{14}) A_3 + i\omega_2 (B_{14} G_{12} - B_{12} G_{13}) A_4 e^{i\sigma_2 T_1} + G_{12} \bar{G} - B_{12} \bar{F} e^{i\sigma_2 T_1} \right]$$

$$D_2 A_2 = \frac{i}{2\omega_2 (B_{12} G_{11} - B_{11} G_{12})} \left[ (B_{14} G_{11} - B_{11} G_{13}) D_1 A_2 + (B_{13} G_{11} - B_{11} G_{14}) D_1 A_1 e^{-i\sigma_2 T_1} \right.$$

$$\left. + i\omega_2 (B_{14} G_{11} - B_{11} G_{13}) A_4 + i\omega_1 (B_{13} G_{11} - B_{11} G_{14}) A_3 e^{-i\sigma_2 T_1} + G_{11} \bar{G} e^{-i\sigma_2 T_1} - B_{11} \bar{F} \right] \quad (2.74)$$

To get the final solution, we apply method of reconstitution[36] using the equations,

$$\begin{aligned}\frac{dA_1}{dt} &= \epsilon D_1 A_1 + \epsilon^2 D_2 A_1 + \dots \\ \frac{dA_2}{dt} &= \epsilon D_1 A_2 + \epsilon^2 D_2 A_2 + \dots\end{aligned}\quad (2.75)$$

Putting the values for differential terms from Eqn.(2.74) into Eqn.(2.75) and using eq (2.71), subsequently setting  $\epsilon = 1$ , so that  $T_0 = T_1 = T_2 = t$ , we get the reconstituted modulation equations.

$$\begin{aligned}\dot{A}_1 &= \left[ 1 + i \frac{(B_{13}G_{12} - G_{14}B_{12})}{4\omega_1(B_{11}G_{12} - G_{11}B_{12})} \right] D_1 A_1 + i \left[ \frac{(B_{14}G_{12} - G_{13}B_{12})}{4\omega_1(B_{11}G_{12} - G_{11}B_{12})} \right] D_1 A_2 e^{i\sigma_2 t} \\ &\quad + i \left[ \frac{(G_{12}\bar{G} - B_{12}\bar{F}e^{i\sigma_2 t})}{2\omega_1(B_{11}G_{12} - G_{11}B_{12})} \right]\end{aligned}\quad (2.76)$$

$$\begin{aligned}\dot{A}_2 &= i \left[ \frac{(B_{13}G_{11} - G_{14}B_{11})}{4\omega_2(B_{12}G_{11} - G_{12}B_{11})} \right] D_1 A_1 e^{-i\sigma_2 t} + \left[ 1 + i \frac{(B_{14}G_{11} - G_{13}B_{11})}{4\omega_2(B_{12}G_{11} - G_{12}B_{11})} \right] D_1 A_2 \\ &\quad + i \left[ \frac{(G_{11}\bar{G}e^{-i\sigma_2 t} - B_{11}\bar{F})}{2\omega_2(B_{12}G_{11} - G_{12}B_{11})} \right]\end{aligned}\quad (2.77)$$

To express the modulation equations in polar form, we transform  $A_1, A_2$  by assuming,

$$A_n = \frac{1}{2} a_n e^{i\beta_n}, \quad n = 1, 2. \quad (2.78)$$

Here  $a_n$  and  $\beta_n$  are real functions of time  $t$ , hence,

$$\begin{aligned}A_1 = \frac{1}{2} a_1 e^{i\beta_1} &\Rightarrow \dot{A}_1 = \frac{1}{2} (a_1 \dot{e}^{i\beta_1} + i a_1 \dot{\beta}_1 e^{i\beta_1}) \\ A_2 = \frac{1}{2} a_2 e^{i\beta_2} &\Rightarrow \dot{A}_2 = \frac{1}{2} (a_2 \dot{e}^{i\beta_2} + i a_2 \dot{\beta}_2 e^{i\beta_2})\end{aligned}\quad (2.79)$$

Inserting Eqn.(2.79) into Eqn.(2.76) and (2.77) and using Eqn.(2.66) we get,

$$\begin{aligned}\frac{1}{2} (a_1 \dot{e}^{i\beta_1} + i a_1 \dot{\beta}_1 e^{i\beta_1}) &= \left( 1 + i \frac{B_{13}G_{12} - G_{14}B_{12}}{4\omega_1(B_{11}G_{12} - G_{11}B_{12})} \right) \left[ \frac{1}{2} \left( \frac{B_3G_2 - B_2G_4}{B_2G_1 - B_1G_2} \right) a_1 e^{i\beta_1} \right. \\ &\quad \left. + \frac{1}{2} \left( \frac{B_4G_2 - B_2G_3}{B_2G_1 - B_1G_2} \right) a_2 e^{i(\sigma_2 t + \beta_2)} - i \left( \frac{B_2G_5 - B_5G_2}{B_2G_1 - B_1G_2} \right) e^{i\sigma_1 t} \right] \\ &\quad + i \left( \frac{B_{14}G_{12} - B_{12}G_{13}}{4\omega_1(B_{11}G_{12} - G_{11}B_{12})} \right) e^{i\sigma_2 t} \left[ \frac{1}{2} \left( \frac{B_4G_1 - B_1G_3}{B_1G_2 - B_2G_1} \right) a_2 e^{i\beta_2} \right. \\ &\quad \left. + \frac{1}{2} \left( \frac{B_3G_1 - B_1G_4}{B_1G_2 - B_2G_1} \right) a_1 e^{i(\beta_1 - \sigma_2 t)} - i \left( \frac{B_1G_5 - B_5G_1}{B_1G_2 - B_2G_1} \right) e^{i(\sigma_1 - \sigma_2)t} \right] \\ &\quad + i \frac{G_{12}}{16\omega_1(B_{11}G_{12} - B_{12}G_{11})} \left[ \bar{g}_1 a_1^2 a_2 e^{i(2\beta_1 - \beta_2 - \sigma_2 t)} + \bar{g}_2 a_2^3 e^{i(\beta_2 + \sigma_2 t)} + \bar{g}_3 a_1^2 a_2 e^{i(\beta_2 + \sigma_2 t)} \right. \\ &\quad \left. + \bar{g}_4 a_1 a_2^2 e^{i(2\beta_2 - \beta_1 + 2\sigma_2 t)} + \bar{g}_5 a_1^3 e^{i\beta_1} + \bar{g}_6 a_1 a_2^2 e^{i\beta_1} \right] - i \frac{B_{12}e^{i\sigma_2 t}}{16\omega_1(B_{11}G_{12} - B_{12}G_{11})} \left[ \bar{f}_1 a_1 a_2^2 e^{i(\sigma_2 t - \beta_1 + 2\beta_2)} \right. \\ &\quad \left. + \bar{f}_2 a_1^3 e^{i(\beta_1 - \sigma_2 t)} + \bar{f}_3 a_1 a_2^2 e^{i(\beta_1 - \sigma_2 t)} + \bar{f}_4 a_1^2 a_2 e^{i(2\beta_1 - \beta_2 - 2\sigma_2 t)} + \bar{f}_5 a_2^3 e^{i\beta_2} + \bar{f}_6 a_1^2 a_2 e^{i\beta_2} \right]\end{aligned}\quad (2.80)$$

$$\begin{aligned}
\frac{1}{2}(\dot{a}_2 e^{i\beta_2} + i a_2 \dot{\beta}_2 e^{i\beta_2}) &= \left(1 + i \frac{B_{14}G_{11} - G_{13}B_{11}}{4\omega_2(B_{12}G_{11} - G_{12}B_{11})}\right) \left[\frac{1}{2} \left(\frac{B_4G_1 - B_1G_4}{B_1G_2 - B_2G_1}\right) a_2 e^{i\beta_2}\right. \\
&\quad \left. + \frac{1}{2} \left(\frac{B_3G_1 - B_1G_4}{B_1G_2 - B_2G_1}\right) a_1 e^{i(\beta_1 - \sigma_2 t)} - i \left(\frac{B_1G_5 - B_5G_1}{B_1G_2 - B_2G_1}\right) e^{i(\sigma_1 - \sigma_2)t}\right] \\
&\quad + i \left(\frac{B_{13}G_{11} - B_{11}G_{14}}{4\omega_2(B_{12}G_{11} - B_{11}G_{12})}\right) e^{-i\sigma_2 t} \left[\frac{1}{2} \left(\frac{B_3G_2 - B_2G_4}{B_2G_1 - B_1G_2}\right) a_1 e^{i\beta_1}\right. \\
&\quad \left. + \frac{1}{2} \left(\frac{B_4G_2 - B_2G_3}{B_2G_1 - B_1G_2}\right) a_2 e^{i(\sigma_2 t + \beta_2)} - i \left(\frac{B_2G_5 - B_5G_2}{B_2G_1 - B_1G_2}\right) e^{i\sigma_1 t}\right] \\
&\quad + i \frac{G_{11} e^{-i\sigma_2 t}}{16\omega_2(B_{12}G_{11} - B_{11}G_{12})} \left[\bar{g}_1 a_1^2 a_2 e^{i(2\beta_1 - \beta_2 - \sigma_2 t)} + \bar{g}_2 a_2^3 e^{i(\beta_2 + \sigma_2 t)} + \bar{g}_3 a_1^2 a_2 e^{i(\beta_2 + \sigma_2 t)}\right. \\
&\quad \left. + \bar{g}_4 a_1 a_2^2 e^{i(2\beta_2 - \beta_1 + 2\sigma_2 t)} + \bar{g}_5 a_1^3 e^{i\beta_1} + \bar{g}_6 a_1 a_2^2 e^{i\beta_1}\right] - i \frac{B_{11}}{16\omega_2(B_{12}G_{11} - B_{11}G_{12})} \left[\bar{f}_1 a_1 a_2^2 e^{i(\sigma_2 t - \beta_1 + 2\beta_2)}\right. \\
&\quad \left. + \bar{f}_2 a_1^3 e^{i(\beta_1 - \sigma_2 t)} + \bar{f}_3 a_1 a_2^2 e^{i(\beta_1 - \sigma_2 t)} + \bar{f}_4 a_1^2 a_2 e^{i(2\beta_1 - \beta_2 - 2\sigma_2 t)} + \bar{f}_5 a_2^3 e^{i\beta_2} + \bar{f}_6 a_1^2 a_2 e^{i\beta_2}\right]
\end{aligned} \tag{2.81}$$

Finally, we convert these above non-autonomous equations into autonomous forms by defining another two new variables,

$$\begin{aligned}
\theta_1 &= (\sigma_1 t - \beta_1), \quad \theta_2 = (\sigma_1 - \sigma_2)t - \beta_2 \\
\Rightarrow \dot{\theta}_1 &= (\sigma_1 - \dot{\beta}_1), \quad \dot{\theta}_2 = (\sigma_1 - \sigma_2) - \dot{\beta}_2
\end{aligned} \tag{2.82}$$

Using Eqn.(2.82), we separate the real and imaginary parts from Eqn.(2.80) and (2.81) to get four first order ordinary differential equations, known as enveloping or modulation equations.

$$\begin{aligned}
a_1 &= h_1 a_1 + h_2 a_2 \cos(\theta_1 - \theta_2) + 2h_3 \sin \theta_1 - \left[\frac{B_{13}G_{12} - B_{12}G_{14}}{4\omega_1(B_{11}G_{12} - B_{12}G_{11})}\right] \left(h_2 a_2 \sin(\theta_1 - \theta_2)\right. \\
&\quad \left. - 2h_3 \cos \theta_1\right) - \left[\frac{B_{14}G_{12} - B_{12}G_{13}}{4\omega_1(B_{11}G_{12} - B_{12}G_{11})}\right] \left(h_4 a_2 \sin(\theta_1 - \theta_2) - 2h_6 \cos \theta_1\right) \\
&\quad + \left[\frac{2G_{12}}{16\omega_1(B_{11}G_{12} - B_{12}G_{11})}\right] \left(\bar{g}_1 a_1^2 a_2 \sin(\theta_1 - \theta_2) - \bar{g}_2 a_2^3 \sin(\theta_1 - \theta_2) - \bar{g}_3 a_1^2 a_2 \sin(\theta_1 - \theta_2)\right. \\
&\quad \left. - \bar{g}_4 a_1 a_2^2 \sin 2(\theta_1 - \theta_2)\right) + \left[\frac{2B_{12}}{16\omega_1(B_{11}G_{12} - B_{12}G_{11})}\right] \left(\bar{f}_1 a_1 a_2^2 \sin 2(\theta_1 - \theta_2)\right. \\
&\quad \left. - \bar{f}_4 a_1^2 a_2 \sin(\theta_1 - \theta_2) + \bar{f}_5 a_2^3 \sin(\theta_1 - \theta_2) + \bar{f}_6 a_1^2 a_2 \sin(\theta_1 - \theta_2)\right) \tag{2.83}
\end{aligned}$$

$$\begin{aligned}
a_1 \dot{\theta}_1 = & \sigma_1 a_1 - h_2 a_2 \sin(\theta_1 - \theta_2) + 2h_3 \cos \theta_1 - \left[ \frac{B_{13}G_{12} - B_{12}G_{14}}{4\omega_1(B_{11}G_{12} - B_{12}G_{11})} \right] \left( h_2 a_2 \cos(\theta_1 - \theta_2) \right. \\
& \left. + h_1 a_1 - 2h_3 \sin \theta_1 \right) - \left[ \frac{B_{14}G_{12} - B_{12}G_{13}}{4\omega_1(B_{11}G_{12} - B_{12}G_{11})} \right] \left( h_4 a_2 \cos(\theta_1 - \theta_2) + h_5 a_1 + 2h_6 \sin \theta_1 \right) \\
& - \left[ \frac{2G_{12}}{16\omega_1(B_{11}G_{12} - B_{12}G_{11})} \right] \left( \bar{g}_1 a_1^2 a_2 \cos(\theta_1 - \theta_2) + \bar{g}_2 a_2^3 \cos(\theta_1 - \theta_2) + \bar{g}_3 a_1^2 a_2 \cos(\theta_1 - \theta_2) \right. \\
& \left. + \bar{g}_4 a_1 a_2^2 \cos 2(\theta_1 - \theta_2) + \bar{g}_5 a_1^3 + \bar{g}_6 a_1 a_2^2 \right) + \left[ \frac{2B_{12}}{16\omega_1(B_{11}G_{12} - B_{12}G_{11})} \right] \left( \bar{f}_1 a_1 a_2^2 \cos 2(\theta_1 - \theta_2) \right. \\
& \left. + \bar{f}_2 a_1^3 + \bar{f}_3 a_1 a_2^2 + \bar{f}_4 a_1^2 a_2 \cos(\theta_1 - \theta_2) + \bar{f}_5 a_2^3 \cos(\theta_1 - \theta_2) + \bar{f}_6 a_1^2 a_2 \cos(\theta_1 - \theta_2) \right) \quad (2.84)
\end{aligned}$$

$$\begin{aligned}
\dot{a}_2 = & h_4 a_2 + h_5 a_1 \cos(\theta_1 - \theta_2) + 2h_6 \sin \theta_2 + \left[ \frac{B_{14}G_{11} - B_{11}G_{13}}{4\omega_2(B_{12}G_{11} - B_{11}G_{12})} \right] \left( h_5 a_1 \sin(\theta_1 - \theta_2) \right. \\
& \left. + 2h_6 \cos \theta_2 \right) + \left[ \frac{B_{13}G_{11} - B_{11}G_{14}}{4\omega_2(B_{12}G_{11} - B_{11}G_{12})} \right] \left( h_1 a_1 \sin(\theta_1 - \theta_2) + 2h_3 \cos \theta_2 \right) \\
& + \left[ \frac{2G_{11}}{16\omega_2(B_{12}G_{11} - B_{11}G_{12})} \right] \left( \bar{g}_1 a_1^2 a_2 \sin 2(\theta_1 - \theta_2) - \bar{g}_4 a_1 a_2^2 \sin(\theta_1 - \theta_2) + \bar{g}_5 a_1^3 \sin(\theta_1 - \theta_2) \right. \\
& \left. + \bar{g}_6 a_1 a_2^2 \sin(\theta_1 - \theta_2) \right) + \left[ \frac{2B_{11}}{16\omega_2(B_{12}G_{11} - B_{11}G_{12})} \right] \left( \bar{f}_1 a_1 a_2^2 \sin(\theta_1 - \theta_2) \right. \\
& \left. - \bar{f}_2 a_1^3 \sin(\theta_1 - \theta_2) - \bar{f}_3 a_1 a_2^2 \sin(\theta_1 - \theta_2) - \bar{f}_4 a_1^2 a_2 \sin 2(\theta_1 - \theta_2) \right) \quad (2.85)
\end{aligned}$$

$$\begin{aligned}
a_2 \dot{\theta}_2 = & (\sigma_1 - \sigma_2) a_2 + h_5 a_1 \sin(\theta_1 - \theta_2) + 2h_6 \cos \theta_2 - \left[ \frac{B_{14}G_{11} - B_{11}G_{13}}{4\omega_2(B_{12}G_{11} - B_{11}G_{12})} \right] \left( h_5 a_1 \cos(\theta_1 - \theta_2) \right. \\
& \left. + h_4 a_2 + 2h_6 \sin \theta_2 \right) - \left[ \frac{B_{13}G_{11} - B_{11}G_{14}}{4\omega_2(B_{12}G_{11} - B_{11}G_{12})} \right] \left( h_1 a_1 \cos(\theta_1 - \theta_2) + h_2 a_2 + 2h_3 \sin \theta_2 \right) \\
& - \left[ \frac{2G_{11}}{16\omega_2(B_{12}G_{11} - B_{11}G_{12})} \right] \left( \bar{g}_1 a_1^2 a_2 \cos 2(\theta_1 - \theta_2) + \bar{g}_2 a_2^3 + \bar{g}_3 a_1^2 a_2 + \bar{g}_4 a_1 a_2^2 \cos(\theta_1 - \theta_2) \right. \\
& \left. + \bar{g}_5 a_1^3 \cos(\theta_1 - \theta_2) + \bar{g}_6 a_1 a_2^2 \cos(\theta_1 - \theta_2) \right) + \left[ \frac{2B_{11}}{16\omega_2(B_{12}G_{11} - B_{11}G_{12})} \right] \left( \bar{f}_1 a_1 a_2^2 \cos(\theta_1 - \theta_2) \right. \\
& \left. + \bar{f}_2 a_1^3 \cos(\theta_1 - \theta_2) + \bar{f}_3 a_1 a_2^2 \cos(\theta_1 - \theta_2) + \bar{f}_4 a_1^2 a_2 \cos 2(\theta_1 - \theta_2) + \bar{f}_5 a_2^3 + \bar{f}_6 a_1^2 a_2 \right) \quad (2.86)
\end{aligned}$$

To determine the periodic response of the beam, we solve Eqn.(2.83)-(2.86) for equilibrium solution by setting time derivatives equals to zero. As the control parameter  $\sigma_1$  is varied, we find the roots of these equation  $a_1, \theta_1, a_2$  and  $\theta_2$  using Newton-Raphson numerical technique. Now, the response of the beam upto second order for  $\epsilon = 1$  is expressed as,

$$\begin{aligned}
P_1(t) = x_1(t) = x_{11} + x_{12} = & \left( 1 + i \frac{\Lambda_{11}}{2} \right) a_1 \cos(\omega_1 t + \beta_1) + \left( 1 + i \frac{\Lambda_{12}}{2} \right) a_2 \cos(\omega_2 t + \beta_2) \\
& + \Lambda_{13} \cos[(\omega_1 + \sigma_1)t] + \frac{1}{2} c_{11} a_1^2 \cos 2(\omega_1 t + \beta_1) + \frac{1}{2} c_{12} a_1^2 + \frac{1}{2} c_{13} a_2^2 \cos 2(\omega_2 t + \beta_2) \\
& + \frac{1}{2} c_{14} a_2^2 + \frac{1}{2} c_{15} a_1 a_2 \cos 2[(\omega_1 - \omega_2)t + \beta_1 - \beta_2] + \frac{1}{2} c_{16} a_1 a_2 \cos 2[(\omega_1 + \omega_2)t + \beta_1 + \beta_2] \quad (2.87)
\end{aligned}$$

$$\begin{aligned}
P_2(t) = x_2(t) = x_{21} + x_{22} &= k_1 \left( 1 + i \frac{\Lambda_{11}}{2} \right) a_1 \cos(\omega_1 t + \beta_1) + k_2 \left( 1 + i \frac{\Lambda_{12}}{2} \right) a_2 \cos(\omega_2 t + \beta_2) \\
&+ \Lambda_{14} \cos[(\omega_1 + \sigma_1)t] + \frac{1}{2} c_{21} a_1^2 \cos 2(\omega_1 t + \beta_1) + \frac{1}{2} c_{22} a_1^2 + \frac{1}{2} c_{23} a_2^2 \cos 2(\omega_2 t + \beta_2) \\
&+ \frac{1}{2} c_{24} a_2^2 + \frac{1}{2} c_{25} a_1 a_2 \cos 2[(\omega_1 - \omega_2)t + \beta_1 - \beta_2] + \frac{1}{2} c_{26} a_1 a_2 \cos 2[(\omega_1 + \omega_2)t + \beta_1 + \beta_2]
\end{aligned} \tag{2.88}$$

Where, different terms  $\Lambda_{11}, \Lambda_{12}, \Lambda_{13}$  and  $\Lambda_{14}$  are defined as follows,

$$\begin{aligned}
\Lambda_{11} &= \left[ \frac{(B_2 G_4 - B_3 G_2)}{\omega_1 (B_1 G_2 - B_2 G_1)} + \frac{(B_1 G_4 - B_3 G_1)}{\omega_2 (B_1 G_2 - B_2 G_1)} \right], \\
\Lambda_{12} &= \left[ \frac{(B_2 G_3 - B_4 G_2)}{\omega_1 (B_1 G_2 - B_2 G_1)} + \frac{(B_4 G_1 - B_1 G_3)}{\omega_2 (B_1 G_2 - B_2 G_1)} \right], \\
\Lambda_{13} &= \left[ \frac{(B_5 G_2 - B_2 G_5)}{\omega_1 (B_1 G_2 - B_2 G_1)} + \frac{(B_1 G_5 - B_5 G_1)}{\omega_2 (B_1 G_2 - B_2 G_1)} \right], \\
\Lambda_{14} &= \left[ k_1 \frac{(B_5 G_2 - B_2 G_5)}{\omega_1 (B_1 G_2 - B_2 G_1)} + k_2 \frac{(B_1 G_5 - B_5 G_1)}{\omega_2 (B_1 G_2 - B_2 G_1)} \right].
\end{aligned} \tag{2.89}$$

### 2.3.3 Stability Analysis

In this section, we discuss about the criteria based on the modulation equations, for which the solution will be stable. The stability of each equilibrium solution is determined using Routh-Hurwitz criterion by calculating the eigenvalues of the Jacobian matrix of the modulation equations evaluated at the equilibrium point.

Solutions where all eigenvalues have negative real parts are stable, otherwise unstable. If  $J$  be the Jacobian matrix of the modulation equations evaluated at equilibrium point, according to this criteria,

$$[J] - \lambda[I] = 0$$

$$\Rightarrow \lambda^4 + R_1 \lambda^3 + R_2 \lambda^2 + R_3 \lambda + R_4 = 0 \tag{2.90}$$

Where,  $R_i$ 's represent the coefficients of different powers of  $\lambda$  in Eqn.(2.90). Then the necessary and sufficient conditions [15] to be satisfied for stability of fixed points so that none of the roots of Eqn.(2.90) has a positive real part are,

$$R_1 R_2 - R_3 > 0 \tag{2.91}$$

$$R_3(R_1 R_2 - R_3) - R_1^2 R_4 > 0 \tag{2.92}$$

$$R_4 > 0 \tag{2.93}$$

The jacobian matrix of the modulation equations used to determine the coefficients  $R_i$  is given in the appendix.

## 2.4 Results and discussion

This section represents the outcomes of the analytical model for the system of single beam excited through one bottom electrode and two side electrodes. First, we present the results of linear frequency analysis after neglecting the nonlinear and forcing terms. The analytical results are compared with the experimental outcomes and are validated. Subsequently, we consider the nonlinear modal equations and explain the results from numerical analysis using MATLAB and the concept of modal coupling is explained.

Before proceeding to the results and analysis, the geometric parameters as well as material properties of the Au-Pd beam under consideration are mentioned in the following Table 2.1 and Table 2.2 respectively.

Table 2.1: Geom. Parameters

Parameters	Value( $\mu m$ )
L	500
B	4
H	0.2
g	4.5
$g_1$	5.6
d	50

Table 2.2: Matl. Properties

Properties	Value
E	2.696E+10 N/m <sup>2</sup>
$\rho$	3500 kg/m <sup>3</sup>
$N_0$	3.7E-5 N
$\alpha_{corr.}$	0.00674
$\epsilon_0$	8.85E-12 F/m
$c_1$	3E-6 N.s/m
$c_3$	1E-6 N.s/m

Considering the above parameters, we do numerical analysis and compare the results with experiments.

### 2.4.1 Linear frequency analysis

To describe the importance of frequency tuning, we analyze a single clamped-clamped beam made up of Au-Pd alloy on silicon substrate. The experiment is performed at low temperature of 77 k. Corresponding to the electrical excitation the dynamic response is measured using laser interferometry based technique.

Figure.(2.4) shows the variation of two modes under different parametric conditions of a single clamped-clamped beam. Figure. (2.4)(a)-(d) show the influence of gap ratio,  $r_1$  when  $d_0 = 50\mu m$

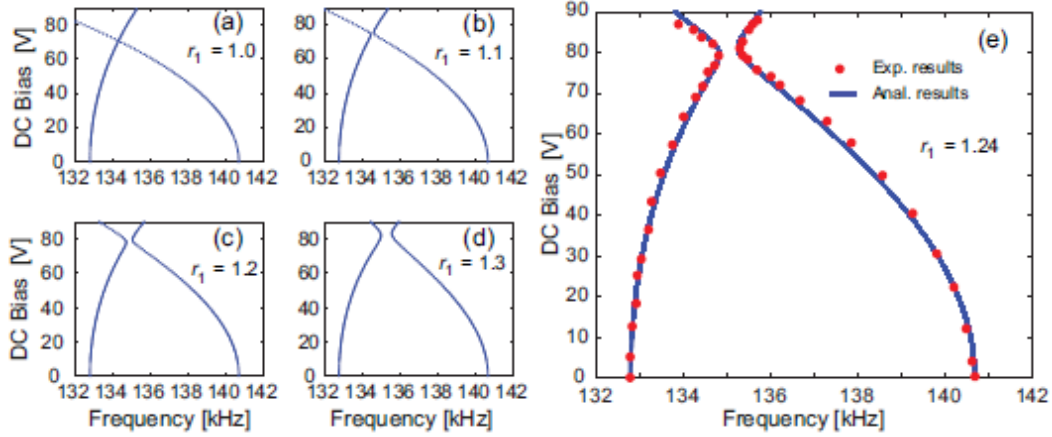


Figure 2.4: (a)-(d) Variation of coupling strength with different gap ratio  $r_1$ ; (e) Comparison of experimental and analytical results for a single beam with geometric parameters  $L = 500 \mu\text{m}$ ,  $H = 4\mu\text{m}$ ,  $B = 200 \text{ nm}$  and  $r_1 = 1.24$ .

and  $g_0 = 4.5\mu\text{m}$ . It is found that the strength of modal coupling of the two modes is negligible when  $r_1 = 1$ , however, its strength increases as  $r_1$  increases to 1.3. Similarly, as  $r_1$  increases, the DC bias at which the coupling occurs also increases. But if one gap is made sufficiently large than the other, then only one side electrode influences the beam similar to Kozinsky experiment([12]). Hence we can control this region by suitably varying side electrode gaps. The Figure.(2.4)(e) presents the experimental evidence of such kind of coupling along with the analytical results for  $r_1 = 1.24$ , when the beam and bottom electrode are supplied with voltage  $V$  and the two side electrodes are grounded. From the Figure.(2.4)(e), it is clear that the coupling between two modes occur at nearly 76 V for  $r_1 = 1.24$ .

## 2.4.2 Numerical solution (based on rk5 or ode45)

To obtain the numerical solutions of nonlinear modal equations, we solve Eqn.(2.41)-(2.44) using Runge-kutta method in MATLAB. First we perform dynamic analysis of the system away from the coupling region at 50 V. The results obtained show no influence of one mode on the other as expected earlier. Then as the DC bias is increased further, fixing the AC excitation amplitude, both the modes come close to each other and start influencing which becomes maximum near the coupling voltage 76 V as shown in Figure.(2.4).

Now, we fix the DC voltage near the coupling region (76 V) and vary the AC amplitude. At low AC excitation, the amplitude-frequency curve of the beam shows only linear region. But as the magnitude of AC increases beyond critical value, nonlinearity in the response arises. Only the stable regions of the solutions are plotted and the unstable or multivalued regions are shown by jumps. By conducting forward and backward sweeps of forcing frequency we can predict the region of instability.



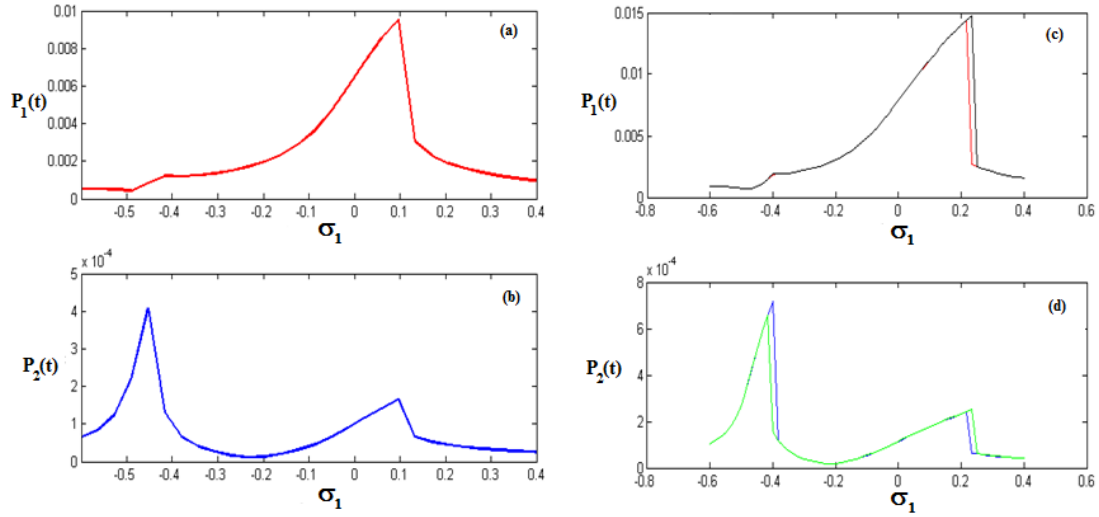


Figure 2.5: (a),(b) Linear frequency response of single beam near coupling region.  $V_{DC} = 76V$ ,  $V_{AC} = 0.05 V$ .  $P_1, P_2$  represent the in-plane and out of plane modal displacements. (c),(d) Nonlinear frequency response of single beam near coupling region showing jumps.  $V_{DC} = 76V$ ,  $V_{AC} = 0.08$ . Forward frequency sweep (red and blue), Reverse frequency sweep (black and green).

### 2.4.3 Solution based on Method of Multiple Scales

To qualitatively analyze the nonlinear responses of the beam, we apply method of multiple scales to obtain the enveloping equations Eqn.(2.83)-(2.86). For steady state response, the time derivatives of different terms on the left hand side of these equations are equated to zero. Consequently we solve four algebraic equations using Newton-Raphson technique in MATLAB. Finally using Eqn.(2.87) and (2.88) the modal displacements in both the directions are calculated. Using Routh-Herwitz criteria, the stable and unstable regions of solution can be separated.

Figure.(2.6) shows the numerical results using Newton-Raphson technique from modulation equations. Here the stable solutions are shown where the unstable region remains un-plotted. We use both forward and reverse sweeps for two different AC voltages to get the points where instability starts. In Figure.(2.7), we have shown the complete nonlinear response using MATCONT for 0.06 V AC. The responses are calculated near the coupling region.

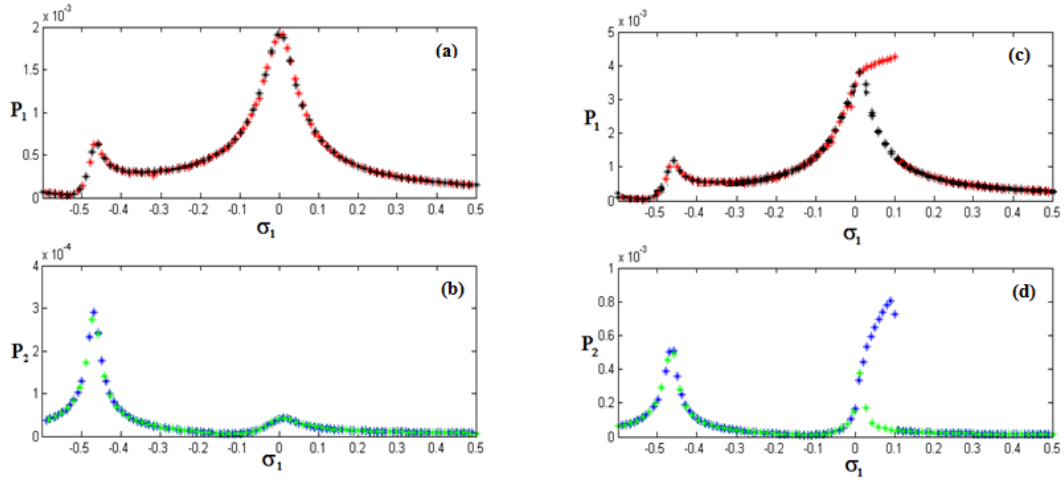


Figure 2.6:  $P_1, P_2$  represent the in-plane and out of plane modal displacements for single beam. (a),(b) Linear frequency response of single beam using method of multiple scales for  $V_{DC} = 76V$ ,  $V_{AC} = 0.03 V$  and (c),(d) presents nonlinear frequency response near coupling region using MMS showing stable and unstable regions at  $V_{DC} = 76V$ ,  $V_{AC} = 0.06 V$ . Forward frequency sweep (red and blue), Reverse frequency sweep (black and green).

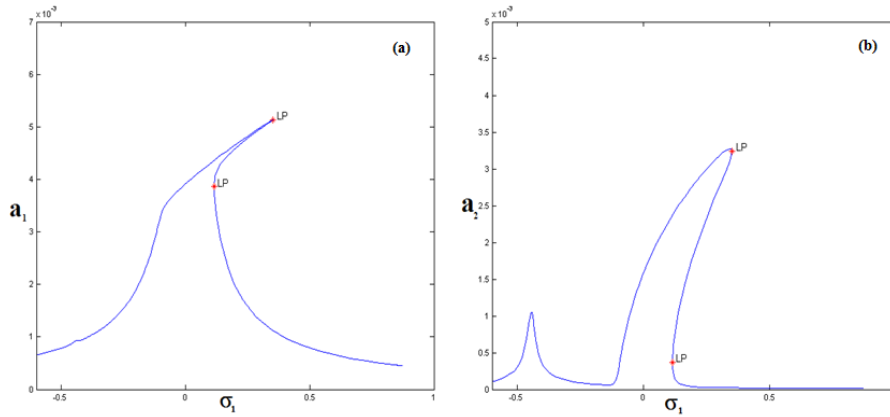


Figure 2.7: Complete amplitude-frequency response obtained by method of multiple scales using MATCONT for  $V_{DC} = 76V$ ,  $V_{AC} = 0.06 V$ . LP shows the limit points. Fig.(2.7)(a) corresponds to the in-plane and (b) corresponds to the out-of-plane movement.

## Chapter 3

# Mathematical modeling and solution of an array of three fixed-fixed beams

In this section, we extend the analysis of single beam system to an array of three beams. All the beams are geometrically similar and fixed at both the ends. The beams are excited by two side electrodes and one bottom electrode as before. We analytically model the system by considering each beam separately which is influenced by the neighboring beams and electrodes. Finally using Rayleigh-Ritz-Galerkin modal superposition concept, we reduce the system using single mode shape. The frequency analysis is carried out based on linear modal matrix and the analytical results are validated by comparing with experimental results.

### 3.1 Full static and dynamic governing equations

For the analysis of the system of 3 beam array, we consider all beams having length  $L$ , width  $B$ , thickness  $H$  and are fixed at both the ends. Beams are separated from each other and side electrodes by side gaps of  $g_n$  and all beams are separated from the bottom electrode by gap  $d$  as shown in Fig.(3.1). For simplicity, we normalize the gap between each beam and its neighbors w.r.t the first beam-electrode separation  $g_0$ , which gives  $r_n = \frac{g_n}{g_0}$  for  $n = 0, 1, 2, 3$ . We consider different residual tensions in the beams due to uneven heating effects.

The motion of each beam is considered to be in two orthogonal directions in the three beam array as in the case of single beam. Hence, we have altogether 6 governing equations to model the system. The forcing on the first and third beams are similar due to symmetry of the system, while that on the middle beam is different. Now, neglecting fringing effects and considering forces due to in-homogeneous electric field, the governing equations of motion for the system are written as,

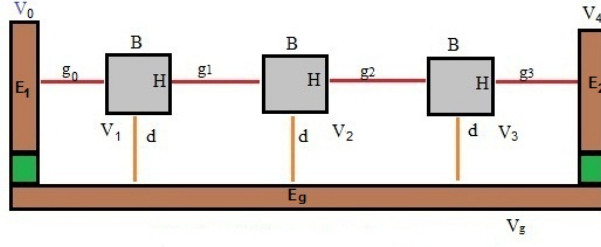


Figure 3.1: Side view of an array of 3 beams separated from each other, the side electrodes  $E_1$  and  $E_2$ , and the ground electrode  $E_g$ . Bottom separation for all beams are  $d$

$$EI_z y_{1xxxx} + \rho A y_{1tt} - [N_1 + \frac{E_x A}{2L} \int_0^L (y_{1x}^2 + z_{1x}^2) dx] y_{1xx} = Q_{1y} \quad (3.1)$$

$$EI_y z_{1xxxx} + \rho A z_{1tt} - [N_1 + \frac{E_x A}{2L} \int_0^L (z_{1x}^2 + y_{1x}^2) dx] z_{1xx} = Q_{1z} \quad (3.2)$$

$$EI_z y_{2xxxx} + \rho A y_{2tt} - [N_2 + \frac{E_x A}{2L} \int_0^L (y_{2x}^2 + z_{2x}^2) dx] y_{2xx} = Q_{2y} \quad (3.3)$$

$$EI_y z_{2xxxx} + \rho A z_{2tt} - [N_2 + \frac{E_x A}{2L} \int_0^L (z_{2x}^2 + y_{2x}^2) dx] z_{2xx} = Q_{2z} \quad (3.4)$$

$$EI_z y_{3xxxx} + \rho A y_{3tt} - [N_3 + \frac{E_x A}{2L} \int_0^L (y_{3x}^2 + z_{3x}^2) dx] y_{3xx} = Q_{3y} \quad (3.5)$$

$$EI_y z_{3xxxx} + \rho A z_{3tt} - [N_3 + \frac{E_x A}{2L} \int_0^L (z_{3x}^2 + y_{3x}^2) dx] z_{3xx} = Q_{3z} \quad (3.6)$$

Subjected to the following boundary conditions for  $n = 1, 2, 3$ .

$$\begin{aligned} y_n(0, t) = y_n(L, t) = 0, & \quad z_n(0, t) = z_n(L, t) = 0, \\ y_{nx}(0, t) = y_{nx}(L, t) = 0, & \quad z_{nx}(0, t) = z_{nx}(L, t) = 0 \end{aligned} \quad (3.7)$$

For  $n = 1, 2, 3$  for three beams.  $N_1, N_2$  and  $N_3$  are the axial tensions in the beams respectively. They may be different because of different initial residual tension or due to thermal gradient induced by LASER heating effect. The actual tension  $N$  can be expressed as  $N = N_0 + N'$ , where  $N_0$  is the pretension in the fabricated device corresponding to the reference temperature and  $N'$  is the additional tension induced in the beam due to the differential thermal contraction of the beam and the substrate [4].

$$N' = -EA(\alpha - \alpha_s)(T - T_0)$$

where  $E$  is the Young's modulus of the beam material, and  $\alpha, \alpha_s$  are the linear coefficients of

thermal expansion of the beam and substrate respectively. Subscripts  $x$  and  $t$  denote the derivatives with respect to  $x$  and  $t$  respectively.  $E$  and  $E_x$  are the Young's modulus of elasticity for all the beams in two orthogonal directions respectively.  $\rho$  is the density of the beam material.  $A$  is the cross section area of each beam. We take the displacements of the beam in two directions as  $y_1 = y_1(x)$ ,  $z_1 = z_1(x)$ ,  $y_2 = y_2(x)$ ,  $z_2 = z_2(x)$ ,  $y_3 = y_3(x)$  and  $z_3 = z_3(x)$ .  $I_z$  and  $I_y$  are the moment of inertia of the cross section for  $y$  and  $z$  deflections respectively. These two quantities are same for all the three beams due to their similar geometric dimensions.

Following the expressions of forcing for single beam, the forcing terms  $Q_y$  and  $Q_z$  for all the 3 beams can be written as follows,

$$Q_{1y} = \frac{1}{2}\epsilon_0(1 - k_1|z_1|)H \left[ \frac{(V_{10} + v(t))^2}{(g_0 - y_1)^2} - \frac{(V_{21} + v(t))^2}{(g_1 + y_1 - y_2)^2} \right] \quad (3.8)$$

$$Q_{1z} = \frac{1}{2}\epsilon_0 B \left[ \frac{(V_{1g} + kv(t))^2}{(d - z_1)^2} \right] + k_2 \left[ (V_{10} + v(t))^2(-z_1) + (V_{21} + v(t))^2(z_2 - z_1) \right] \quad (3.9)$$

$$Q_{2y} = \frac{1}{2}\epsilon_0(1 - k_1|z_2|)H \left[ \frac{(V_{21} + v(t))^2}{(g_1 + y_1 - y_2)^2} - \frac{(V_{32} + v(t))^2}{(g_2 + y_2 - y_3)^2} \right] \quad (3.10)$$

$$Q_{2z} = \frac{1}{2}\epsilon_0 B \left[ \frac{(V_{2g} + kv(t))^2}{(d - z_2)^2} \right] + k_2 \left[ (V_{21} + v(t))^2(z_1 - z_2) + (V_{32} + v(t))^2(z_3 - z_2) \right] \quad (3.11)$$

$$Q_{3y} = \frac{1}{2}\epsilon_0(1 - k_1|z_3|)H \left[ \frac{(V_{32} + v(t))^2}{(g_2 + y_2 - y_3)^2} - \frac{(V_{43} + v(t))^2}{(g_3 + y_3 - y_4)^2} \right] \quad (3.12)$$

$$Q_{3z} = \frac{1}{2}\epsilon_0 B \left[ \frac{(V_{3g} + kv(t))^2}{(d - z_3)^2} \right] + k_2 \left[ (V_{32} + v(t))^2(z_2 - z_3) + (V_{43} + v(t))^2(z_4 - z_3) \right] \quad (3.13)$$

Where  $\epsilon_0 = 8.85 \times 10^{-12}$  F/m is the free space permittivity.  $V$  and  $v(t)$  are the DC and AC components of applied voltage. Since we are applying AC to alternate beams,  $k = 0$  for beams with even numbering, otherwise it is equal to 1.

We non-dimensionalize Eqn.(3.1)- (3.6) by substituting the following new variables as denoted by hat in the governing equations,

$$\hat{x} = \frac{x}{L}, \hat{y}_1 = \frac{y_1}{g}, \hat{y}_2 = \frac{y_2}{g}, \hat{y}_3 = \frac{y_3}{g}, \hat{z}_1 = \frac{z_1}{d}, \hat{z}_2 = \frac{z_2}{d}, \hat{z}_3 = \frac{z_3}{d}, \hat{t} = \frac{t}{T} \quad (3.14)$$

$T$  is the time scale to non-dimensionalize time  $t$  and is equal to  $\sqrt{\frac{\rho B H L^4}{E I_z}}$ . Now, dropping hats, we get non-dimensionalized form of equations as,

$$y_{1xxxx} + y_{1tt} - [N_1 + \alpha_1\Gamma(y_1, y_1) + \alpha_2\Gamma(z_1, z_1)]y_{1xx} = \alpha_3 \left[ \frac{(V_{10} + v(t))^2}{r_0^2 \left(1 + \frac{-y_1}{r_0}\right)^2} - \frac{(V_{21} + v(t))^2}{r_1^2 \left(1 + \frac{(y_1 - y_2)}{r_1}\right)^2} \right] \quad (3.15)$$

$$z_{1xxxx} + \alpha_4 z_{1tt} - \alpha_4 [N_1 + \alpha_1\Gamma(y_1, y_1) + \alpha_2\Gamma(z_1, z_1)]z_{1xx} = \alpha_5 \frac{(V_{1g} + kv(t))^2}{(1 - z_1)^2} + \alpha_6 \left[ [V_{10} + v(t)]^2(-z_1) + [V_{21} + v(t)]^2(z_2 - z_1) \right] \quad (3.16)$$

$$y_{2xxxx} + y_{2tt} - [N_2 + \alpha_1\Gamma(y_2, y_2) + \alpha_2\Gamma(z_2, z_2)]y_{2xx} = \alpha_3 \left[ \frac{(V_{21} + v(t))^2}{r_1^2 \left(1 + \frac{(y_1 - y_2)}{r_1}\right)^2} - \frac{(V_{21} + v(t))^2}{r_2^2 \left(1 + \frac{(y_2 - y_3)}{r_2}\right)^2} \right] \quad (3.17)$$

$$z_{2xxxx} + \alpha_4 z_{2tt} - \alpha_4 [N_2 + \alpha_1\Gamma(y_2, y_2) + \alpha_2\Gamma(z_2, z_2)]z_{2xx} = \alpha_5 \frac{(V_{2g} + kv(t))^2}{(1 - z_2)^2} + \alpha_6 \left[ [V_{21} + v(t)]^2(z_1 - z_2) + [V_{32} + v(t)]^2(z_3 - z_2) \right] \quad (3.18)$$

$$y_{3xxxx} + y_{3tt} - [N_3 + \alpha_1\Gamma(y_3, y_3) + \alpha_2\Gamma(z_3, z_3)]y_{3xx} = \alpha_3 \left[ \frac{(V_{32} + v(t))^2}{r_2^2 \left(1 + \frac{(y_2 - y_3)}{r_2}\right)^2} - \frac{(V_{43} + v(t))^2}{r_3^2 \left(1 + \frac{(y_3)}{r_3}\right)^2} \right] \quad (3.19)$$

$$z_{3xxxx} + \alpha_4 z_{3tt} - \alpha_4 [N_3 + \alpha_1\Gamma(y_3, y_3) + \alpha_2\Gamma(z_3, z_3)]z_{3xx} = \alpha_5 \frac{(V_{3g} + kv(t))^2}{(1 - z_3)^2} + \alpha_6 \left[ [V_{32} + v(t)]^2(z_2 - z_3) - [V_{43} + v(t)]^2(z_3) \right] \quad (3.20)$$

Subjected to new sets of boundary conditions for  $n = 1, 2, 3$ ,

$$\begin{aligned} y_n(0, t) = y_n(1, t) = 0, & \quad z_n(0, t) = z_n(1, t) = 0, \\ y_{nx}(0, t) = y_{nx}(1, t) = 0, & \quad z_{nx}(0, t) = z_{nx}(1, t) = 0 \end{aligned} \quad (3.21)$$

All the coefficients appearing in these equations are given in the Eqn.(2.10). Now we consider

the displacements in the form:

$$\begin{aligned}
y_1(x, t) &= u_{s1}(x) + u_1(x, t), & z_1(x, t) &= w_{s1}(x) + w_1(x, t) \\
y_2(x, t) &= u_{s2}(x) + u_2(x, t), & z_2(x, t) &= w_{s2}(x) + w_2(x, t) \\
y_3(x, t) &= u_{s3}(x) + u_3(x, t), & z_3(x, t) &= w_{s3}(x) + w_3(x, t)
\end{aligned} \tag{3.22}$$

To find the static deflections  $u_{sn}(x)$  and  $w_{sn}(x)$  of the beam for  $n = 1, 2, 3$ , we have to solve the resulting equations after substituting eq(3.22) in eq(3.15)-(3.20) and then making all time derivatives and dynamic terms equal to zero. Finally the static equations are written as follows,

$$\begin{aligned}
u_{s1xxxx} - [N_1 + \alpha_1 \Gamma(u_{s1}, u_{s1}) + \alpha_2 \Gamma(w_{s1}, w_{s1})]u_{s1xx} &= \alpha_3 \left[ \frac{(V_{10})^2}{r_0^2 \left(1 + \frac{(-u_{s1})}{r_0}\right)^2} - \frac{(V_{21})^2}{r_1^2 \left(1 + \frac{(u_{s1} - u_{s2})}{r_1}\right)^2} \right]
\end{aligned} \tag{3.23}$$

$$\begin{aligned}
w_{s1xxxx} - \alpha_4 [N_1 + \alpha_1 \Gamma(u_{s1}, u_{s1}) + \alpha_2 \Gamma(w_{s1}, w_{s1})]w_{s1xx} &= \alpha_5 \frac{(V_{1g})^2}{(1 - w_{s1})^2} \\
&+ \alpha_6 \left[ V_{10}^2 (-w_{s1}) + V_{21}^2 (w_{s2} - w_{s1}) \right]
\end{aligned} \tag{3.24}$$

$$\begin{aligned}
u_{s2xxxx} - [N_2 + \alpha_1 \Gamma(u_{s2}, u_{s2}) + \alpha_2 \Gamma(w_{s2}, w_{s2})]u_{s2xx} &= \alpha_3 \left[ \frac{(V_{21})^2}{r_1^2 \left(1 + \frac{(u_{s1} - u_{s2})}{r_1}\right)^2} - \frac{(V_{32})^2}{r_2^2 \left(1 + \frac{(u_{s2} - u_{s3})}{r_2}\right)^2} \right]
\end{aligned} \tag{3.25}$$

$$\begin{aligned}
w_{s2xxxx} - \alpha_4 [N_2 + \alpha_1 \Gamma(u_{s2}, u_{s2}) + \alpha_2 \Gamma(w_{s2}, w_{s2})]w_{s2xx} &= \alpha_5 \frac{(V_{2g})^2}{(1 - w_{s2})^2} \\
&+ \alpha_6 \left[ V_{21}^2 (w_{s1} - w_{s1}) + V_{32}^2 (w_{s3} - w_{s2}) \right]
\end{aligned} \tag{3.26}$$

$$\begin{aligned}
u_{s3xxxx} - [N_3 + \alpha_1 \Gamma(u_{s3}, u_{s3}) + \alpha_2 \Gamma(w_{s3}, w_{s3})]u_{s3xx} &= \alpha_3 \left[ \frac{(V_{32})^2}{r_2^2 \left(1 + \frac{(u_{s2} - u_{s3})}{r_2}\right)^2} - \frac{(V_{43})^2}{r_3^2 \left(1 + \frac{(u_{s3})}{r_3}\right)^2} \right]
\end{aligned} \tag{3.27}$$

$$\begin{aligned}
w_{s3xxxx} - \alpha_4 [N_3 + \alpha_1 \Gamma(u_{s3}, u_{s3}) + \alpha_2 \Gamma(w_{s3}, w_{s3})]w_{s3xx} &= \alpha_5 \frac{(V_{3g})^2}{(1 - w_{s3})^2} \\
&+ \alpha_6 \left[ V_{32}^2 (w_{s2} - w_{s3}) - V_{43}^2 (w_{s3}) \right]
\end{aligned} \tag{3.28}$$

Again substituting eq(3.22) in eq(3.15)-(3.20), using the static equations (3.23),(3.28) and expand-

ing the forcing terms about equilibrium by Taylor series expansion method, the dynamic governing equations are obtained. To perform the linear frequency analysis, we neglect all nonlinear and forcing terms in these equations. Finally, the linear dynamic equations are given as follows,

$$\begin{aligned}
u_{1xxxx} + u_{1tt} - [2\alpha_1\Gamma(u_{s1}, u_1) + 2\alpha_2\Gamma(w_{s1}, w_1)]u_{s1xx} - [N_1 + \alpha_1\Gamma(u_{s1}, u_{s1}) \\
+ \alpha_2\Gamma(w_{s1}, w_{s1})]u_{1xx} = 2\alpha_3 \left[ V_{10}^2 \left( \frac{u_1}{r_0^3 \left( 1 + \frac{(-u_{s1})}{r_0} \right)^3} \right) \right. \\
\left. - (V_{21})^2 \left( \frac{u_2 - u_1}{r_1^3 \left( 1 + \frac{(u_{s1} - u_{s2})}{r_1} \right)^3} \right) \right] \quad (3.29)
\end{aligned}$$

$$\begin{aligned}
w_{1xxxx} + \alpha_4 w_{1tt} - \alpha_4 [2\alpha_1\Gamma(u_{s1}, u_1) + 2\alpha_2\Gamma(w_{s1}, w_1)]w_{s1xx} - \alpha_4 [N_1 \\
+ \alpha_1\Gamma(u_{s1}, u_{s1}) + \alpha_2\Gamma(w_{s1}, w_{s1})]w_{1xx} = 2\alpha_5 \frac{V_{1g}^2}{(1 - w_{s1})^3} w_1 \\
+ \alpha_6 \left[ V_{10}^2 (-w_1) + V_{21}^2 (w_2 - w_1) \right] \quad (3.30)
\end{aligned}$$

$$\begin{aligned}
u_{2xxxx} + u_{2tt} - [2\alpha_1\Gamma(u_{s2}, u_2) + 2\alpha_2\Gamma(w_{s2}, w_2)]u_{s2xx} - [N_2 + \alpha_1\Gamma(u_{s2}, u_{s2}) \\
+ \alpha_2\Gamma(w_{s2}, w_{s2})]u_{2xx} = 2\alpha_3 \left[ V_{21}^2 \left( \frac{u_2 - u_1}{r_1^3 \left( 1 + \frac{(u_{s2} - u_{s2})}{r_1} \right)^3} \right) \right. \\
\left. - (V_{32})^2 \left( \frac{u_3 - u_2}{r_2^3 \left( 1 + \frac{(u_{s2} - u_{s3})}{r_2} \right)^3} \right) \right] \quad (3.31)
\end{aligned}$$

$$\begin{aligned}
w_{2xxxx} + \alpha_4 w_{2tt} - \alpha_4 [2\alpha_1\Gamma(u_{s2}, u_2) + 2\alpha_2\Gamma(w_{s2}, w_2)]w_{s2xx} - \alpha_4 [N_2 \\
+ \alpha_1\Gamma(u_{s2}, u_{s2}) + \alpha_2\Gamma(w_{s2}, w_{s2})]w_{2xx} = 2\alpha_5 \frac{V_{2g}^2}{(1 - w_{s2})^3} w_2 \\
+ \alpha_6 \left[ V_{21}^2 (w_1 - w_2) + V_{32}^2 (w_3 - w_2) \right] \quad (3.32)
\end{aligned}$$

$$\begin{aligned}
u_{3xxxx} + u_{3tt} - [2\alpha_1\Gamma(u_{s3}, u_3) + 2\alpha_2\Gamma(w_{s3}, w_3)]u_{s3xx} - [N_3 + \alpha_1\Gamma(u_{s3}, u_{s3}) \\
+ \alpha_2\Gamma(w_{s3}, w_{s3})]u_{3xx} = 2\alpha_3 \left[ V_{32}^2 \left( \frac{u_3 - u_2}{r_2^3 \left( 1 + \frac{(u_{s2} - u_{s3})}{r_2} \right)^3} \right) \right. \\
\left. + (V_{43})^2 \left( \frac{u_3}{r_3^3 \left( 1 + \frac{(u_{s3})}{r_3} \right)^3} \right) \right] \quad (3.33)
\end{aligned}$$

$$\begin{aligned}
w_{3xxxx} + \alpha_4 w_{3tt} - \alpha_4 [2\alpha_1\Gamma(u_{s3}, u_3) + 2\alpha_2\Gamma(w_{s3}, w_3)]w_{s3xx} - \alpha_4 [N_3 \\
+ \alpha_1\Gamma(u_{s3}, u_{s3}) + \alpha_2\Gamma(w_{s3}, w_{s3})]w_{3xx} = 2\alpha_5 \frac{V_{3g}^2}{(1 - w_{s3})^3} w_3 \\
+ \alpha_6 \left[ V_{32}^2 (w_2 - w_3) - V_{43}^2 (w_3) \right] \quad (3.34)
\end{aligned}$$



subjected to the following boundary conditions,

$$\begin{aligned}
u_1(0, t) = u_1(1, t) &= w_1(0, t) = w_1(1, t) = 0 \\
u_{1x}(0, t) = u_{1x}(1, t) &= w_{1x}(0, t) = w_{1x}(1, t) = 0 \\
u_2(0, t) = u_2(1, t) &= w_2(0, t) = w_2(1, t) = 0 \\
u_{2x}(0, t) = u_{2x}(1, t) &= w_{2x}(0, t) = w_{2x}(1, t) = 0 \\
u_3(0, t) = u_3(1, t) &= w_3(0, t) = w_3(1, t) = 0 \\
u_{3x}(0, t) = u_{3x}(1, t) &= w_{3x}(0, t) = w_{3x}(1, t) = 0
\end{aligned} \tag{3.35}$$

### 3.2 Frequency analysis for N = 3 beam.

To perform the frequency analysis, we reduce the above static and linear dynamic equations using single mode Galerkin procedure. We assume the static and dynamic deflections of the beam along both the planes as:

$$\begin{aligned}
u_{s1}(x) &= A_{11}(y, z)\phi(x); & w_{s1}(x) &= A_{12}(y, z)\phi(x); \\
u_1(x, t) &= P_{11}(t)\phi(x); & w_1(x, t) &= P_{12}(t)\phi(x); \\
\\
u_{s2}(x) &= A_{21}(y, z)\phi(x); & w_{s2}(x) &= A_{22}(y, z)\phi(x); \\
u_2(x, t) &= P_{21}(t)\phi(x); & w_2(x, t) &= P_{22}(t)\phi(x); \\
\\
u_{s3}(x) &= A_{31}(y, z)\phi(x); & w_{s3}(x) &= A_{32}(y, z)\phi(x); \\
u_3(x, t) &= P_{31}(t)\phi(x); & w_3(x, t) &= P_{32}(t)\phi(x);
\end{aligned} \tag{3.36}$$

Here,  $\phi(x) = \sqrt{\frac{2}{3}}(1 - \cos(2\pi x))$  as assumed earlier, so that it satisfies orthogonality conditions. Finally the reduced order static equations are given as,

$$\begin{aligned}
\frac{16}{9}\pi^4\alpha_1 A_{11}^3 + \left(\frac{16}{3}\pi^4 + \frac{16}{9}\pi^4\alpha_2 A_{12}^2 + \frac{4}{3}\pi^2 N_1\right)A_{11} - \alpha_3 \left[ \frac{V_{10}^2}{r_0^2} \sqrt{\frac{2/3}{(1 + 2\sqrt{\frac{2}{3}}\frac{(-A_{11})}{r_0})^3}} \right. \\
\left. - \frac{V_{21}^2}{r_1^2} \sqrt{\frac{2/3}{(1 + 2\sqrt{\frac{2}{3}}\frac{(A_{11}-A_{21})}{r_1})^3}} \right] = 0
\end{aligned} \tag{3.37}$$

$$\begin{aligned}
\frac{16}{9}\pi^4\alpha_2 A_{12}^3 + \left(\frac{16}{3}\frac{\pi^4}{\alpha_4} + \frac{16}{9}\pi^4\alpha_1 A_{11}^2 + \frac{4}{3}\pi^2 N_1\right)A_{12} - \frac{\alpha_5}{\alpha_4} V_{1g}^2 \sqrt{\frac{2/3}{(1 - 2\sqrt{\frac{2}{3}}A_{12})^3}} \\
+ \frac{\alpha_6}{\alpha_4} \left( [V_{10}^2 + V_{21}^2]A_{12} + V_{21}^2 A_{22} \right) = 0
\end{aligned} \tag{3.38}$$

$$\begin{aligned} \frac{16}{9}\pi^4\alpha_1 A_{21}^3 + \left(\frac{16}{3}\pi^4 + \frac{16}{9}\pi^4\alpha_2 A_{22}^2 + \frac{4}{3}\pi^2 N_2\right)A_{21} - \alpha_3 \left[ \frac{V_{21}^2}{r_1^2} \sqrt{\frac{2/3}{(1 + 2\sqrt{\frac{2}{3}}\frac{(A_{11}-A_{21}))}{r_1})^3}} \right. \\ \left. - \frac{V_{32}^2}{r_2^2} \sqrt{\frac{2/3}{(1 + 2\sqrt{\frac{2}{3}}\frac{(A_{21}-A_{31}))}{r_2})^3}} \right] = 0 \end{aligned} \quad (3.39)$$

$$\begin{aligned} \frac{16}{9}\pi^4\alpha_2 A_{22}^3 + \left(\frac{16}{3}\frac{\pi^4}{\alpha_4} + \frac{16}{9}\pi^4\alpha_1 A_{21}^2 + \frac{4}{3}\pi^2 N_2\right)A_{22} - \frac{\alpha_5}{\alpha_4} V_{2g}^2 \sqrt{\frac{2/3}{(1 - 2\sqrt{\frac{2}{3}}A_{22})^3}} \\ - \frac{\alpha_6}{\alpha_4} \left( V_{21}^2 A_{12} - [V_{21}^2 + V_{32}^2]A_{22} + V_{32}^2 A_{32} \right) = 0 \end{aligned} \quad (3.40)$$

$$\begin{aligned} \frac{16}{9}\pi^4\alpha_1 A_{31}^3 + \left(\frac{16}{3}\pi^4 + \frac{16}{9}\pi^4\alpha_2 A_{32}^2 + \frac{4}{3}\pi^2 N_3\right)A_{31} - \alpha_3 \left[ \frac{V_{32}^2}{r_2^2} \sqrt{\frac{2/3}{(1 + 2\sqrt{\frac{2}{3}}\frac{(A_{21}-A_{31}))}{r_2})^3}} \right. \\ \left. - \frac{V_{43}^2}{r_3^2} \sqrt{\frac{2/3}{(1 + 2\sqrt{\frac{2}{3}}\frac{(A_{31}))}{r_3})^3}} \right] = 0 \end{aligned} \quad (3.41)$$

$$\begin{aligned} \frac{16}{9}\pi^4\alpha_2 A_{32}^3 + \left(\frac{16}{3}\frac{\pi^4}{\alpha_4} + \frac{16}{9}\pi^4\alpha_1 A_{31}^2 + \frac{4}{3}\pi^2 N_3\right)A_{32} - \frac{\alpha_5}{\alpha_4} V_{3g}^2 \sqrt{\frac{2/3}{(1 - 2\sqrt{\frac{2}{3}}A_{32})^3}} \\ - \frac{\alpha_6}{\alpha_4} \left( V_{32}^2 A_{22} - [V_{32}^2 + V_{43}^2]A_{32} \right) = 0 \end{aligned} \quad (3.42)$$

Similarly, reducing the dynamic equations (3.29)-(3.34), we obtain the modal equations in matrix form as,

$$\begin{bmatrix} \ddot{P}_{11} \\ \ddot{P}_{12} \\ \ddot{P}_{21} \\ \ddot{P}_{22} \\ \ddot{P}_{31} \\ \ddot{P}_{32} \end{bmatrix} + \begin{bmatrix} \lambda_{11} & c_1 & c_2 & 0 & 0 & 0 \\ c_3 & \lambda_{12} & 0 & 0 & 0 & 0 \\ c_5 & 0 & \lambda_{21} & c_4 & c_1 & 0 \\ 0 & 0 & c_7 & \lambda_{22} & 0 & 0 \\ 0 & 0 & c_9 & 0 & \lambda_{31} & c_8 \\ 0 & 0 & 0 & 0 & c_{10} & \lambda_{32} \end{bmatrix} \begin{bmatrix} P_{11} \\ P_{12} \\ P_{21} \\ P_{22} \\ P_{31} \\ P_{32} \end{bmatrix} = 0$$

Where,  $c_j$ 's are the coupling terms and  $\lambda_{ij}$ 's are the unperturbed natural frequencies of the array of beams given below.

$$\lambda_{11} = \left[ \frac{16}{3}\pi^4 + \frac{16}{9}\pi^4\alpha_2 A_{12}^2 + \frac{16}{3}\pi^4\alpha_1 A_{11}^2 + \frac{4}{3}\pi^2 N_1 - 2\alpha_3 \left( \frac{V_{10}^2}{r_0^3(1 - 2\sqrt{\frac{2}{3}}\frac{(A_{11})}{r_0})^{\frac{5}{2}}} + \frac{V_{21}^2}{r_1^3(1 - 2\sqrt{\frac{2}{3}}\frac{(A_{21}-A_{11})}{r_1})^{\frac{5}{2}}} \right) \right] \quad (3.43)$$

$$\lambda_{12} = \left[ \frac{16}{3}\frac{\pi^4}{\alpha_4} + \frac{16}{9}\pi^4\alpha_1 A_{11}^2 + \frac{16}{3}\pi^4\alpha_2 A_{12}^2 + \frac{4}{3}\pi^2 N_1 - 2\frac{\alpha_5}{\alpha_4} V_{1g}^2 (1 - 2\sqrt{\frac{2}{3}} A_{12})^{-\frac{5}{2}} + \frac{\alpha_6}{\alpha_4} (V_{10}^2 + V_{21}^2) \right] \quad (3.44)$$

$$\lambda_{21} = \left[ \frac{16}{3}\pi^4 + \frac{16}{9}\pi^4\alpha_2 A_{22}^2 + \frac{16}{3}\pi^4\alpha_1 A_{21}^2 + \frac{4}{3}\pi^2 N_2 - 2\alpha_3 \left( \frac{V_{21}^2}{r_1^3(1 - 2\sqrt{\frac{2}{3}}\frac{(A_{21}-A_{11})}{r_1})^{\frac{5}{2}}} + \frac{V_{32}^2}{r_2^3(1 - 2\sqrt{\frac{2}{3}}\frac{(A_{31}-A_{21})}{r_2})^{\frac{5}{2}}} \right) \right] \quad (3.45)$$

$$\lambda_{22} = \left[ \frac{16}{3}\frac{\pi^4}{\alpha_4} + \frac{16}{9}\pi^4\alpha_1 A_{21}^2 + \frac{16}{3}\pi^4\alpha_2 A_{22}^2 + \frac{4}{3}\pi^2 N_2 - 2\frac{\alpha_5}{\alpha_4} V_{2g}^2 (1 - 2\sqrt{\frac{2}{3}} A_{22})^{-\frac{5}{2}} + \frac{\alpha_6}{\alpha_4} (V_{21}^2 + V_{32}^2) \right] \quad (3.46)$$

$$\lambda_{31} = \left[ \frac{16}{3}\pi^4 + \frac{16}{9}\pi^4\alpha_2 A_{32}^2 + \frac{16}{3}\pi^4\alpha_1 A_{31}^2 + \frac{4}{3}\pi^2 N_3 - 2\alpha_3 \left( \frac{V_{32}^2}{r_2^3(1 - 2\sqrt{\frac{2}{3}}\frac{(A_{31}-A_{21})}{r_2})^{\frac{5}{2}}} + \frac{V_{43}^2}{r_3^3(1 - 2\sqrt{\frac{2}{3}}\frac{-A_{31}}{r_3})^{\frac{5}{2}}} \right) \right] \quad (3.47)$$

$$\lambda_{32} = \left[ \frac{16}{3}\frac{\pi^4}{\alpha_4} + \frac{16}{9}\pi^4\alpha_1 A_{31}^2 + \frac{16}{3}\pi^4\alpha_2 A_{32}^2 + \frac{4}{3}\pi^2 N_3 - 2\frac{\alpha_5}{\alpha_4} V_{3g}^2 (1 - 2\sqrt{\frac{2}{3}} A_{32})^{-\frac{5}{2}} + \frac{\alpha_6}{\alpha_4} (V_{32}^2 + V_{43}^2) \right] \quad (3.48)$$

$$\begin{aligned}
c_1 &= \frac{32}{9} \alpha_2 A_{11} A_{12} \pi^4; c_2 = 2\alpha_3 \frac{V_{32}^2}{r_1^3 (1 - 2\sqrt{\frac{2}{3}} (\frac{A_{21}-A_{11}}{r_1})^{5/2}}); c_3 = \frac{32}{9} \alpha_1 A_{11} A_{12} \pi^4; c_4 = \frac{32}{9} \alpha_2 A_{21} A_{22} \pi^4; \\
c_5 &= 2\alpha_3 \frac{V_{32}^2}{r_1^3 (1 - 2\sqrt{\frac{2}{3}} (\frac{A_{21}-A_{11}}{r_1})^{5/2}}); c_6 = 2\alpha_3 \frac{V_{43}^2}{r_2^3 (1 - 2\sqrt{\frac{2}{3}} (\frac{A_{31}-A_{21}}{r_2})^{5/2}}); c_7 = \frac{32}{9} \alpha_1 A_{21} A_{22} \pi^4; \\
c_8 &= \frac{32}{9} \alpha_2 A_{31} A_{32} \pi^4; c_9 = 2\alpha_3 \frac{V_{43}^2}{r_2^3 (1 - 2\sqrt{\frac{2}{3}} (\frac{A_{31}-A_{21}}{r_2})^{5/2}}); c_{10} = \frac{32}{9} \alpha_1 A_{31} A_{32} \pi^4
\end{aligned} \tag{3.49}$$

Solving this eigenvalue problem gives the linear frequencies of the coupled system. By suitably varying the gaps between beams and applying DC bias, we get multiple modal coupling in the array.

### 3.3 Results and discussions

We present the results for linear frequency analysis based on the analytical model for three beam array and compare it with experimental data. The beams used in the experiment are made up of Au-Pd alloy on a silicon substrate using bulk micro-machining process[9]. All the geometric parameters as well as material properties of the Au-Pd beam under consideration for the numerical analysis of three beams are mentioned in the following Table 3.1 and Table 3.2 respectively. We

Table 3.1: Geom. Parameters

Parameters	Value( $\mu m$ )
$L$	500
$B$	2
$H$	0.2
$g$	4.8
$g_1$	4.9
$g_2$	5
$g_3$	4.6
$d$	50

solve for the modal frequencies of all the beams using MATLAB and plot them to compare with experimental results.

Table 3.2: Matl. Properties

Properties	Value
$E$	1.85E+11 N/m <sup>2</sup>
$\rho$	4870 kg/m <sup>3</sup>
$N_1$	3.3E-5 N
$N_2$	3.498E-5 N
$N_3$	3.729E-5 N
$\alpha_{corr.}$	0.00462
$\epsilon_0$	8.85E-12 F/m

The experimental arrangement of beams in three beam array are shown in the Figure.(3.2). All the beams are fixed at their both ends and separated from the side and bottom electrodes. The experiments are performed at 77 K.



Figure 3.2: A picture of 3-beams array with two side electrodes and a bottom electrode.

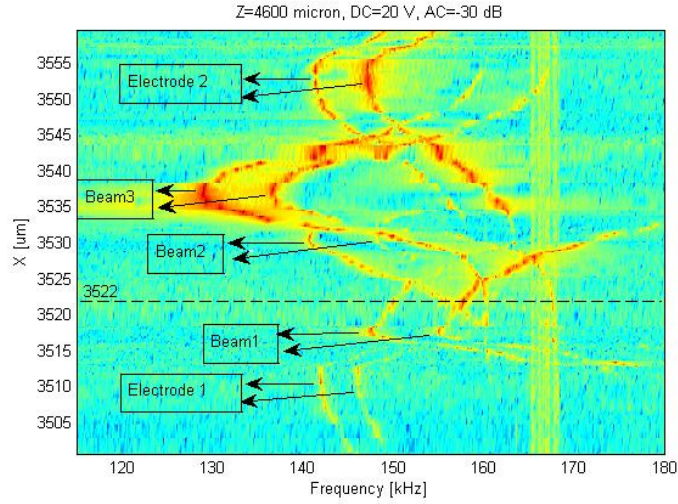


Figure 3.3: Influence of laser heating on frequency across beam width (X -direction is taken along the width).

Frequency variation in an array of three beams due to temperature change by LASER heating shows the presence of mixing regions where different modes come closer and interact with each other. Figure.(3.3) shows the frequency variation due to this effect experimentally. Due to uneven heating along the width, the variation is not uniform.

Taking the parameters as given in Table 3.1 and Table 3.2, the variation of two modal frequencies for each beam in the array subjected to different dc biasing at a fixed temperature distribution are calculated and compared both experimentally and analytically in Figure.(3.4). Both the results agree well with each other. Figure.(3.5) also presents different modal coupling regions which can be controlled by choosing proper gaps between beams. At about 70 V DC, coupling between different modes of beam becomes prominent. But each individual beam behaves as that of single beam discussed in the previous section. Modes of different beams couple at different voltages due to difference in side electrode gaps and other parameters.

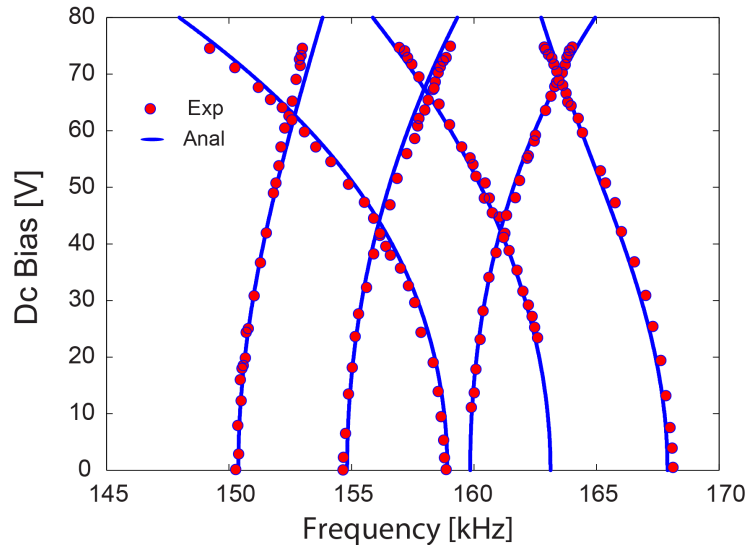


Figure 3.4: Frequency variation due to dc bias when the laser is positioned near  $X=3522 \mu\text{m}$ . Experimental (red dotted) vs. analytical (blue solid line).

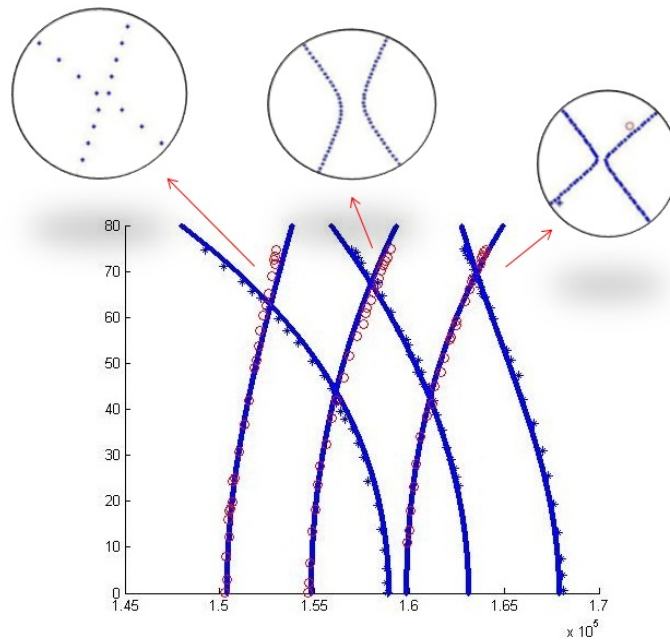


Figure 3.5: Frequency variation in three beam array showing modal couplings (zoomed).

## Chapter 4

# Mathematical modeling and solution of an array of $N$ fixed-fixed beams

Similar to the case of three doubly clamped beams excited electrostatically along in-plane and out of plane directions, in this section we consider an array of  $N$  fixed-fixed beams and generalize our formulations for linear frequency analysis. We consider the motion of each beam to be influenced by the adjacent beams or electrodes in the in-plane direction and by the bottom electrode in the other direction. At the same time, the influence of other neighboring electrodes are ignored. Finally we analyze a case of 40 beam array and compare the analytical result with the experimental outcomes.

### 4.1 Full static and dynamic governing equations

To analytically model the system of  $N$  beams, we consider all beams having length  $L$ , width  $B$ , thickness  $H$  and are clamped at both the ends. Beams are separated from each other and side electrodes by side gaps of  $g_n$  and by the same bottom gap  $d$  as shown in Fig.(4.1). For simplicity, we normalize the gap between each beam and its neighbors w.r.t  $g_0$ , which gives the ratio  $r_n = \frac{g_n}{g_0}$  for  $n = 0, 1, \dots, N$ .

Considering motion of each beam in two orthogonal directions in the array, we get total of  $2N$  governing equations. Neglecting poison's effect, fringing effects and considering forces due to in-homogeneous electric field, the governing equations of motion for the  $n^{th}$  beam are written as,

$$EI_z y_{nxxxx} + \rho A y_{ntt} - [N_n + \frac{E_x A}{2L} \int_0^L (y_{nx}^2 + z_{nx}^2) dx] y_{nxx} = Q_{ny} \quad (4.1)$$

$$EI_y z_{nxxxx} + \rho A z_{ntt} - [N_n + \frac{E_x A}{2L} \int_0^L (z_{nx}^2 + y_{nx}^2) dx] z_{nxx} = Q_{nz} \quad (4.2)$$

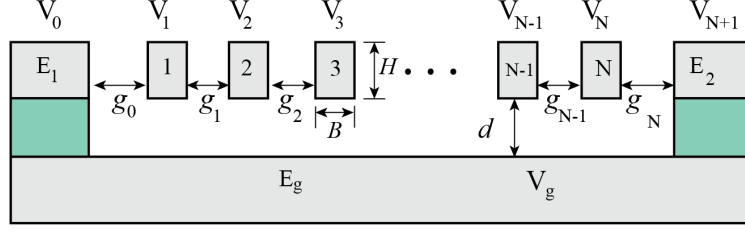


Figure 4.1: Side view of an array of  $N$  beams separated from each other, the side electrodes  $E_1$  and  $E_2$ , and the ground electrode  $E_g$

Subjected to the boundary conditions,

$$\begin{aligned} y_n(0, t) = y_n(L, t) = 0, & \quad z_n(0, t) = z_n(L, t) = 0, \\ y_{nx}(0, t) = y_{nx}(L, t) = 0, & \quad z_{nx}(0, t) = z_{nx}(L, t) = 0 \end{aligned} \quad (4.3)$$

$E$  and  $E_x$  are the Young's modulus of elasticity for the transversely isotropic beam in  $x$  plane and  $x$ -direction respectively.  $\rho$  is the density of the beam material.  $N_n$ ,  $I_z$  and  $I_y$  are the residual tensions for the  $n^{th}$  beam and moment of inertia of the cross section for  $y$  and  $z$  motions respectively.  $A(= BH)$  is the cross section area of the beam. Subscripts  $x$  and  $t$  denote the derivatives with respect to  $x$  and  $t$  respectively.  $y_n = y_n(x)$  and  $z_n = z_n(x)$  are the displacements of the beam in two directions.

As discussed earlier, the forcing terms  $Q_{ny}$  and  $Q_{nz}$  for the  $n^{th}$  beam can be written as follows,

$$Q_{ny} = \frac{1}{2}\epsilon_0(1 - k_1|z_n|)H \left[ \frac{(V_{(n)(n-1)} + v(t))^2}{(g_{(n-1)} + y_{(n-1)} - y_n)^2} - \frac{(V_{(n)(n+1)} + v(t))^2}{(g_n + y_n - y_{(n+1)})^2} \right] \quad (4.4)$$

$$\begin{aligned} Q_{nz} = \frac{1}{2}\epsilon_0 B \left[ \frac{(V_{(n)(g)} + kv(t))^2}{(d - z_n)^2} \right] + k_2 \left[ (V_{(n)(n-1)} + v(t))^2 (z_{(n-1)} - z_n) \right. \\ \left. + (V_{(n+1)(n)} + v(t))^2 (z_{(n+1)} - z_n) \right] \end{aligned} \quad (4.5)$$

Where  $\epsilon_0 = 8.85 \times 10^{-12}$  F/m is the free space permittivity.  $V$  and  $v(t)$  are the DC and AC components of applied voltage. Since we are applying AC to alternate beams,  $k = 0$  for beams with even numbering, otherwise it is equal to 1.

We non-dimensionalize Eqn.(4.1) and (4.2) by substituting the following new variables as denoted by hat in the governing equations,

$$\hat{x} = \frac{x}{L}, \hat{y}_n = \frac{y_n}{g}, \hat{z}_n = \frac{z_n}{d}, \hat{t} = \frac{t}{T} \quad (4.6)$$

$T$  is the time scale used to non-dimensionalize time  $t$  and is equal to  $\sqrt{\frac{\rho B H L^4}{E I_z}}$ . Then dropping hats for convenience, we get non-dimensionalized form of equations,



$$y_{nxxxx} + y_{ntt} - [N_n + \alpha_1 \Gamma(y_n, y_n) + \alpha_2 \Gamma(z_n, z_n)] y_{nxx} = \alpha_3 \left[ \frac{(V_{n(n-1)} + v(t))^2}{r_{(n-1)}^2 \left(1 + \frac{(y_{(n-1)} - y_n)}{r_{(n-1)}}\right)^2} - \frac{(V_{n(n+1)} + v(t))^2}{r_n^2 \left(1 + \frac{(y_n - y_{(n+1)})}{r_n}\right)^2} \right] \quad (4.7)$$

$$z_{nxxxx} + \alpha_4 z_{ntt} - \alpha_4 [N_n + \alpha_1 \Gamma(y_n, y_n) + \alpha_2 \Gamma(z_n, z_n)] z_{nxx} = \alpha_5 \frac{(V_{n(g)} + kv(t))^2}{(1 - z_n)^2} + \alpha_6 \left[ [V_{n(n-1)} + v(t)]^2 (z_{n-1} - z_n) + [V_{n(n+1)} + v(t)]^2 (z_{n+1} - z_n) \right] \quad (4.8)$$

Subjected to new sets of boundary conditions,

$$\begin{aligned} y_n(0, t) = y_n(1, t) = 0, & \quad z_n(0, t) = z_n(1, t) = 0, \\ y_{nx}(0, t) = y_{nx}(1, t) = 0, & \quad z_{nx}(0, t) = z_{nx}(1, t) = 0 \end{aligned} \quad (4.9)$$

All the coefficients appearing in these equations are given in the previous section in Eqn.(2.10). Now we consider the displacements in the form:

$$y_n(x, t) = u_{sn}(x) + u_n(x, t), \quad z_n(x, t) = w_{sn}(x) + w_n(x, t) \quad (4.10)$$

To find the static deflections  $u_{sn}(x)$  and  $w_{sn}(x)$  of the beam, we have to solve the resulting equations after substituting eq(4.10) in eq(4.8), (4.9) and then neglecting all dynamic terms by making them zero. Finally the static equations are written as follows,

$$u_{snxxxx} - [N_n + \alpha_1 \Gamma(u_{sn}, u_{sn}) + \alpha_2 \Gamma(w_{sn}, w_{sn})] u_{snxx} = \alpha_3 \left[ \frac{(V_{n(n-1)})^2}{r_{n-1}^2 \left(1 + \frac{(u_{s(n-1)} - u_{sn})}{r_{n-1}}\right)^2} - \frac{(V_{n(n+1)})^2}{r_n^2 \left(1 + \frac{(u_{sn} - u_{s(n+1)})}{r_n}\right)^2} \right] \quad (4.11)$$

$$w_{snxxxx} - \alpha_4 [N_n + \alpha_1 \Gamma(u_{sn}, u_{sn}) + \alpha_2 \Gamma(w_{sn}, w_{sn})] w_{snxx} = \alpha_5 \frac{(V_{n(g)})^2}{(1 - w_{sn})^2} + \alpha_6 \left[ V_{n(n-1)}^2 (w_{s(n-1)} - w_{sn}) + V_{n(n+1)}^2 (w_{s(n+1)} - w_{sn}) \right] \quad (4.12)$$

Using the static equations (4.11),(4.12) and expanding the forcing terms about equilibrium using Taylor series expansion method, the dynamic equations are obtained. To perform the linear frequency analysis, we neglect all nonlinear and forcing terms in these equations. Finally, the linear dynamic equations are given as follows,

$$\begin{aligned}
u_{nxxxx} + u_{ntt} - [2\alpha_1\Gamma(u_{sn}, u_n) + 2\alpha_2\Gamma(w_{sn}, w_n)]u_{snxx} - [N_n + \alpha_1\Gamma(u_{sn}, u_{sn}) \\
+ \alpha_2\Gamma(w_{sn}, w_{sn})]u_{nxx} = 2\alpha_3 \left[ V_{n(n-1)}^2 \left( \frac{u_n - u_{n-1}}{r_{n-1}^3 \left( 1 + \frac{(u_{s(n-1)} - u_{sn})}{r_{n-1}} \right)^3} \right) \right. \\
\left. - (V_{n(n+1)})^2 \left( \frac{u_{n+1} - u_n}{r_n^3 \left( 1 + \frac{(u_{sn} - u_{s(n+1)})}{r_n} \right)^3} \right) \right] \quad (4.13)
\end{aligned}$$

$$\begin{aligned}
w_{nxxxx} + \alpha_4 w_{ntt} - \alpha_4 [2\alpha_1\Gamma(u_{sn}, u_n) + 2\alpha_2\Gamma(w_{sn}, w_n)]w_{snxx} - \alpha_4 [N_n \\
+ \alpha_1\Gamma(u_{sn}, u_{sn}) + \alpha_2\Gamma(w_{sn}, w_{sn})]w_{nxx} = 2\alpha_5 \frac{V_{(n)(g)}^2}{(1 - w_{sn})^3} w_n \\
+ \alpha_6 \left[ V_{n(n-1)}^2 (w_{n-1} - w_n) + V_{n(n+1)}^2 (w_{n+1} - w_n) \right] \quad (4.14)
\end{aligned}$$

subjected to the following boundary conditions,

$$\begin{aligned}
u_n(0, t) = u_n(1, t) &= w_n(0, t) = w_n(1, t) = 0 \\
u_{nx}(0, t) = u_{nx}(1, t) &= w_{nx}(0, t) = w_{nx}(1, t) = 0 \quad (4.15)
\end{aligned}$$

## 4.2 Linear frequency analysis for N beams.

We reduce the static and linear dynamic governing equations considering single mode shape. Hence, the static and dynamic deflections of the beam along both the planes are assumed as:

$$\begin{aligned}
u_{sn}(x) = A_{n1}(y, z)\phi(x); \quad w_{sn}(x) = A_{n2}(y, z)\phi(x); \\
u_n(x, t) = P_{n1}(t)\phi(x); \quad w_n(x, t) = P_{n2}(t)\phi(x); \quad (4.16)
\end{aligned}$$

Here,  $\phi(x) = \sqrt{\frac{2}{3}}(1 - \cos(2\pi x))$  such that  $\int_0^1 (\phi_1(x))^2 dx = 1$  and it satisfies the geometric boundary conditions. Finally the reduced order static equations are given as,

$$\begin{aligned}
\frac{16}{9}\pi^4 \alpha_1 A_{n1}^3 + \left( \frac{16}{3}\pi^4 + \frac{16}{9}\pi^4 \alpha_2 A_{n2}^2 + \frac{4}{3}\pi^2 N_n \right) A_{n1} - \alpha_3 \left[ \frac{V_{(n-1)(n)}^2}{r_{n-1}^2} \sqrt{\frac{2/3}{\left( 1 + 2\sqrt{\frac{2}{3}} \frac{(A_{(n-1)1} - A_{(n)1})}{r_{n-1}}} \right)^3}} \right. \\
\left. - \frac{V_{(n)(n+1)}^2}{r_n^2} \sqrt{\frac{2/3}{\left( 1 + 2\sqrt{\frac{2}{3}} \frac{(A_{n1} - A_{(n+1)1})}{r_n}} \right)^3}} \right] = 0 \quad (4.17)
\end{aligned}$$

$$\begin{aligned}
\frac{16}{9}\pi^4 \alpha_2 A_{n2}^3 + \left( \frac{16}{3}\frac{\pi^4}{\alpha_4} + \frac{16}{9}\pi^4 \alpha_1 A_{n1}^2 + \frac{4}{3}\pi^2 N_n \right) A_{n2} - \frac{\alpha_5}{\alpha_4} V_{(n)(g)}^2 \sqrt{\frac{2/3}{\left( 1 - 2\sqrt{\frac{2}{3}} A_{n2} \right)^3}} \\
- \frac{\alpha_6}{\alpha_4} \left( V_{(n)(n-1)}^2 A_{(n-1)2} - [V_{(n)(n-1)}^2 + V_{(n+1)(n)}^2] A_{n2} + V_{(n+1)(n)}^2 A_{(n+1)2} \right) = 0 \quad (4.18)
\end{aligned}$$

Where,  $A_{01} = A_{(N+1)1} = 0$  correspond to displacements of two fixed side electrodes  $E_1$  and  $E_2$ . Applying the same Galerkin Procedure as discussed earlier to the dynamic equations (4.13) and (4.14), we obtain the modal equations as,

$$\begin{aligned} \ddot{P}_{n1}(t) + \left[ \frac{16}{3}\pi^4 + \frac{16}{9}\pi^4\alpha_2 A_{n2}^2 + \frac{16}{3}\pi^4\alpha_1 A_{n1}^2 + \frac{4}{3}\pi^2 N_n - 2\alpha_3 \left( \frac{V_{(n)(n-1)}^2}{r_{n-1}^3 (1 - 2\sqrt{\frac{2}{3}} \frac{(A_{n1} - A_{(n-1)1})}{r_{n-1}})^{\frac{5}{2}}} \right. \right. \\ \left. \left. + \frac{V_{(n)(n+1)}^2}{r_n^3 (1 - 2\sqrt{\frac{2}{3}} \frac{(A_{(n+1)1} - A_{n1})}{r_n})^{\frac{5}{2}}} \right) \right] P_{n1}(t) + 2\alpha_3 \left( \frac{V_{(n)(n+1)}^2}{r_n^3 (1 - 2\sqrt{\frac{2}{3}} \frac{(A_{(n+1)1} - A_{n1})}{r_n})^{\frac{5}{2}}} \right) P_{(n+1)1}(t) \\ + 2\alpha_3 \left( \frac{V_{(n-1)n}^2}{r_{n-1}^3 (1 - 2\sqrt{\frac{2}{3}} \frac{(A_{n1} - A_{(n-1)1})}{r_{n-1}})^{\frac{5}{2}}} \right) P_{(n-1)1}(t) = -\frac{32}{9}\alpha_2 A_{n1} A_{n2} \pi^4 P_{n2}(t) \end{aligned} \quad (4.19)$$

$$\begin{aligned} \ddot{P}_{n2}(t) + \left[ \frac{16}{3} \frac{\pi^4}{\alpha_4} + \frac{16}{9}\pi^4\alpha_1 A_{n1}^2 + \frac{16}{3}\pi^4\alpha_2 A_{n2}^2 + \frac{4}{3}\pi^2 N_n - 2\frac{\alpha_5}{\alpha_4} V_{(n)(g)}^2 (1 - 2\sqrt{\frac{2}{3}} A_{n2})^{-\frac{5}{2}} \right. \\ \left. + \frac{\alpha_6}{\alpha_4} (V_{(n)(n-1)}^2 + V_{(n+1)(n)}^2) \right] P_{n2}(t) \\ - \left( \frac{\alpha_6}{\alpha_4} V_{(n)(n-1)}^2 \right) P_{(n-1)2} - \left( \frac{\alpha_6}{\alpha_4} V_{(n+1)(n)}^2 \right) P_{(n+1)2} = -\frac{32}{9}\alpha_1 A_{n1} A_{n2} \pi^4 P_{n1}(t) \end{aligned} \quad (4.20)$$

Finally, the modal equations take the matrix form,  $\ddot{P} + [M]P = 0$ .

Here,

$$[P] = [P_{11} \ P_{12} \ \dots \ P_{k1} \ P_{k2} \ \dots \ P_{N1} \ P_{N2}]^T$$

$$[M] = \begin{bmatrix} \lambda_{11} & c_{1io} & c_{12i} & \dots & \cdot & \cdot & \cdot & \cdot & \cdot & \cdot & \cdot & \cdot & 0 & 0 \\ c_{1oi} & \lambda_{12} & 0 & c_{12o} & \dots & \cdot & \cdot & \cdot & \cdot & \cdot & \cdot & \cdot & 0 & 0 \\ \cdot & \cdot & \cdot & \cdot & \cdot & \cdot & \cdot & \cdot & \cdot & \cdot & \cdot & \cdot & \cdot & \cdot \\ \cdot & \cdot & \cdot & \cdot & \cdot & \cdot & \cdot & \cdot & \cdot & \cdot & \cdot & \cdot & \cdot & \cdot \\ \cdot & \cdot & \cdot & \cdot & \dots & c_{k(k-1)i} & 0 & \lambda_{k1} & c_{kio} & c_{k(k+1)i} & \dots & \cdot & \cdot & \cdot \\ \cdot & \cdot & \cdot & \cdot & \cdot & \dots & c_{(k-1)ko} & c_{koi} & \lambda_{k2} & 0 & c_{(k+1)ko} & \dots & \cdot & \cdot \\ \cdot & \cdot & \cdot & \cdot & \cdot & \cdot & \cdot & \cdot & \cdot & \cdot & \cdot & \cdot & \cdot & \cdot \\ 0 & \cdot & \cdot & \cdot & \cdot & \cdot & \cdot & \cdot & \cdot & \dots & c_{N(N-1)i} & 0 & \lambda_{N1} & c_{Nio} \\ 0 & \cdot & \cdot & \cdot & \cdot & \cdot & \cdot & \cdot & \cdot & \dots & 0 & c_{(N-1)No} & c_{Noi} & \lambda_{N2} \end{bmatrix}$$

where,

$$\lambda_{n1} = \left[ \frac{16}{3}\pi^4 + \frac{16}{9}\pi^4\alpha_2 A_{n2}^2 + \frac{16}{3}\pi^4\alpha_1 A_{n1}^2 + \frac{4}{3}\pi^2 N_n - 2\alpha_3 \left( \frac{V_{(n)(n-1)}^2}{r_{n-1}^3 (1 - 2\sqrt{\frac{2}{3}} \frac{(A_{n1} - A_{(n-1)1})}{r_{n-1}})^{\frac{5}{2}}} + \frac{V_{(n)(n+1)}^2}{r_n^3 (1 - 2\sqrt{\frac{2}{3}} \frac{(A_{(n+1)1} - A_{n1})}{r_n})^{\frac{5}{2}}} \right) \right] \quad (4.23)$$

$$\lambda_{n2} = \left[ \frac{16}{3} \frac{\pi^4}{\alpha_4} + \frac{16}{9}\pi^4\alpha_1 A_{n1}^2 + \frac{16}{3}\pi^4\alpha_2 A_{n2}^2 + \frac{4}{3}\pi^2 N_n - 2 \frac{\alpha_5}{\alpha_4} V_{(n)(g)}^2 (1 - 2\sqrt{\frac{2}{3}} A_{n2})^{-\frac{5}{2}} + \frac{\alpha_6}{\alpha_4} (V_{(n)(n-1)}^2 + V_{(n+1)(n)}^2) \right] \quad (4.24)$$

$$c_{n(n-1)i} = 2\alpha_3 \left( \frac{V_{(n-1)n}^2}{r_{n-1}^3 (1 - 2\sqrt{\frac{2}{3}} \frac{(A_{n1} - A_{(n-1)1})}{r_{n-1}})^{\frac{5}{2}}} \right)$$

$$c_{n(n+1)i} = 2\alpha_3 \left( \frac{V_{(n)(n+1)}^2}{r_n^3 (1 - 2\sqrt{\frac{2}{3}} \frac{(A_{(n+1)1} - A_{n1})}{r_n})^{\frac{5}{2}}} \right) \quad (4.25)$$

$$c_{nio} = \frac{32}{9}\alpha_2 A_{n1} A_{n2} \pi^4; \quad c_{n(n-1)o} = -\frac{\alpha_6}{\alpha_4} V_{(n)(n-1)}^2$$

$$c_{noi} = \frac{32}{9}\alpha_1 A_{n1} A_{n2} \pi^4; \quad c_{n(n+1)o} = -\frac{\alpha_6}{\alpha_4} V_{(n+1)(n)}^2 \quad (4.26)$$

In the above expressions,  $i$  and  $o$  denote two different modes, say, in-plane and out-of-plane modes.  $\lambda_{n1}$  and  $\lambda_{n2}$  correspond to the unperturbed natural frequencies of the  $n^{th}$  beam along  $i$  and  $o$  modes, respectively.  $c_{nio}$  denotes modal coupling of  $i$  and  $o$  modes of  $n^{th}$  beam, and  $c_{n(n-1)i}$  and  $c_{n(n+1)i}$  denote the  $i$  mode interaction of adjacent beams. Similarly,  $c_{n(n-1)o}$  and  $c_{n(n+1)o}$  denote the  $o$  mode interaction of adjacent beams. Finally, the frequencies corresponding different modes of each beam can be found from the eigenvalues of matrix [M].

### 4.3 Results and discussions

In this section, we discuss the outcomes of frequency analysis for an array of 40 beams numerically using Eqn.(4.17)-(4.20). We also present the experimental results for 40 beam array. The thickness of all the beams in the array are assumed to vary in between 2-4 $\mu$ m.

The beams are made of AuPd alloy on a silicon substrate using a bulk micro-machining process as discussed in case of single and three beam array. The fabricated beams are separated from their adjacent beams by different gaps  $g_i$ ,  $i = 0, 1, \dots, N$ , which are taken in the range of 4.0  $\mu$ m to 6.0  $\mu$ m. Other physical properties are as discussed in Table.(3.1) and Table.(3.2). The initial tensions  $N_i$  can be found by comparing the analytical and experimental results. In our case we take a maximum variation of 8 percent in initial tension of beams. Figure.(4.2)(a) shows the variation of the modal

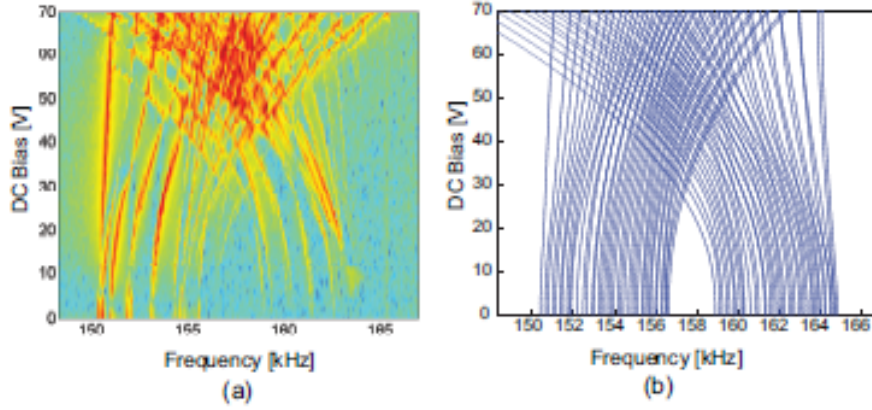


Figure 4.2: (a) Experimental result for frequency variation in an array of 40 beams showing multiple modal coupling; (b) The corresponding analytical result for  $L = 500 \mu\text{m}$ ,  $H = 2\text{-}4\mu\text{m}$ ,  $B = 200 \text{ nm}$  and alternate beams are applied with voltage  $V_{DC}$ .

frequencies for an array of 40 beams. Due to uneven laser heating, the frequencies corresponding to each beam are different. Such frequency distribution can be obtained by varying initial tension,  $N$ . When the DC bias voltage of alternate beams increases to 70 V, each beam behaves similar to that of a single beam Figure.(2.3)(e). But, unlike the single beam, an array of multiple beams shows multiple coupling regions. Figure.(4.2)(b) shows the analytical approximation of frequency variation in 40 beam array. There exist multiple modal coupling between different modes of a beam as well as modes of different beams.

## Chapter 5

# Conclusions and Future work

In this chapter we summarize the entire work and conclude the outcomes based on our analytical model. We have developed an approximate analytical model for a single fixed-fixed beam as well as an array of three beams excited simultaneously by two side electrodes and one bottom electrode. We tune the frequencies of the beams electrostatically, by applying potential differences between beams and electrodes and excite them in two mutually perpendicular directions, namely in-plane and out-of-plane. It is found that by suitably controlling the inter beam or beam-electrode gaps, we can get regions where two or more modes interact with each other and exchange energy between them. Again by varying the tensions in the beams we get wide operating natural frequencies of a beam. So by controlling the gaps and induced tensions in the beams, one can attain a desired frequency. Moreover, the pull-in voltage can also be increased by simultaneously exciting both modes and maintaining a proper gap.

After conducting the frequency analysis based on linear dynamic equations, we study the nonlinear dynamic behavior of the single beam system near and away from the coupling region. We apply method of multiple scales to the modal equations to find the dynamic response of the single beam. Here, we describe the case of 1:1 internal resonance where the in-plane mode couples with the out-of-plane mode and vice versa. Subsequently, we extend our formulations and generalize our model for an array of  $N$  beams. As a particular case, we do frequency analysis corresponding to 40 beam array and explain the concept of multiple modal coupling through the results. Finally we validate our model by comparing with the experimental results. Hence the frequency tuning mechanism by selecting differential gaps are important from MEMS design point of view. At the same time, by controlling the coupling region it is possible to get highly stable MEMS devices along with more pull-in voltages.

At last, while discussing the scope of works, it should be clear that the model we have developed is an approximate one. More accurate formulations can be done by considering several other effects such as fringing effects, effect of forcing due to just next as well as other neighboring members. The nonlinear coupling analysis can also be extended to an array of beams where multiple modal interactions are prominent and this concept can be applied for stabilizing the amplitude and frequency of oscillation in MEMS devices.

## Appendix

$$\begin{aligned}
t_1 &= \frac{16}{9}\alpha_1\pi^4, \quad t_2 = \frac{16}{3}\alpha_1A_1\pi^4, \quad t_3 = \frac{16}{9}\alpha_2\pi^4, \quad t_4 = \frac{32}{9}\alpha_2A_2\pi^4, \\
t_5 &= \frac{2\alpha_3}{(1-2\sqrt{\frac{2}{3}}A_1)^{5/2}}, \quad t_6 = \frac{2\alpha_3}{r_1^3(1+2\sqrt{\frac{2}{3}}\frac{A_1}{r_1})^{5/2}}, \quad t_7 = \frac{16}{9}\alpha_2A_1\pi^4, \\
t_8 &= \frac{32}{9}\alpha_2A_1A_2\pi^4, \quad t_9 = \frac{\sqrt{\frac{2}{3}}\alpha_3}{(1-2\sqrt{\frac{2}{3}}A_1)^{3/2}}, \quad t_{10} = \frac{\sqrt{\frac{2}{3}}\alpha_3}{r_1^2(1+2\sqrt{\frac{2}{3}}\frac{A_1}{r_1})^{3/2}}; \\
s_1 &= \frac{16}{9}\alpha_2\pi^4, \quad s_2 = \frac{16}{3}\alpha_2A_2\pi^4, \quad s_3 = \frac{16}{9}\alpha_1\pi^4, \quad s_4 = \frac{32}{9}\alpha_1A_1\pi^4, \\
s_5 &= \frac{2\alpha_5}{\alpha_4(1-2\sqrt{\frac{2}{3}}A_2)^{5/2}}, \quad s_6 = \frac{\alpha_6}{\alpha_4}, \quad s_7 = \frac{16}{9}\alpha_1A_2\pi^4, \\
s_8 &= \frac{32}{9}\alpha_1A_1A_2\pi^4, \quad s_9 = \frac{\sqrt{\frac{2}{3}}\alpha_5}{\alpha_4(1-2\sqrt{\frac{2}{3}}A_2)^{3/2}}, \quad s_{10} = \frac{\alpha_6}{\alpha_4}A_2; \tag{5.1}
\end{aligned}$$

$$\eta_{11} = 2V_{10}V_{ac}, \quad \eta_{12} = 2V_{21}V_{ac}, \quad \eta_{21} = 2V_{1g}V_{ac}, \quad \eta_2 = \frac{V_{ac}^2}{2}, \tag{5.2}$$

$$\begin{aligned}
B_1 &= 2\omega_1(1+k_1\bar{k}_1), & B_2 &= 2\omega_2(1+k_2\bar{k}_1), \\
B_3 &= \omega_1(C_1+C_3k_1\bar{k}_1), & B_4 &= \omega_2(C_1+C_3k_2\bar{k}_1), \\
B_5 &= \left[ \frac{t_9\eta_{11} - t_{10}\eta_{12} + \bar{k}_1s_9\eta_{21} - \bar{k}_1s_{10}(\eta_{11} + \eta_{12})}{2} \right];
\end{aligned}$$

$$\begin{aligned}
G_1 &= 2\omega_1(1+k_1\bar{k}_2), & G_2 &= 2\omega_2(1+k_2\bar{k}_2), \\
G_3 &= \omega_2(C_1+C_3k_2\bar{k}_2), & G_4 &= \omega_1(C_1+C_3k_1\bar{k}_2), \\
G_5 &= \left[ \frac{t_9\eta_{11} - t_{10}\eta_{12} + \bar{k}_2s_9\eta_{21} - \bar{k}_2s_{10}(\eta_{11} + \eta_{12})}{2} \right]; \tag{5.3}
\end{aligned}$$

$$\begin{aligned}
B_{11} &= (1+k_1\bar{k}_1), & B_{12} &= (1+k_2\bar{k}_1), \\
B_{13} &= (C_1+C_3k_1\bar{k}_1), & B_{14} &= (C_1+C_3k_2\bar{k}_1); \\
G_{11} &= (1+k_1\bar{k}_2), & G_{12} &= (1+k_2\bar{k}_2), \\
G_{13} &= (C_1+C_3k_2\bar{k}_2), & G_{14} &= (C_1+C_3k_1\bar{k}_2); \tag{5.4}
\end{aligned}$$

$$\begin{aligned}
c_{11} &= \frac{(-4\omega_1^2 t_4 k_1 - t_8 s_2 k_1^2 - t_8 s_7 - t_8 s_4 k_1 + \lambda_2^2 t_4 k_1 + \lambda_2^2 t_2 + \lambda_2^2 t_7 k_1^2 - 4\omega_1^2 t_7 k_1^2 - 4\omega_1^2 t_2)}{(t_8 s_8 - \lambda_2^2 \lambda_1^2 + 4\lambda_2^2 \omega_1^2 + 4\omega_1^2 \lambda_1^2 - 16\omega_1^4)}; \\
c_{21} &= -\frac{(-\lambda_1^2 s_7 + 4\omega_1^2 s_7 + t_2 s_8 - \lambda_1^2 s_2 k_1^2 - \lambda_1^2 s_4 k_1 + 4\omega_1^2 s_2 k_1^2 + 4\omega_1^2 s_4 k_1 + t_7 s_8 k_1^2 + t_4 k_1 s_8)}{(t_8 s_8 - \lambda_2^2 \lambda_1^2 + 4\lambda_2^2 \omega_1^2 + 4\omega_1^2 \lambda_1^2 - 16\omega_1^4)}; \\
c_{12} &= \frac{(-t_8 s_2 k_1^2 - t_8 s_7 - t_8 s_4 k_1 + \lambda_2^2 t_2 + \lambda_2^2 t_7 k_1^2 + \lambda_2^2 t_4 k_1)}{(t_8 s_8 - \lambda_2^2 \lambda_1^2)}; \\
c_{22} &= -\frac{(-\lambda_1^2 s_2 k_1^2 - \lambda_1^2 s_7 - \lambda_1^2 s_4 k_1 + t_2 s_8 + t_7 k_1^2 s_8 + t_4 k_1 s_8)}{(t_8 s_8 - \lambda_2^2 \lambda_1^2)}; \\
c_{13} &= \frac{(-4\omega_2^2 t_4 k_2 - t_8 s_2 k_2^2 - t_8 s_7 - t_8 s_4 k_2 + \lambda_2^2 t_4 k_2 + \lambda_2^2 t_2 + \lambda_2^2 t_7 k_2^2 - 4\omega_2^2 t_7 k_2^2 - 4\omega_2^2 t_2)}{(t_8 s_8 - \lambda_2^2 \lambda_1^2 + 4\lambda_2^2 \omega_2^2 + 4\omega_2^2 \lambda_1^2 - 16\omega_2^4)}; \\
c_{23} &= -\frac{(-\lambda_1^2 s_7 + 4\omega_2^2 s_7 + t_2 s_8 - \lambda_1^2 s_2 k_2^2 - \lambda_1^2 s_4 k_2 + 4\omega_2^2 s_2 k_2^2 + 4\omega_2^2 s_4 k_2 + t_7 s_8 k_2^2 + t_4 k_2 s_8)}{(t_8 s_8 - \lambda_2^2 \lambda_1^2 + 4\lambda_2^2 \omega_2^2 + 4\omega_2^2 \lambda_1^2 - 16\omega_2^4)}; \\
c_{14} &= \frac{(-t_8 s_2 k_2^2 - t_8 s_7 - t_8 s_4 k_2 + \lambda_2^2 t_2 + \lambda_2^2 t_7 k_2^2 + \lambda_2^2 t_4 k_2)}{(t_8 s_8 - \lambda_2^2 \lambda_1^2)}; \\
c_{24} &= -\frac{(-\lambda_1^2 s_2 k_2^2 - \lambda_1^2 s_7 - \lambda_1^2 s_4 k_2 + t_2 s_8 + t_7 k_2^2 s_8 + t_4 k_2 s_8)}{(t_8 s_8 - \lambda_2^2 \lambda_1^2)};
\end{aligned}$$

$$\begin{aligned}
c_{15N} &= -2t_8 s_2 k_1 k_2 - 2\omega_1^2 t_2 + 2\lambda_2^2 t_7 k_1 k_2 - 2\omega_1^2 t_7 k_1 k_2 - t_8 s_4 k_2 + 2\omega_1 \omega_2 t_4 k_1 + 2\omega_1 \omega_2 t_4 k_2 \\
&\quad - 2\omega_2^2 t_7 k_1 k_2 + \lambda_2^2 t_4 k_1 - t_8 s_4 k_1 + 4\omega_1 \omega_2 t_7 k_1 k_2 - 2t_8 s_7 + 2\lambda_2^2 t_2 - \omega_1^2 t_4 k_1 - \omega_1^2 t_4 k_2 \\
&\quad - \omega_2^2 t_4 k_2 - 2\omega_2^2 t_2 + 4\omega_1 \omega_2 t_2 - \omega_2^2 t_4 k_1 + \lambda_2^2 t_4 k_2; \\
c_{15D} &= -2\lambda_2^2 \omega_1 \omega_2 - 2\lambda_1^2 \omega_1 \omega_2 + t_8 s_8 - \omega_1^4 - \omega_2^4 - \lambda_1^2 \lambda_2^2 + \lambda_2^2 \omega_1^2 + \lambda_2^2 \omega_2^2 + \omega_1^2 \lambda_1^2 + 4\omega_1^3 \omega_2 \\
&\quad - 6\omega_1^2 \omega_2^2 + 4\omega_1 \omega_2^3 + \omega_2^2 \lambda_1^2; \\
c_{25N} &= -4\omega_1 \omega_2 s_2 k_1 k_2 - \lambda_1^2 s_4 k_2 - \lambda_1^2 s_4 k_1 + \omega_1^2 s_4 (k_1 + k_2) - 4\omega_1 \omega_2 s_7 + \omega_2^2 s_4 (k_2 + k_1) \\
&\quad + t_4 s_8 (k_1 + k_2) - 2\lambda_1^2 s_7 + 2(\omega_1^2 + \omega_2^2) s_7 + 2t_2 s_8 - 2\lambda_1^2 s_2 k_1 k_2 + 2\omega_1^2 s_2 k_1 k_2 \\
&\quad - 2\omega_1 \omega_2 s_4 (k_1 + k_2) + 2\omega_2^2 s_2 k_1 k_2 + 2t_7 k_1 k_2 s_8; \\
c_{25D} &= -2\lambda_2^2 \omega_1 \omega_2 - 2\lambda_1^2 \omega_1 \omega_2 + t_8 s_8 - \omega_1^4 - \omega_2^4 - \lambda_1^2 \lambda_2^2 + \lambda_2^2 \omega_1^2 + \lambda_2^2 \omega_2^2 + \omega_1^2 \lambda_1^2 + 4\omega_1^3 \omega_2 \\
&\quad - 6\omega_1^2 \omega_2^2 + 4\omega_1 \omega_2^3 + \omega_2^2 \lambda_1^2; \\
c_{16N} &= -2t_8 s_2 k_1 k_2 - 2(\omega_1^2 + \omega_2^2) t_2 + 2\lambda_2^2 t_7 k_1 k_2 - 2(\omega_1^2 + \omega_2^2) t_7 k_1 k_2 - 2\omega_1 \omega_2 t_4 (k_1 + k_2) \\
&\quad + \lambda_2^2 t_4 (k_1 + k_2) - t_8 s_4 (k_1 + k_2) - 4\omega_1 \omega_2 t_7 k_1 k_2 - 2t_8 s_7 + 2\lambda_2^2 t_2 \\
&\quad - \omega_1^2 t_4 (k_1 + k_2) - \omega_2^2 t_4 (k_1 + k_2) - 4\omega_1 \omega_2 t_2; \\
c_{16D} &= 2\lambda_2^2 \omega_1 \omega_2 + 2\lambda_1^2 \omega_1 \omega_2 + t_8 s_8 - \omega_1^4 - \omega_2^4 - \lambda_1^2 \lambda_2^2 + \lambda_2^2 \omega_1^2 + \lambda_2^2 \omega_2^2 + \omega_1^2 \lambda_1^2 - 4\omega_1^3 \omega_2 \\
&\quad - 6\omega_1^2 \omega_2^2 - 4\omega_1 \omega_2^3 + \omega_2^2 \lambda_1^2; \\
c_{26N} &= -[4\omega_1 \omega_2 s_2 k_1 k_2 - \lambda_1^2 s_4 k_1 - \lambda_1^2 s_4 k_2 + \omega_1^2 s_4 (k_1 + k_2) + 4\omega_1 \omega_2 s_7 + \omega_2^2 s_4 (k_2 + k_1) \\
&\quad + t_4 s_8 (k_1 + k_2) - 2\lambda_1^2 s_7 + 2(\omega_1^2 + \omega_2^2) s_7 + 2t_2 s_8 - 2\lambda_1^2 s_2 k_1 k_2 + 2\omega_1^2 s_2 k_1 k_2 \\
&\quad + 2\omega_1 \omega_2 s_4 (k_1 + k_2) + 2\omega_2^2 s_2 k_1 k_2 + 2t_7 k_1 k_2 s_8]; \\
c_{26D} &= 2\lambda_2^2 \omega_1 \omega_2 + 2\lambda_1^2 \omega_1 \omega_2 + t_8 s_8 - \omega_1^4 - \omega_2^4 - \lambda_1^2 \lambda_2^2 + \lambda_2^2 \omega_1^2 + \lambda_2^2 \omega_2^2 + \omega_1^2 \lambda_1^2 - 4\omega_1^3 \omega_2 \\
&\quad - 6\omega_1^2 \omega_2^2 - 4\omega_1 \omega_2^3 + \omega_2^2 \lambda_1^2;
\end{aligned}$$

$$c_{15} = \frac{c_{15N}}{c_{15D}}, \quad c_{25} = \frac{c_{25N}}{c_{25D}}; \quad c_{16} = \frac{c_{16N}}{c_{16D}}; \quad c_{26} = \frac{c_{26N}}{c_{26D}}; \quad (5.5)$$



$$\begin{aligned}
g_{11} &= t_3 k_1^2 + t_4 c_{25} + t_4 c_{21} + t_4 c_{11} k_2 + 2t_3 k_1 k_2 + t_4 c_{15} k_1 + 2t_7 k_1 c_{25} + 2t_7 k_2 c_{21} + 3t_1 + 2t_2 c_{15} + 2t_2 c_{11}; \\
g_{12} &= 3t_1 + 4t_7 k_2 c_{24} + 2t_7 k_2 c_{23} + t_4 c_{13} k_2 + 2t_4 c_{14} k_2 + 4t_2 c_{14} + 2t_2 c_{13} + 3t_3 k_2^2 + 2t_4 c_{24} + t_4 c_{23}; \\
g_{13} &= 2t_4 c_{12} k_2 + 2t_7 k_1 c_{25} + 4t_3 k_1 k_2 + 2t_7 k_1 c_{26} + t_4 c_{15} k_1 + 6t_1 + 2t_2 c_{15} + 2t_2 c_{16} + 4t_2 c_{12} + 2t_3 k_1^2 \\
&+ t_4 c_{25} + t_4 c_{26} + 2t_4 c_{22} + t_4 c_{16} k_1 + 4t_7 k_2 c_{22}; \\
g_{14} &= 3t_1 + t_4 c_{15} k_2 + 2t_7 c_{25} k_2 + t_4 k_1 c_{13} + 2t_3 k_1 k_2 + 2t_7 k_1 c_{23} + t_3 k_2^2 + t_4 c_{25} + t_4 c_{23} + 2t_2 c_{15} + 2t_2 c_{13}; \\
g_{15} &= t_4 c_{11} k_1 + 2t_4 c_{12} k_1 + 4t_7 k_1 c_{22} + 2t_7 k_1 c_{21} + 4t_2 c_{12} + 2t_2 c_{11} + 3t_3 k_1^2 + 2t_4 c_{22} + t_4 c_{21} + 3t_1; \\
g_{16} &= 2t_2 c_{15} + 2t_2 c_{16} + 4t_2 c_{14} + 2t_3 k_2^2 + t_4 c_{26} + t_4 c_{25} + 2t_4 c_{24} + 6t_1 + 4t_7 k_1 c_{24} + 2t_7 k_2 c_{26} + 2t_7 k_2 c_{25} \\
&+ 4t_3 k_1 k_2 + t_4 c_{15} k_2 + 2t_4 k_1 c_{14} + t_4 c_{16} k_2;
\end{aligned}$$

$$\begin{aligned}
g_{21} &= 2s_2(c_{25}k_1 + c_{21}k_2) + 3s_1k_1^2k_2 + 2s_7(c_{11} + c_{15}) + s_3(2k_1 + k_2) + s_4(c_{21} + c_{25} + k_2c_{11} + k_1c_{15}); \\
g_{22} &= 2s_2(2k_2c_{24} + k_2c_{23}) + s_1(3k_2^3) + 2s_7(c_{13} + 2c_{14}) + s_3(3k_2) + s_4(c_{23} + 2c_{24} + c_{13}k_2 + 2c_{14}k_2); \\
g_{23} &= 2s_2(2c_{22}k_2 + c_{25}k_1 + c_{26}k_1) + s_1(6k_1^2k_2) + 2s_7(c_{15} + c_{16} + 2c_{12}) + s_3(4k_1 + 2k_2) \\
&+ s_4(c_{25} + c_{26} + 2c_{22} + 2c_{12}k_2 + c_{15}k_1 + c_{16}k_1); \\
g_{24} &= 2s_2(c_{23}k_1 + c_{25}k_2) + s_1(3k_1k_2^2) + 2s_7(c_{13} + c_{15}) + s_3(k_1 + 2k_2) + s_4(c_{23} + c_{25} + c_{13}k_1 + c_{15}k_2); \\
g_{25} &= 2s_2(2k_1c_{22} + k_1c_{21}) + s_1(3k_1^3) + 2s_7(2c_{12} + c_{11}) + s_3(3k_1) + s_4(c_{21} + 2c_{22} + c_{11}k_1 + 2c_{12}k_1); \\
g_{26} &= 2s_2(2c_{24}k_1 + c_{25}k_2 + c_{26}k_2) + s_1(6k_1k_2^2) + 2s_7(c_{15} + c_{16} + 2c_{14}) + s_3(2k_1 + 4k_2) \\
&+ s_4(c_{25} + c_{26} + 2c_{24} + 2c_{14}k_1 + c_{15}k_2 + c_{16}k_2);
\end{aligned}$$

$$\begin{aligned}
f_{11} &= 2t_2(c_{13} + c_{15}) + 3t_1 + 2t_7(c_{23}k_1 + c_{25}k_2) + t_3(k_2^2 + 2k_1k_2) + t_4(c_{23} + c_{25} + c_{13}k_1 + c_{15}k_2); \\
f_{12} &= 2t_2(2c_{12} + c_{11}) + 3t_1 + 2t_7(2c_{22}k_1 + c_{21}k_1) + t_3(3k_1^2) + t_4(2c_{22} + c_{21} + c_{11}k_1 + 2c_{12}k_1); \\
f_{13} &= 2t_2(c_{15} + c_{16} + 2c_{14}) + 6t_1 + 2t_7(2c_{24}k_1 + c_{25}k_2 + c_{26}) + t_3(2k_2^2 + 4k_1k_2) \\
&+ t_4(c_{25} + c_{26} + 2c_{24} + 2c_{14}k_1 + c_{15}k_2 + c_{16}k_2); \\
f_{14} &= 2t_2(c_{15} + c_{11}) + 3t_1 + 2t_7(c_{25}k_1 + c_{21}k_2) + t_3(2k_1k_2 + k_1^2) + t_4(c_{21} + c_{25} + c_{11}k_2 + c_{15}k_1); \\
f_{15} &= 2t_2(2c_{14} + c_{13}) + 3t_1 + 2t_7(2c_{24}k_2 + c_{23}k_2) + t_3(3k_2^2) + t_4(2c_{24} + c_{23} + c_{13}k_2 + 2c_{14}k_2); \\
f_{16} &= 2t_2(c_{15} + c_{16} + 2c_{12}) + 6t_1 + 2t_7(2c_{22}k_2 + c_{26}k_1) + t_3(4k_1k_2 + 2k_1^2) \\
&+ t_4(c_{25} + c_{26} + 2c_{22} + 2c_{12}k_2 + c_{15}k_1 + c_{16}k_1);
\end{aligned}$$

$$\begin{aligned}
f_{21} &= 2s_2(c_{23}k_1 + c_{25}k_2) + s_1(3k_1k_2^2) + 2s_7(c_{13} + c_{15}) + s_3(k_1 + 2k_2) + s_4(c_{23} + c_{25} + c_{13}k_1 + c_{15}k_2); \\
f_{22} &= 2s_2(2c_{24}k_1 + c_{25}k_2 + c_{26}k_2) + s_1(6k_1k_2^2) + 2s_7(c_{15} + c_{16} + 2c_{14}) + s_3(2k_1 + 4k_2) \\
&\quad + s_4(c_{25} + c_{26} + 2c_{24} + 2c_{14}k_1 + c_{15}k_2 + c_{16}k_2); \\
f_{23} &= 2s_2(2c_{22}k_1 + c_{21}k_1) + s_1(3k_1^3) + 2s_7(2c_{12} + c_{11}) + s_3(3k_1) + s_4(2c_{22} + c_{21} + c_{11}k_1 + 2c_{12}k_1); \\
f_{24} &= 2s_2(c_{25}k_1 + c_{21}k_2) + s_1(3k_1^2k_2) + 2s_7(c_{15} + c_{11}) + s_3(2k_1 + k_2) + s_4(c_{21} + c_{25} + c_{11}k_2 + c_{15}k_1); \\
f_{25} &= 2s_2(2c_{22}k_2 + c_{25}k_1 + c_{26}k_1) + s_1(6k_1^2k_2) + 2s_7(c_{15} + c_{16} + 2c_{12}) + s_3(4k_1 + 2k_2) \\
&\quad + s_4(c_{25} + c_{26} + 2c_{22} + 2c_{12}k_2 + c_{15}k_1 + c_{16}k_1); \\
f_{26} &= 2s_2(2c_{24}k_2 + c_{23}k_2) + s_1(3k_2^3) + 2s_7(2c_{14} + c_{13}) + s_3(3k_2) + s_4(2c_{24} + c_{23} + c_{13}k_2 + 2c_{14}k_2);
\end{aligned} \tag{5.6}$$

$$\begin{aligned}
\bar{G} &= \bar{g}_1\bar{A}_2A_1^2e^{-i\sigma_2T_1} + \bar{g}_2\bar{A}_2A_2^2e^{i\sigma_2T_1} + \bar{g}_3A_1A_2\bar{A}_1e^{i\sigma_2T_1} + \bar{g}_4A_2^2\bar{A}_1e^{2i\sigma_2T_1} + \bar{g}_5A_1^2\bar{A}_1 + \bar{g}_6A_1\bar{A}_2A_2; \\
\bar{F} &= \bar{f}_1\bar{A}_1A_2^2e^{i\sigma_2T_1} + \bar{f}_2\bar{A}_1A_1^2e^{-i\sigma_2T_1} + \bar{f}_3A_1A_2\bar{A}_2e^{-i\sigma_2T_1} + \bar{f}_4A_1^2\bar{A}_2e^{-2i\sigma_2T_1} + \bar{f}_5A_2^2\bar{A}_2 + \bar{f}_6A_1\bar{A}_1A_2;
\end{aligned} \tag{5.7}$$

$$\begin{aligned}
h_1 &= \left( \frac{B_3G_2 - B_2G_4}{B_2G_1 - B_1G_2} \right), & h_2 &= \left( \frac{B_4G_2 - B_2G_3}{B_2G_1 - B_1G_2} \right); \\
h_3 &= \left( \frac{B_2G_5 - B_5G_2}{B_2G_1 - B_1G_2} \right), & h_4 &= \left( \frac{B_4G_1 - B_1G_3}{B_1G_2 - B_2G_1} \right); \\
h_5 &= \left( \frac{B_3G_1 - B_1G_4}{B_1G_2 - B_2G_1} \right), & h_6 &= \left( \frac{B_1G_5 - B_5G_1}{B_1G_2 - B_2G_1} \right);
\end{aligned} \tag{5.8}$$

$$\begin{aligned}
J_{11} &= h_1 + \left[ \frac{2G_{12}}{16\omega_1(B_{11}G_{12} - B_{12}G_{11})} \right] \left( 2\bar{g}_1a_1a_2 \sin(\theta_1 - \theta_2) - 2\bar{g}_3a_1a_2 \sin(\theta_1 - \theta_2) \right. \\
&\quad \left. - \bar{g}_4a_2^2 \sin 2(\theta_1 - \theta_2) \right) + \left[ \frac{2B_{12}}{16\omega_1(B_{11}G_{12} - B_{12}G_{11})} \right] \left( \bar{f}_1a_2^2 \sin 2(\theta_1 - \theta_2) \right. \\
&\quad \left. - 2\bar{f}_4a_1a_2 \sin(\theta_1 - \theta_2) + 2\bar{f}_6a_1a_2 \sin(\theta_1 - \theta_2) \right) \\
J_{12} &= -h_2a_2 \sin(\theta_1 - \theta_2) + 2h_3 \cos \theta_1 - \left[ \frac{B_{13}G_{12} - B_{12}G_{14}}{4\omega_1(B_{11}G_{12} - B_{12}G_{11})} \right] \left( h_2a_2 \cos(\theta_1 - \theta_2) \right. \\
&\quad \left. + 2h_3 \sin \theta_1 \right) - \left[ \frac{B_{14}G_{12} - B_{12}G_{13}}{4\omega_1(B_{11}G_{12} - B_{12}G_{11})} \right] \left( h_4a_2 \cos(\theta_1 - \theta_2) + 2h_6 \sin \theta_1 \right) \\
&+ \left[ \frac{2G_{12}}{16\omega_1(B_{11}G_{12} - B_{12}G_{11})} \right] \left( \bar{g}_1a_1^2a_2 \cos(\theta_1 - \theta_2) - \bar{g}_2a_2^3 \cos(\theta_1 - \theta_2) - \bar{g}_3a_1^2a_2 \cos(\theta_1 - \theta_2) \right. \\
&\quad \left. - 2\bar{g}_4a_1a_2^2 \cos 2(\theta_1 - \theta_2) \right) + \left[ \frac{2B_{12}}{16\omega_1(B_{11}G_{12} - B_{12}G_{11})} \right] \left( 2\bar{f}_1a_1a_2^2 \cos 2(\theta_1 - \theta_2) \right. \\
&\quad \left. - \bar{f}_4a_1^2a_2 \cos(\theta_1 - \theta_2) + \bar{f}_5a_2^3 \cos(\theta_1 - \theta_2) + \bar{f}_6a_1^2a_2 \cos(\theta_1 - \theta_2) \right)
\end{aligned}$$

$$\begin{aligned}
J_{13} = & h_2 \cos(\theta_1 - \theta_2) - \left[ \frac{B_{13}G_{12} - B_{12}G_{14}}{4\omega_1(B_{11}G_{12} - B_{12}G_{11})} \right] \left( h_2 \sin(\theta_1 - \theta_2) \right. \\
& \left. \right) - \left[ \frac{B_{14}G_{12} - B_{12}G_{13}}{4\omega_1(B_{11}G_{12} - B_{12}G_{11})} \right] \left( h_4 \sin(\theta_1 - \theta_2) \right) \\
+ & \left[ \frac{2G_{12}}{16\omega_1(B_{11}G_{12} - B_{12}G_{11})} \right] \left( \bar{g}_1 a_1^2 \sin(\theta_1 - \theta_2) - 3\bar{g}_2 a_2^2 \sin(\theta_1 - \theta_2) - \bar{g}_3 a_1^2 \sin(\theta_1 - \theta_2) \right. \\
& \left. - 2\bar{g}_4 a_1 a_2 \sin 2(\theta_1 - \theta_2) \right) + \left[ \frac{2B_{12}}{16\omega_1(B_{11}G_{12} - B_{12}G_{11})} \right] \left( 2\bar{f}_1 a_1 a_2 \sin 2(\theta_1 - \theta_2) \right. \\
& \left. - \bar{f}_4 a_1^2 \sin(\theta_1 - \theta_2) + 3\bar{f}_5 a_2^2 \sin(\theta_1 - \theta_2) + \bar{f}_6 a_1^2 \sin(\theta_1 - \theta_2) \right)
\end{aligned}$$

$$\begin{aligned}
J_{41} = & h_2 a_2 \sin(\theta_1 - \theta_2) - \left[ \frac{B_{13}G_{12} - B_{12}G_{14}}{4\omega_1(B_{11}G_{12} - B_{12}G_{11})} \right] \left( -h_2 a_2 \cos(\theta_1 - \theta_2) \right) \\
& - \left[ \frac{B_{14}G_{12} - B_{12}G_{13}}{4\omega_1(B_{11}G_{12} - B_{12}G_{11})} \right] \left( -h_4 a_2 \cos(\theta_1 - \theta_2) \right) \\
+ & \left[ \frac{2G_{12}}{16\omega_1(B_{11}G_{12} - B_{12}G_{11})} \right] \left( -\bar{g}_1 a_1^2 a_2 \cos(\theta_1 - \theta_2) + \bar{g}_2 a_2^3 \cos(\theta_1 - \theta_2) + \bar{g}_3 a_1^2 a_2 \cos(\theta_1 - \theta_2) \right. \\
& \left. + 2\bar{g}_4 a_1 a_2^2 \cos 2(\theta_1 - \theta_2) \right) + \left[ \frac{2B_{12}}{16\omega_1(B_{11}G_{12} - B_{12}G_{11})} \right] \left( -2\bar{f}_1 a_1 a_2^2 \cos 2(\theta_1 - \theta_2) \right. \\
& \left. + \bar{f}_4 a_1^2 a_2 \cos(\theta_1 - \theta_2) - \bar{f}_5 a_2^3 \cos(\theta_1 - \theta_2) - \bar{f}_6 a_1^2 a_2 \cos(\theta_1 - \theta_2) \right)
\end{aligned}$$

# References

- [1] Hossein Pakdast, and Marco Lazzarino, Triple coupled cantilever systems for mass detection and localization, *Sensors and Actuators A: Physical* **175**, 127-131, 2012
- [2] M. Spletzer, A. Raman, H. Sumali, and J. P. Sullivan, Highly sensitive mass detection and identification using vibration localization in coupled microcantilever arrays, *Applied Physics Letter* **92**, 114102(1)-114102(3), 2008
- [3] Y. T. Yang, C. Callegari, X. L. Feng, K. L. Ekinici, and M. L. Roukes, Zeptogram-Scale Nanomechanical Mass Sensing, *Nano Letters* **6**(4), 583-586, 2006
- [4] Ashok Kumar Pandey, Oded Gottlieb, Oleg Shtempluck, and Eyal Buks, Performance of an AuPd micromechanical resonator as a temperature sensor, *Applied Physics Letters* **96**, 203105(1)-205103(3), 2010
- [5] H. W. Ch. Postma, I. Kozinsky, A. Husain, and M. L. Roukes, Dynamic range of nanotube- and nanowire-based electromechanical systems, *Applied Physics Letters* **86**(4), 223105(1)-223105(3), 2005
- [6] N. Suzuki, H. Tanigawa, and K. Suzuki, Zeptogram-Scale Nanomechanical Mass Sensing, *Journal of Micromechanics and Microengineering* **23**, 045018(1)-045018(12), 2013
- [7] Wan-Sul Lee, Kie-Chan Kwon, Bong-Kyu Kim, Ji-Hyon Cho, and Sung-Kie Youn, Frequency Shifting Analysis of Electrostatically Tunable Micro-mechanical Actuator, *Journal of Modeling and Simulation of Microsystems* **2**(1), 83-88, 2001
- [8] Quirin P. Unterreithmeier, Eva M. Weig, and Jorg P. Kotthaus, Universal transduction scheme for nanomechanical systems based on dielectric forces, *Nature Letters* **458**, 1001-1004, 2009
- [9] Eyal Buks, and Michael L. Roukes, Electrically Tunable Collective Response in a Coupled Micromechanical Array, *Journal of Microelectromechanical Systems* **11**(6), 802-807, 2002
- [10] Todd Remptema, and Liwei Lin, Active frequency tuning for micro resonators by localized thermal stressing effects, *Sensors and Actuators A* **91**, 326-332, 2001
- [11] Hari S. Solanki, Shamashis Sengupta, Sajal Dhara, Vibhor Singh, Sunil Patil, Rohan Dhall, Jeevak Parpia, Arnab Bhattacharya, and Mandar M. Deshmukh, Tuning mechanical modes and influence of charge screening in nanowire resonators, *Physical Review B* **81**, 115459(1)-115459(7), 2010

- [12] I. Kozinsky, H. W. Ch. Postma, I. Bargatin and M. L. Roukes, Tuning nonlinearity, dynamic range, and frequency of nanomechanical resonators, *Applied Physics Letters* **88**, 253101(1)-253101(3), 2006
- [13] Nguyen C.T., MEMS technology for timing and frequency control, *IEEE trans.* **54**, 251-270, 2007
- [14] I. Kozinsky, Nonlinear Nanoelectromechanical Systems, *PhD Thesis, Caltec, California* , 2007
- [15] A.H. Nayfeh, Nonlinear Interactions, Analytical, Computational and Experimental Methods, *Book, Wiley- Interscience, John Wiley and sons Inc. 1st ed.*, 2004
- [16] A.H. Nayfeh and P. Frank Pai, Linear and Nonlinear Structural Mechanics, *Book, Wiley-VCH, weinheim 1st ed.*, 2004
- [17] A.H. Nayfeh, Introduction to perturbation techniques, *Book, Wiley-interscience, John Wiley and sons Inc. Library edition*, 1993
- [18] H.K. Lee, P.A. Ward, A.E. Duwel, J.C. Salvia, Y.Q. Qu, R. Melamud, S.A. Chandorkar, M.A. Hopcroft, B. Kim, and T.W. Kenny, Verification of phase noise model for MEMS oscillators operating in the nonlinear regime, *Solid-state Sensors, Actuators and Microsystems Conferenece, Transducer* , 510-513, 2011
- [19] Dario Antonio, Damian H. Zanette, and Daniel Lopez, Frequency stabilization in nonlinear micromechanical oscillators, *Nature communications* **3**(806), 1-6, 2012
- [20] Akira Abe, Validity and accuracy of solutions for nonlinear vibration analyses of suspended cables with one to one internal resonance, *Nonlinear Analysis: Real World Applications* **11**, 2594-2602, 2010
- [21] Yan Yan, Wenquan Wang, and Lixiang Zhang, Applied multiscale method to analysis of nonlinear vibration for double-walled carbon nanotubes, *Applied Mathematical Modelling* **35**, 2279-2289, 2011
- [22] S. Murat Bagdatli, H. Ridvan Oz, and Erdogan Ozkaya, Nonlinear transverse vibrations and 3:1 internal resonances of a tensioned beam on multiple supports, *Mathematical and Computational Applications* **16**(1), 203-215, 2011
- [23] Usama H. Hegazy, 3:1 internal resonance of a string-beam coupled system with cubic nonlinearities, *Commun Nonlinear Sci Numer Simulat* **15**, 4219-4229, 2010
- [24] A. F. El-Bassiouny, Three-to-one Internal Resonance in The Non Linear Oscillation of Shallow Arch, *Physica Scripta* **72**, 439-450, 2005
- [25] Ashwin Vyas, Dimitriou Peroulis, and Anil Bajaj, A Microresonator Design Based on Nonlinear 1:2 Internal Resonance in Flexural Structural Modes, *Journal of Microelectromechanical Systems* **18**(3), 744-762, 2009
- [26] Mohammed F. Daqaq, Eihab M. Abdel-Rahman, and Ali H. Nayfeh, Two-to-one internal resonance in microscanners, *Nonlinear Dynamics* **57**, 231-251, 2009

- [27] Manu Agarwal, Kwan Kyu Park, Rob N. Candler, Bongsang Kim, Matthew A. Hopcroft, Saurabh A. Chandorkar, Chandra M. Jha, Renata Melamud, Thomas W. Kenny and Boris Murmann, Nonlinear Characterization of Electrostatic MEMS Resonators, *IEEE Conference* **15**, 209-212, 2006
- [28] Stav Zaitsev, Oleg Shtempluck, Eyal Buks, and Oded Gottlieb, Nonlinear damping in a micromechanical oscillator, *Nonlinear Dynamics* **67**, 859-883, 2012
- [29] Hyung Kyu Lee, Renata Melamud, Saurabh Chandorkar, James Salvia, Shingo Yoneoka, and Thomas W. Kenny, Stable Operation of MEMS Oscillators Far Above the Critical Vibration Amplitude in the Nonlinear Regime, *Journal of Microelectromechanical system* **20**(6), 1228-1230, 2011
- [30] S. Gutschmidt, and O. Gottlieb, Internal resonance and bifurcations of an array below the first pull-in instability, *International Journal of Bifurcation and Chaos* **20**(3), 605-618, 2010
- [31] S. Gutschmidt, and O. Gottlieb, Nonlinear dynamic behavior of a microbeam array subject to parametric actuation at low, medium and large DC-voltages, *Nonlinear Dynamics* **67**, 1-36, 2012
- [32] A. Isacson, and J. M. Kinaret, Parametric resonances in electrostatically interacting carbon nanotube arrays, *Condensed Matter, Mesoscale and Nanoscale Physics* **arXiv:0812.3515**, 1-11, 2008
- [33] L. Chotorlishvili, A. Ugulava, G. Mchedlishvili, A. Komnik, S. Wimberger, and J. Berakdar, Nonlinear dynamics of two coupled nanoelectromechanical resonators, *Journal of Physics B* **44**, 215402(1)-215402(9), 2011
- [34] S. S. Verbridge, D. F. Shapiro, H. G. Craighead and J. M. Parpia, Nonlinear dynamics of two coupled nanoelectromechanical resonators, *Nano Lett.* **7**(6), 1728, 2007
- [35] Ashok Kumar Pandey, Venkatesh K.P. and Rudra Pratap, Effect of Metal Coating and Residual Stress on the Resonant Frequency of MEMS Resonators, *Sadhana* **34**(4), 1-11, 2009
- [36] Nayfeh A.H., Resolving controversies in the application of the method of multiple scales and the generalized method of averaging, *Nonlinear Dyn.* **40**, 61-102, 2005